TRANSPORTATION RESEARCH

RECORD

No. 1434

Pavement Design, Management, and Performance; Soils, Geology, and Foundations

---

Subsurface Drainage, Soil-Fluid Interface Phenomena, and Management of Unpaved Surfaces

A peer-reviewed publication of the Transportation Research Board

TRANSPORTATION RESEARCH BOARD
NATIONAL RESEARCH COUNCIL

NATIONAL ACADEMY PRESS
WASHINGTON, D.C. 1994

Transportation Research Record 1434
ISSN 0361-1981
ISBN 0-309-05511-3
Price: $25

Subscriber Categories
IIB pavement design, management, and performance
IIIA soils, geology, and foundations

Printed in the United States of America

Transportation Research Record 1434

Contents

Foreword

The 13 papers in this volume are arranged in three general groups. The first six papers are on issues related to subsurface drainage of slopes, embankments, and pavement subgrades. The first three describe precipitate formation in subsurface drainage systems because of chemical breakdown of certain types of aggregates, and the remaining three relate to drainage of granular bases, open-graded layers, and jointed concrete pavement.

The next three papers describe phenomena at the soil-fluid interface. The movement of fluids in the subsurface is an important consideration in designing road structures to ensure adequate drainage and to safeguard against contaminant migration into the right-of-ways from a contaminated subsurface.

The last group of papers describes management systems for unpaved and aggregate-surfaced roads. These papers provide either an overall look at the management systems, both computerized and manual, or specific details of system components that are applicable to unpaved surfaces.

PART 1

Subsurface Drainage

Alkaline Leachate and Calcareous Tufa Originating from Slag in a Highway Embankment near Baltimore, Maryland

BRUCE W. BOYER

A series of springs located along the lower contact of a slag bed 3 to 7 m thick sandwiched within an embankment for Interstate 695 in Baltimore County, Maryland, discharges water with a pH of 12.5 to 13 and a dissolved calcium concentration of roughly 1000 mg/L. Further reactions with atmospheric CO_2 cause this leachate to precipitate copious quantities of calcite ($CaCO_3$) in the form of surficial tufa, interstitial cement within the fill, or fine powdery sediment in surface water. Because of its high pH, the leachate is classed as a hazardous waste, and the Maryland State Highway Administration has been required to construct a fenced enclosure and containment pond for the springs and to haul away the leachate or treat it before discharge. The cost of remediation had reached $1,000,000 by early 1994, when a treatment plant using hydrochloric acid to neutralize the leachate was about to begin operation. This case history demonstrates that great caution should be exercised in use of industrial by-products as construction materials. Although other recent studies have clarified the mechanism of tufa formation, unanswered questions remain regarding the mobility and fate of labile constituents other than calcium. Such questions must be answered before such reactive materials are dispersed into the environment in the name of recycling.

During April 1986 the Maryland Department of the Environment (MDE) notified the State Highway Administration (SHA) of a suspected chemical spill on the right-of-way for Interstate 695 (Baltimore Beltway) near North Point Boulevard. The spill consisted of a wet white solid on the face of an embankment below one of the ramps. SHA hired a contractor to remove this material. However, in October 1987, MDE found more of the material and requested further action. When the contractor again attempted to scrape up the deposit, its apparent source was exposed—a spring on the embankment. Since the effluent from this spring had a pH greater than 12.5, it was classified as a hazardous waste, and MDE directed SHA to contain the discharge. SHA responded by constructing a lined containment pond in November 1987. Water from this pond was periodically pumped out by a tank truck and hauled to a secure permitted disposal site in another state. The cost of this procedure (about $7,000/week) prompted a search for a more cost-effective system and motivated a hydrogeologic study to determine the source of the caustic discharge and identification of any other responsible parties.

INVESTIGATION

Six alkaline springs have been found in the problem area; two are perennial; the others flow only following precipitation events. The springs can be located even when they are inactive because they are all marked by patches of unvegetated soil and distinctive white mineral deposits (often forming plumes that can be traced upslope to a point source), which range from loose powdery sediment to rigid crusts 20 mm or more in thickness. The crusts contain numerous pores—molds of grass stems and other debris trapped by the growing crust. On the basis of petrography, chemical analysis, X-ray diffraction, and strong effervescence in dilute hydrochloric acid, the crust has been determined to be largely calcite (calcium carbonate). It resembles calcareous tufa, a deposit that forms around some natural springs. Calcite also occurs in the fine sediment that carpets the bottom of the containment pond as paper-thin rafts (like miniature ice floes) or a continuous skin on the surface of the pond and as an interstitial cement that has lithified the soil of the embankment near the perennial springs to a depth of at least 300 mm.

The embankment in the study area is composed mostly of sandy soil obtained by stripping native material from a large area immediately east of the embankment, where aerial photographs record a history of agricultural land use with no evidence of industrial waste generation or disposal. Discontinuous clay lenses occur, mostly in the lower part of the embankment. Sandwiched within this natural material is a layer of slag that is apparently continuous for hundreds of meters but varies greatly in thickness. The slag consists mostly of sand to gravel-sized fragments of dark gray rocklike material, which often contains vesicles (round voids) formed by gas bubbles trapped within the molten slag. Most of the slag fragments have softer, light gray weathered "rinds" that effervesce in hydrochloric acid, indicating the presence of calcite. The slag also contains varying amounts of silt- to clay-sized material, which is not readily identifiable, although it resembles the slag in color. It may be residue formed by weathering and leaching of slag or some other industrial waste.

The slag layer is believed to be the source of the alkaline seepage for the following reasons:

1. Samples of slag from borings and surface exposures on the embankment gave reaction pH values of 12 to 13 when mixed with distilled water. When leached with nitric acid, they yielded very high concentrations of dissolved calcium and magnesium. In contrast, soil samples of the nonslag embankment materials have reaction pH values closer to neutral (5.5 to 8.0) and calcium concentrations averaging only 0.2 percent of those in the slag samples.
2. All the observed alkaline springs are located along the line where the bottom of a slag bed intersects the embankment surface.

Maryland State Highway Administration, 2323 W. Joppa Road, Brooklandville, Md. 21022.

3. The greatest volume of alkaline seepage is observed near the area where the slag is thickest.
4. The major chemical constituents of the seepage occur in proportions consistent with an origin by leaching of slag.

There is some doubt regarding the exact nature of the material within the slag bed that is responsible for the high pH of the leachate. The reaction pH of blast furnace slag is normally in the range of 9 to 11; in one study, blast furnace slag from eight different sources yielded reaction pH values ranging from 9.4 to 11.7, with an average of 10.6 (*1*). This suggests that blast furnace slag alone could not be responsible for the high pH observed in the present study. However, there are published references to other steel industry wastes that are more strongly alkaline, for example, arc furnace dust (reaction pH 11.7 to 12.8), ladle refining slag (11.0 to 12.7), A.O.D. converter dust (11.5 to 12.25) (*2*), an "alkaline sludge" from coal tar processing with a pH of 14.0 and high concentrations of phenols (*3*), and steel slag and slacker aggregate (*4*). According to the contractor, the slag was "borrowed" from an abandoned railroad spur fill constructed 40 years ago. The contractor believes that the material may have been blast furnace slag, open hearth slag (a type of steel slag), or "plant refuse" described as "a conglomerate of residual slag and debris from pit operations and refuse from plant operations after primary extraction of metallics by crane magnets."

HYDROGEOLOGY

The mostly likely conceptual model for groundwater flow within the embankment is shown in Figure 1. The model assumes that direct precipitation or stormwater runoff readily infiltrates the sandy natural soil above the slag. The groundwater then moves downward through the slag until it encounters the less permeable clayey layers (aquitards) beneath the slag, which cause formation of one or more perched water lenses that spread vertically and laterally until they reach the surface of the embankment and erupt as springs. If these lenses are not replenished by infiltration, they will eventually shrink or totally disappear as water seeps down and out of the embankment; this explains why most of the alkaline springs are ephemeral and cease flowing in a downward sequence. The peculiar shape of the slag layer serves to funnel groundwater from a large catchment area toward the perennial springs on the east side of the embankment.

The hydrogeologic model assumes that slag is the most permeable material within the embankment. Available data on hydrologic parameters of slag are very limited. The coefficient of permeability (hydraulic conductivity) of compacted granulated slag is reported to be roughly equal to that of "clean" sand and gravel (*5*). It is somewhat puzzling that a suspected high-conductivity perched aquifer should exhibit slow protracted drainage through perennial springs. However, there are several factors that could explain this. First, slag may have unusual aquifer properties. Because the surface of slag particles is rough and vesicular, a layer composed of such particles should have an intergranular pore geometry different from that of, for example, a typical quartzose sand or gravel. Also because of the vesicles, a slag bed should have intragranular as well as intergranular porosity. The result could be that a slag layer would have a higher specific yield and a more protracted period of gravity drainage than many natural aquifer materials whose particle size distribution (as determined by sieving, for example) is similar. Another factor could be that seepage from the overlying less permeable natural soil recharges the slag aquifer at a rate roughly balancing the rate of spring discharge. Finally, it is possible that aquifer discharge is choked by progressive carbonate cementation of areas where seepage might otherwise occur, thereby ponding leachate within the slag.

GEOCHEMISTRY

The major chemical species found in inorganic chemical analyses of water from the main perennial spring are shown in Table 1. The water is characterized by high concentrations of calcium, hydroxyl, chloride, sodium, and potassium ions. When the analysis is recalculated as milliequivalents per liter, it becomes evident that Na^+ is almost exactly balanced by Cl^-, and Ca^{2+} is approximately balanced by $(OH)^-$. The most likely explanation for this pattern is that the leachate forms mainly by dissolution of two solids, NaCl and CaO [or $Ca(OH)_2$].

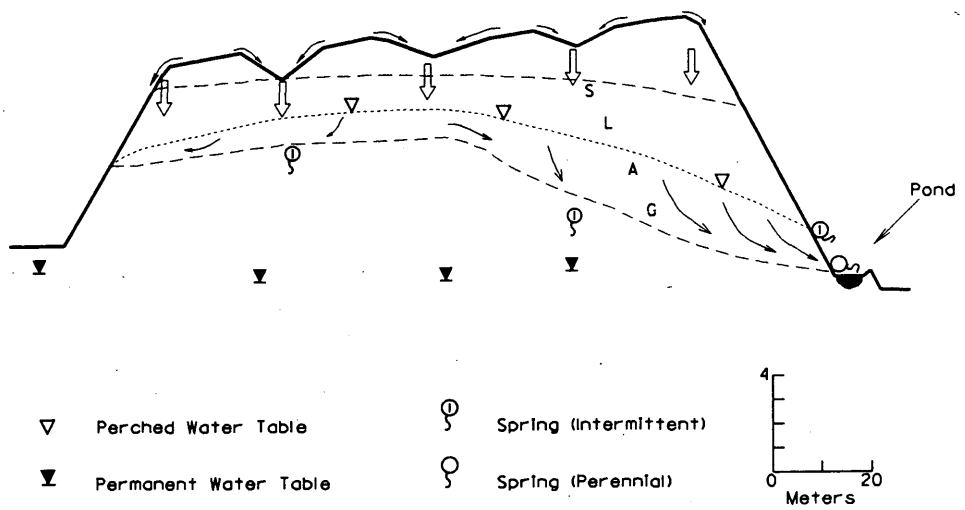

FIGURE 1 Cross section of embankment with conceptual groundwater flow model.

TABLE 1 Concentration of Major Ions in I-695 Slag Leachate

	Ion					
Units	Ca^{2+}	OH^-	Na^+	Cl^-	K^+	Al^{3+}
Mg/l[a]	1137	1048	557	859	50[c]	13.5
Meq/l[b]	56.74	61.62	24.23	24.24	1.28	1.50

[a]Milligrams per liter
[b]Milliequivalents per liter
[c]Estimate based on a different analysis

Recent studies (*4*) have identified free lime (CaO) as the source of the high calcium levels in steel slag leachate. Free lime (also known as quicklime) cannot coexist with liquid water because it irreversibly hydrates to portlandite, $Ca(OH)_2$, at earth-surface conditions. This suggests that, given sufficient contact time, the solubility of portlandite could set an upper limit on the concentrations of Ca and $(OH)^-$ in slag leachate if the system is isolated from CO_2. The slag layer at North Point is largely protected from contact with atmospheric CO_2 by the relatively thick blanket of overburden, the cemented soil zones, and the presence of perennially water-saturated conditions in part of the slag. These factors favor generation of a leachate dominated by calcium and hydroxide ions. Once this leachate comes into contact with air, however, CO_2 will begin to dissolve into the leachate, forming H_2CO_3, most of which will quickly dissociate to form $(CO_3)^{2+}$, which in turn will react with Ca^{2+} to form $CaCO_3$ (calcite). The solubility of portlandite is roughly 2 orders of magnitude greater than that of calcite at room temperature. This means that uncarbonated slag leachate will reach supersaturation with respect to calcite even if only tiny amounts of CO_2 dissolve into it, because the Ca^{2+} content has built up to very high levels as the result of prior exclusion of CO_2. Thus, steel slag leachate is unlike many natural waters in that it can precipitate calcite without having the solubility of calcite reduced by heating, evaporation, or degassing of CO_2 from the solution, although these factors can increase the degree of supersaturation and thereby speed up precipitation.

Because the North Point leachate was not analyzed for carbonate and bicarbonate, published analyses from Ohio (*6*), which did include these important species and were otherwise similar to the North Point analyses, were used as input to WATEQ4F, a computer program that calculates degree of saturation of a solution with respect to various mineral species (*7*). The results (Table 2) confirm that the most alkaline Ohio underdrain slag leachate is a solution that is nearly saturated with respect to portlandite and supersaturated with respect to calcite even at a cool springtime temperature (13°C) and even though it has absorbed very little CO_2 (as much as water at equilibrium with a partial pressure of $10^{-11.2}$ atm CO_2). This concentration is far below the atmospheric concentration of CO_2 ($10^{-3.5}$ atm) and even farther below those found in many soils, where plant and microbial respiration produces CO_2. The result is that slag leachate not only will continue to absorb and react with CO_2 whenever it contacts the open air in drainpipes or surface slopes, as is well known (*4*), but also will react with CO_2 in soil pores. This property may explain the origin of the case-hardened soils observed at North Point.

Further evidence that precipitation of calcite from carbonate-poor slag leachate requires only addition of CO_2, not heating or evaporation, was provided by a simple experiment conducted in

TABLE 2 Log_{10} of Activity of Chemical Species in Solution and Saturation Indexes of Calcite and Portlandite

	Type of Solution		
Species	H_2O @ Equilibrium With $Ca(OH)_2$, No CO_2, 25° C	Steel Slag Leachate, Ohio, 13° C[a]	H_2O @ Equilibrium With $CaCO_3$ & Air, 25°C
H^+	-12.5	-12.8	-8.4
OH^-	- 1.5	- 1.6	-5.6
Ca^{2+}	- 2.1	- 2.4	-3.7
CO_3^{2-}	(Not present)	- 3.8	-4.7
HCO_3^-	"	- 6.1	-2.9
H_2CO_3	"	-12.5	-5.0
P_{CO2}	"	-11.2	-3.5
S. I.[b] Calcite	"	2.3	0.0
S. I. Portlandite	0.0	- 0.6	-9.7

[a]Concentrations from analysis in Reference (*6*); converted to activities using (*7*)
[b]Positive S.I. indicates supersaturation, negative S.I. indicates undersaturation, zero indicates saturation

the Maryland SHA chemistry laboratory. Pure CO_2 from a pressurized tank was bubbled into a sample of North Point leachate, causing a rapid precipitation of calcite accompanied by a steady decline in pH. This process is in dramatic contrast to carbonate precipitation in most natural environments, which is often triggered by a rise in pH or a loss of CO_2 from solution.

Magnesium was not detected in the North Point leachate, and very low levels of magnesium have also been reported in slag leachate in other areas (*6*). This lack of magnesium is surprising, since magnesium is a major constituent of most slag and is a common cation in natural groundwater. Either magnesium is not dissolving from the slag or it is dissolving and then reprecipitating within the slag layer or somewhere between the slag and the spring. Computer manipulation of leachate analyses suggests that both of these alternatives are plausible. A published analysis of slag leachate from Ohio (*6*), which contained a relatively high level of magnesium (4.4 mg/L) and was otherwise similar to the North Point leachate, was used as input to WATEQ4F. Since no data were available on dissolved silica, various assumed contents of silica were added to the analysis. The results indicated that if the Ohio slag leachate contained as little as 0.01 ppm dissolved silica (a level several orders of magnitude below that found in most natural surface and groundwaters), it would be strongly oversaturated with respect to several high-temperature alkaline-earth (Ca- or Mg-bearing) silicates that have been reported to occur in fresh blast furnace slag or are similar to silicates known to occur in slag (e.g., forsterite, Mg_2SiO_4, and diopside, $CaMgSi_2O_6$). This finding suggests that these minerals, which do weather (albeit slowly) in normally acid natural groundwaters, are unlikely to decompose in the alkaline environment of slag leachate, and it tends to support the conclusion of other reports (*4*) that the solutes in slag leachate are largely derived from other sources, such as free lime (CaO). The WATEQ4F results also indicate that if slag leachate did originally contain even small quantities of dissolved silica and magnesium or acquired them by mixing with natural water, the resulting solution could be supersaturated with respect to several Mg-bearing silicate minerals (talc and sepiolite), which are known to form at relatively low temperatures. Even without dissolved silica, the Ohio leachate is supersaturated with respect to several low-temperature magnesian carbonate and hydroxide minerals, including artinite, $MgCO_3 \cdot Mg(OH)_2 \cdot 3H_20$, and brucite, $Mg(OH)_2$. Formation of brucite at earth-surface conditions is quite plausible. In fact, standard laboratory methods for titration of calcium hardness call for raising the pH to 12 to 13 (the same range observed in some slag leachates) in order to eliminate magnesium interference by precipitating all Mg as $Mg(OH)_2$ (*8*). If the slag leachate contained dissolved aluminum (as the North Point leachate does) in addition to low levels of silica and magnesium, the resulting hypothetical solution would be strongly supersaturated with respect to chlorite, a common product of natural low-temperature weathering of magnesian rocks. Although chlorite and other layer silicates are difficult to synthesize directly from solution at low temperatures, they are readily formed by modification of preexisting clays (*9*).

The above discussion indicates that there are a number of plausible mechanisms that could be expected to scavenge Mg from slag leachate. It also points to the need for research into the mobility and fate of silica, alumina, and other constituents of slag. Although calcitic tufa is the most conspicuous chemical product of steel slag leachate, many other less obvious reactions are possible. For example, the chemical environment in slag leachate is quite similar to that within water-saturated cement paste, which suggests that the alkali-silica reaction could occur (especially when deicing salt is present) or that cementitious minerals could form in or near buried slag. Such reactions could be beneficial or deleterious, depending on site-specific conditions and design goals.

The most important inorganic chemical constituents in the alkaline seepage that cannot be readily explained by leaching of slag are sodium and chloride. These two ions occur in roughly the same 1:1 molar ratio as in common salt (NaCl). Some industrial wastes contain NaCl brine, but a more likely source is highway deicing salt. A rough estimate of the amount of NaCl deposited on I-695 in the probable catchment area of the springs is about 27 000 kg/year. Much of this salt dissolves and infiltrates the embankment. Although not all of it reaches the alkaline springs, enough probably does to account for the roughly 680 kg/year of NaCl discharged to the containment pond.

Ions not directly involved in carbonate equilibria may have significant effects on the precipitation of calcite. If water temperature and concentrations of Ca^{2+} and $(CO_3)^{2-}$ are the same in two solutions but one solution has a higher concentration of other dissolved ions, that solution will be less saturated with respect to calcite because the activity coefficients of Ca^{2+} and $(CO_3)^{2-}$ will be reduced. The most significant of these "passive" ions at North Point and in typical highway underdrain water are Na^+ and Cl^-; since concentration of these ions varies greatly depending on weather conditions and time of year, they may be important influences on seasonal variations in tufa precipitation.

If the flow rate and dissolved solids content (excluding NaCl) of the springs are extrapolated, the embankment is losing roughly 1000 kg of solids in solution every year. The long-term effect of this process on embankment stability is unknown.

The containment pond in which the spring water accumulates often has a peculiar turquoise color. This was a cause of concern, because some heavy metal ions (copper, chromium, and vanadium) can produce blue or green colors in solution. However, these elements are not present in detectable amounts in the pond or spring water. The color is believed to have a benign origin. The water of many natural springs fed by carbonate (limestone or dolomite) aquifers also has a blue or blue-green appearance. There are at least eight springs named Blue Spring in Missouri alone (*10*), and Maryland has the Potomac Blue Spring south of Cumberland. The cause of this color is probably the differential scattering of white light by particles of suspended carbonate minerals less than 1 m in diameter. This "Tyndall scattering" is basically the same mechanism that makes the clear daylight sky appear blue.

Water from the main perennial spring contains two semivolatile organic compounds (29 ppb napthalene and less than 10 ppb methylnapthalene). Furthermore, the strong mothball-like odor of napthalene is evident in some boring samples of the slag bed, and all slag samples tested averaged about 1.5 percent organic matter, which is significantly higher than the results for the nonslag soil samples. The semivolatile polycyclic aromatics detected are coal-tar derivatives, produced when coal is converted to coke, which is then used to fuel the same furnaces that produce slag as a by-product. The prime contractor for the I-695/North Point Boulevard complex is also a major supplier of slag aggregate and has a contract to do hauling at the giant Bethlehem Steel Sparrows Point plant. This coincidence makes it more likely that the contractor emplaced within the embankment slag contaminated by coal-tar sludge and possibly other industrial wastes from Sparrows Point.

REMEDIATION

Capping the spring is not a valid solution. Even if the conspicuous perennial discharges could be sealed, the groundwater would simply back up until new outlets were established; the effect would be cosmetic at best. Furthermore, it is undesirable to impede drainage in an embankment, because this could increase pore pressures to the point that slope failure occurs.

Removing the slag would entail excavating hundreds of lane-feet of pavement and thousands of cubic yards of overburden, as well as the slag itself, which might then have to be disposed of as a hazardous waste. The monetary and other cost (traffic disruption, etc.) of rebuilding the embankment would be out of proportion to any benefit to be obtained.

Various techniques for encapsulating or isolating buried wastes to prevent interaction with groundwater are possible (e.g., slurry walls, grout injection). However, the volume and areal extent of the slag would make this strategy expensive, and introducing impermeable materials into an embankment would produce complex and probably adverse affects on groundwater drainage.

Reducing leachate generation by minimizing infiltration into the top of the embankment offers a reasonable first solution, and one that could be pursued incrementally. Relatively inexpensive measures include repairing distressed ditch pavement, paving ditches, and installing rebuts to catch pavement runoff before it can flow onto grassy surfaces and infiltrate. As an extreme measure, the entire top of the embankment could be capped with impermeable material. However, since drainage control could not guarantee a total absence of spring flow, management chose to have the leachate treated and discharged. A pilot study indicated that bubbling CO_2 gas through the leachate rapidly reduced the pH to nonhazardous levels, but this technique was never employed on a full-scale basis because of concern about the large quantities of calcite sludge that it would have generated. Instead, a temporary treatment plant housed in a truck trailer used HCl to neutralize the leachate. Continuing problems with vandalism and corrosion of the trailer by HCl fumes caused a return to pump-and-haul disposal while a permanent treatment plant, also using HCl, was constructed. Doubts remain about the suitability of a system that will require repeated skilled maintenance and monitoring and that involves leaving a hazardous acid substance in a vandal-prone unmanned structure.

CONCLUSIONS

Slag leachate acquires its high pH and calcium content through hydrolysis of a man-made metastable compound (quicklime) in a microenvironment largely closed to CO_2. Once it moves out of this environment and becomes subject to buffering by atmospheric CO_2, it dissolves CO_2, precipitates calcite, and exhibits a decline in pH. This process could be accelerated by bubbling CO_2 or air through the leachate.

On the basis of the contractor's account of its provenance, the slag may have experienced decades of exposure before emplacement in the I-695 embankment, which is itself over 20 years old. This suggests that aging or weathering of some slags does not guarantee their inability to generate troublesome leachate.

Conspicuous tufa is not the only form of calcite precipitated from slag leachate. Cemented soils also form, affecting drainage and vegetation of the subgrade. Precipitation of other minerals, including carbonates, hydroxides, and silicates, is thermodynamically favorable.

The caustic seepage from the I-695 embankment teaches an expensive lesson; costs of remediation had reached $1,000,000 by early 1994. Whatever the original motive for its use, slag has certainly not turned out to be cost-effective in this instance. Highway agencies are coming under increasing pressure to use industrial wastes in construction. Some of these materials are attractive from the standpoint of initial cost, performance specifications, and availability, but they may involve risks that must be carefully studied before these materials are accepted. More research needs to be done on the mobility and fate of weathering products and leachate constituents before industrial waste products are widely dispersed into the environment in the name of recycling.

REFERENCES

1. *Slag and Its Relation to the Corrosion Characteristics of Ferrous Metals.* Bulletin MF 172-13. National Slag Association, Alexandria, Va., undated.
2. Philipp, J. A., R. Endell, J. Raquin, and O. Dechelette. Leaching Test Characterization of Iron and Steel Industry Waste. In *Hazardous and Industrial Solid Waste Testing and Disposal* (D. Lorenzen and others, eds.), Special Technical Publication 933, ASTM, Philadelphia, Pa., 1986, Vol. 6, pp. 7–27.
3. Sundaresan, B. B., P. V. R. Subrahmanyam, and A. D. Bhide. The Hazardous Waste Scene in India. In *Hazardous and Industrial Waste Management and Testing: Third Symposium* (L. Jackson, A. Rohlik, and R. Conway, eds.), Special Technical Publication 851, ASTM, Philadelphia, Pa., 1984, pp. 291–304.
4. Hurd, J. O. Effect of Slag Type on Tufa Precipitate Formation. In *Transportation Research Record 1192*, TRB, National Research Council, Washington, D.C., pp. 79–84.
5. *Granulated Blast Furnace Slag.* The Standard Slag Company, Youngstown, Ohio, undated.
6. Feldman, R. M. *Tufa Precipitation and Its Effect on Drainage of Highway Pavement.* Report FHWA/0H-81/010. Kent State University, Kent, Ohio, 1981.
7. Ball, J. W., and D. K. Nordstrom. *User's Manual for WATEQ4F, with Revised Thermodynamic Data Base and Test Cases for Calculating Speciation of Major, Trace, and Redox Elements in Natural Waters.* U.S. Geological Survey Open-File Report 91-183. Menlo Park, Calif., 1991, 189 pp.
8. *Water Analysis Handbook,* 2nd ed. Hach Company, Loveland, Colo., 1992.
9. Jones, B. F. Clay Mineral Diagenesis in Lacustrine Sediments. In *Studies in Diagenesis* (F. A. Mumpton, ed.), U.S. Geological Survey Bulletin 1578, 1986.
10. Vineyard, J. D., and G. L. Feder. *Springs of Missouri.* Missouri Department of Natural Resources, 1982, 212 pp.

Publication of this paper sponsored by Committee on Subsurface Drainage.

Characterization of Base and Subbase Iron and Steel Slag Aggregates Causing Deposition of Calcareous Tufa in Drains

JIWAN D. GUPTA, WILLIAM A. KNELLER, RANGAMANNAR TAMIRISA, AND EWA SKRZYPCZAK-JANKUN

Tufaceouslike materials are observed clogging pavement drains along highways in northeastern Ohio. These materials have also been found in catch basins and spillways. Previous studies suggest that the original free lime (CaO) in slags used as subbase materials is responsible for the deposition of the tufa. To characterize these slags, X-ray diffraction, energy dispersive X-ray, surface area measurements, CaO solubility in anhydrous ethylene glycol ("sugar test"), and other physicochemical tests were conducted on air-cooled blast furnace (ACBF), open-hearth (OH), and basic oxygen furnace (BOF) slags. ACBF iron slag is composed of crystalline akermanite ($Ca_2MgSi_2O_7$). Results of the sugar test indicate that this slag does not contain any residual or easily available free lime. The ACBF sample exhibited the lowest surface area and therefore is the least reactive with CO_2-charged waters. The OH and BOF slags, however, exhibit the presence of CaO or its weathering equivalents such as $Ca(OH)_2$ and $CaCO_3$. All these steel slags exhibit a high tufa-generating potential. Analysis of the physicochemical tests of these steel slags indicates that they are composed mainly of β-dicalcium silicate (larnite), calcium ferrites, wüstite (FeO), free lime (CaO), periclase (MgO), portlandite [$Ca(OH)_2$], and calcite ($CaCO_3$). These slags also exhibit high surface areas and are more reactive with CO_2-charged waters. Most highway departments require that steel slags be aged or cured for at least 6 months before they are used. Sugar tests conducted on samples obtained from different horizontal depths (up to 10 ft) in a stockpile showed that the CaO (free lime) content increases with increasing depth into the stockpile. Evidently some of the free lime is encapsulated by insoluble silicates or is in occluded pores and has not come in contact with CO_2-charged porewater. Therefore, aging of slags by exposure to weathering does not necessarily decrease the free lime content enough to prevent the formation of tufa. It is concluded that the presence of CaO, MgO, $Ca(OH)_2$, and $CaCO_3$ in slags is critical in determining their tufa potential for use as base and subbase aggregates.

Iron and steel slags have been used as base and subbase aggregates in several northeastern Ohio pavement construction projects. Along these highways, tufaceouslike materials have been observed clogging many subdrains (*1*). These materials have also been found in catch basins and spillways. Some of the drain outlets have been observed completely clogged with tufa, creating water retention and soft-pavement conditions. Furthermore, frost action on the retained water results in severe distresses that also cause premature failure of the pavement. Tufa deposition in these pavement structures, therefore, leads to early pavement deterioration and costly maintenance.

J. D. Gupta and R. Tamirisa, Department of Civil Engineering, University of Toledo, Ohio 43606–3390. W. A. Kneller, Department of Geology, University of Toledo, Ohio 43606–3390. E. Skrzypczak-Jankun, Department of Chemistry, University of Toledo, Ohio 43606-3390.

The main component of tufaceous precipitates is calcium carbonate. It is termed *tufa* because it is similar to deposits that occur in natural systems. Bates and Jackson (*2*) define tufa as a natural chemical sedimentary rock composed of calcium carbonate formed as precipitate by the evaporation of natural water rich in dissolved calcium carbonate. Research studies (*3,4*) have suggested that free lime (CaO) in these slags is responsible for producing tufa.

FORMATION OF TUFA

The chemical reactions between free lime and rainwater occur under the pavement surface. The free lime reacts with rainwater and forms calcium hydroxide $Ca(OH)_2$ in pavement drains. The formation of tufa from free lime is explained by the following chemical reaction:

$$CaO + H_2O = Ca(OH)_2 \quad (1)$$

The calcium hydroxide solution in the drain water produces pH values of more than 11.0. Also, high concentrations of carbon dioxide from the atmosphere and automobile exhaust react with rainwater forming carbonic acid (H_2CO_3):

$$CO_2 + H_2O \leftrightarrow H_2CO_3 \quad (2)$$

The carbonic acid reacts with calcium hydroxide forming calcium bicarbonate [$Ca(HCO_3)_2$], which is more soluble in water than $CaCO_3$.

$$2H_2CO_3 + Ca(OH)_2 \leftrightarrow Ca(HCO_3)_2 + 2H_2O \quad (3)$$

At the orifices of drains and in catch basins, the water from this enriched solution of calcium bicarbonate evaporates because of warm temperatures, and the carbon dioxide escapes into the atmosphere. This condition leads to the precipitation of calcium carbonate and the formation of tufa:

$$Ca(HCO_3)_2 \leftrightarrow CaCO_3 (\downarrow) + H_2O (\uparrow) + CO_2 (\uparrow) \quad (4)$$

Warm temperatures lead to increased rates of deposition of tufa, whereas at cold temperatures the CO_2 remains in solution and favors dissolution. These conditions lead to increased tufa precipitation during the summer months and less precipitation during

the winter months. These chemical reactions clearly indicate that the concentration of free lime, water, carbon dioxide, temperature, and humidity are the main elements that control the precipitation of tufaceous deposits in drains and catchment basins of highways.

SCOPE OF PAPER

The objective of this research is to study the physicochemical properties of tufa and iron and steel slags. In pursuit of this objective, various laboratory experiments were conducted to determine the tufa-producing potential of the slags. The tufa and slag samples are described in this paper, as well as the laboratory experiments. Research findings and conclusions are presented with regard to the potential use of steel slags.

TUFA AND SLAG SAMPLES

Tufa Samples

A field trip was arranged through Ohio Department of Transportation (ODOT) to collect tufa samples from different locations in which slags were used as subbase aggregates. Five tufa samples were obtained from different locations in Cuyahoga County where pavement subdrains were clogged by tufa. Site investigation revealed that different types of slag had been used as the subbase aggregate at each site. At these sites, tufa was observed to be clogging drains 5 to 6 years after the original emplacement of the pavement.

Slag Samples

Eight 80- to 100-lb slag samples were provided by ODOT. These samples consisted of one aged air-cooled blast furnace (ACBF) slag, three aged open-hearth (OH) slags, and four basic oxygen furnace (BOF) slags (two aged and two unaged). The aged samples were from the stockpiles exposed to the atmosphere for more than 6 months. The actual period of aging, however, was not known. The unaged samples were from either fresh stockpiles or stockpiles stored for less than 3 months.

LABORATORY STUDIES

Chemical and X-ray Diffraction Analyses of Tufa Samples

Pure tufa contains only calcium carbonate, but the tufa samples obtained from the field contained some impurities such as organic matter, quartz, and elements leached out from the slag aggregate. The chemical analysis included the removal of organic materials by hydrogen peroxide (30 percent) oxidation, determination of the percent insoluble residue (ISR), calcium carbonate, R_2O_3 (oxides of Al, Fe, Mn, and P), and loss on ignition (LOI).

Table 1 shows the results of the chemical analysis on these tufa samples, including the organic matter content, which varies from 0.67 to 1.06 percent; the R_2O_3 content, which varies from 4.0 to 14.0 percent; and the LOI, which varies from 35 to 42 percent. These LOI values mostly correspond to the loss of carbon dioxide on heating the tufa. In Sample 1 the calcium carbonate content is 84.75 percent and the corresponding LOI is 37.30 percent as compared with 44 percent for pure calcium carbonate. The same is true for all other tufa samples. The main component in all tufa samples therefore is calcium carbonate regardless of the steel slag used as a base or subbase material. Insoluble residue values varied from 0.53 to 8.24 percent. These are due mainly to the insoluble impurities such as quartz or possibly clays. X-ray diffraction of the tufa samples verified the results of the chemical analysis. Figure 1 shows the X-ray diffractograms of the tufa samples. These diffractograms show that the tufa markedly consists of calcite ($CaCO_3$), quartz (SiO_2), and minor amounts of dolomite [$(Ca,Mg)(CO_3)_2$]. The dolomite most likely is a contaminant derived from the dolomitic aggregate in the concrete.

Oxide Analysis of Slags

The oxide analysis provided the percentage of the elements as oxides present in the slag samples. This analysis was done in accordance with ASTM E886-88, a procedure to identify elements such as aluminum, calcium, iron, magnesium, phosphorus, potassium, silicon, sodium, and sulfur by X-ray fluorescence (XRF) methods. ASTM procedures E790 and C114-16.2 were used also to identify the moisture content and LOI, respectively.

Table 2 shows the results of oxide analysis of the slag samples. The dominant element in the slags as an oxide is calcium. The next two most abundant oxides are those of silicon and iron. Oxides of calcium in the OH slags vary from 34 to 41 percent,

TABLE 1 Chemical Analysis of Tufa Samples (Values in Percentages)

Sample Number	Organic Matter	ISR[a]	R_2O_3[b]	$CaCO_3$[c]	Total Percent	LOI[d]
1	0.91	8.24	6.10	84.75	100	37.30
2	0.86	3.50	9.60	86.04	100	36.67
3	0.67	0.53	4.23	94.57	100	41.67
4	0.76	5.40	13.37	80.47	100	35.47
5	1.06	0.55	4.80	93.59	100	41.37

a - Insoluble Residue
b - Could be Fe, Al, Mg, P, or Mn
c - Calcium Carbonate
d - Loss On Ignition

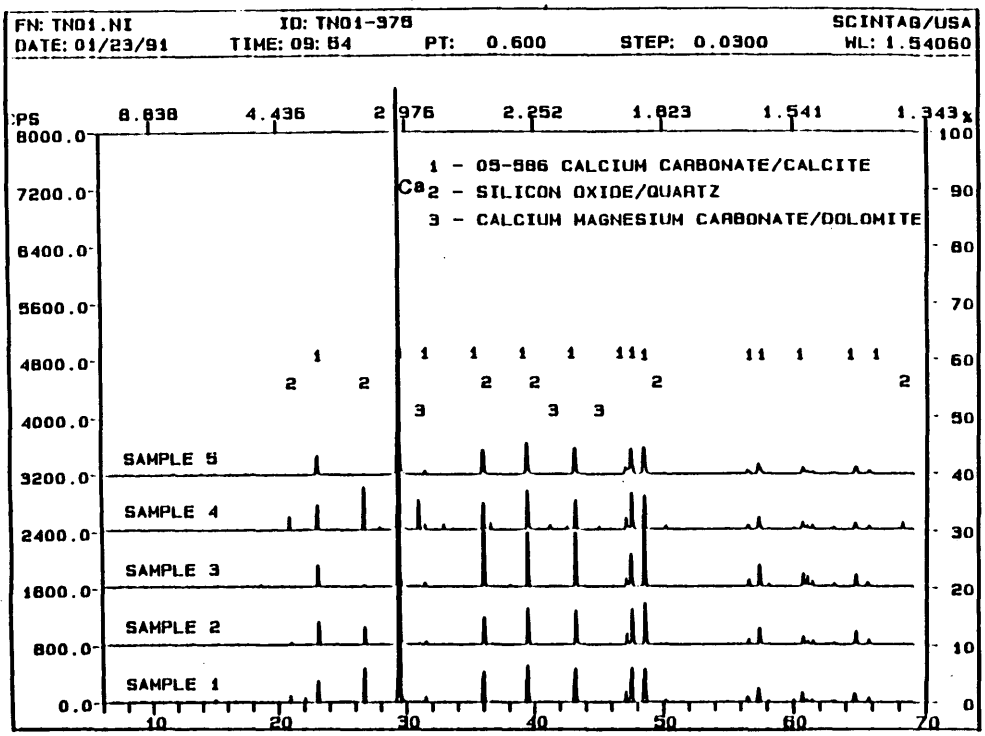

FIGURE 1 X-ray diffractograms of tufa Samples 1 to 5.

whereas in the BOF slags, it varies from 35 to 51 percent. The ACBF slag contains about 40 percent oxides of calcium and has the highest silica content (38 percent), whereas the silica content in other slags varies from 15 to 25 percent. Furthermore, the ACBF slag has the highest content of aluminum and magnesium and the least percentage of oxides of iron as compared with other slags. Table 2 shows that the ACBF slag does not contain any measurable LOI, which indicates that no carbonates are present. The OH and BOF slags contain aluminum (3 to 4.5 percent), iron (15 to 25 percent), magnesium (5 to 9.5 percent), and manganese (2 to 5 percent). These slags contain carbonates, as indicated by their LOIs, which range from 1.5 to 10.5 percent. All slag samples contain minor amounts of oxides of phosphorus, potassium, sulfur, and sodium and contain trace amounts of oxides of strontium, barium, chromium, and vanadium.

The data in Table 2 help to identify various chemical and mineral phases present in the slags during the X-ray analysis. It is noteworthy that the calcium oxide content shown in Table 2 is the total possible calcium oxide inclusive of any free lime in the slags.

X-Ray Diffraction Analysis

X-ray powder diffraction analysis determined the gross mineralogy of the slags. Oven-dried slag samples (between −275 and +325 sieve size) were used in the X-ray diffraction analyses. All powder diffraction data were accrued using SCINTAG Powder Diffractometer XDS2000, with a Cu tube operated at 45 kV and 40 mA. A high-purity solid-state germanium (HPGE) detector cooled by liquid nitrogen was also used. The SCINTAG software package (DMS 2000 version 1.88 with JCPDS data base version .40) was employed for all calculations carried out on a Micro Vax 3100 computer. The diffraction patterns for all samples were recorded by continuous scan at a scanning speed of 3 degrees/min

TABLE 2 Oxide Analysis of Slag Samples

Sample #	Slag Type	Oxides												
		Al_2O_3	Cao	Fe_2O_3	MgO	MnO	P_2O_5	K_2O	SiO_2	Na_2O	SO_2	Moisture	LOI	Oth[a]
1	ACBF	8.52	40.09	0.85	10.80	0.71	0.02	0.24	38.09	0.23	0.24	0.04	-	0.2
2	OH	3.50	36.02	26.57	9.84	3.31	0.26	0.01	15.19	0.06	1.70	0.42	3.1	-
3	OH	3.57	40.76	23.81	7.81	5.26	0.10	0.01	13.73	0.01	0.01	0.78	1.5	1.1
4	OH	4.66	34.02	15.41	5.04	3.39	0.10	0.17	26.06	0.08	0.01	0.57	10.5	-
5	BOF	3.75	35.27	24.08	10.52	2.81	0.29	0.01	12.77	0.08	0.01	3.08	5.5	1.8
6	BOF	4.46	38.49	26.33	8.35	4.48	0.13	0.01	12.41	0.07	0.01	0.61	2.1	2.5
7	BOF	2.97	48.02	15.05	9.67	3.12	0.22	0.01	13.21	0.01	0.01	1.65	6.1	-
8	BOF	3.01	50.81	15.62	5.32	3.56	0.30	0.01	15.04	0.01	0.04	2.88	3.4	-

a Oth - Others commonly include SrO, BaO, TiO_2, Cr_2O_3, and V_2O_5

with a "step size" of 0.03 degree/min. Search-and-match routines were used against the JCPDS data base for the identification of the resulting peaks. The search was limited to the elements H, Na, K, Mg, Ca, Al, Fe, C, Si, P, N, S, O, and Cl. The peaks below 5 percent of relative intensity were not taken into account for the preliminary search. The solution was accepted if it fell into the error window of 0.3 percent of a given d-spacing. Because the samples were weathered, many secondary minerals can occur concommittantly with the primary slag minerals. This condition creates a sample composed of multiphases and produces overlapping peaks on the diffractograms. Therefore, some of the mineral species in Table 3 may be spurious. To decrease this spurious tendency, the minerals in Table 3 were verified by petrographic analysis using a polarizing light microscope in both the transmission and reflection modes. Those minerals that were verified by petrographic polarizing microscope are indicated by a footnote in Table 3. In addition, those minerals in Table 3 that are not footnoted have been known to occur in slags.

X-ray diffractograms of ACBF slag (Figure 2) show that akermanite and an unnamed mineral (Fe-Mg-Al-SiO) occur as the major phases. Other compounds such as rhodochrosite, mackinawite, iron calcium sulfide carbonate hydrate, and an unnamed mineral are present as minor or trace phases. Some of these phases may be artifacts induced by overlapping. Figure 3 shows the X-ray diffractograms for three OH slag samples. In all the samples, silica, mayenite, augite, hematite, magnesite, and gehlenite are present as major phases. Other compounds and minerals are present in trace amounts.

Figure 4 shows the X-ray diffractograms of the BOF slag samples. Comparison of all the BOF slag samples indicates that Samples 5 and 6 contain silica, grossular, magnesium calcium carbonates, calcium iron oxide (ferrite), and portlandite $Ca(OH)_2$, whereas slag Samples 7 and 8 contain larnite (β-Ca_2SiO_4), portlandite [$Ca(OH)_2$], wüstite (FeO), and clinoferrosilite ($FeSiO_3$) as major phases. Other possible compounds in the BOF slags occur as minor phases: iron oxides, ferrites, phosphates, silicates, and sulfides.

Various mineralogical phases are identified by a computer search match for the slag samples. Approximately 50 different species were identified by the computer search match in all the samples. The 50 mineral species are grouped into 6 major mineral types (see Table 3): silicates, oxides and hydroxides, carbonates, phosphates, sulfides, and chlorides. These species are further identified according to their relative abundances as A for presence in abundance, P for present but in less quantity, M for presence in minor quantity, and T for presence as a trace.

The most important mineralogical phases for this research study are the presence of calcite ($CaCO_3$), perclase (MgO), or portlandite [$Ca(OH)_2$] in the slag samples because they can increase the tufa precipitate potential. In OH slag Sample 2, both calcite and portlandite occur, whereas OH slag Sample 4 contains only calcite. The OH samples have been exposed to weathering for as long as 80 years and at least for 15 years. The latter estimate of exposure is based on the fact that 1978 was the last year that OH slag was generated. Apparently all the CaO and $Ca(OH)_2$ in Sample 4 has been totally carbonated. The BOF slag Samples 5, 7, and 8 contain both portlandite and calcite except for Sample 6, which contains only calcite. Again this depends on the degree of exposure to the atmosphere. Thus the OH and BOF slags exhibit a higher potential for producing tufa. The time required and the volume of tufa precipitate may vary among slag types depending on many factors: reactivity of slags, surface area, particle size, pore size distribution, amount of water, absorption, and so on.

ACBF slag does not contain either calcite or portlandite. It consists mainly of calcium magnesium aluminum iron silicates. In the past, ACBF slags have exhibited the most inertness of all aggregates and therefore should not produce any tufa. This statement is reinforced strongly by the absence of mineral species responsible for tufa precipitation.

Surface Area Measurements

The surface area of a material controls the rate of chemical reaction between solids and gases or liquids. The surface area measurements of the slag samples were conducted to differentiate the relative reactivity of these slags. From knowledge of the surface area measurements and mass percentage of the total reactive free lime in the slag, it is possible to predict their tufa potential properties.

Surface area (SA) measurements using slags sized between -275 and $+325$ mesh were made on a micromeritics Gemini 2360 Analyzer, which is fast and simple to operate. The units of measurement are named after the authors who developed the procedures and formulas to calculate SA measurements of solids. The Brunauer, Emmett, and Teller (BET) method calculates multipoint and single-point SAs, whereas the Langmuir method calculates multipoint SAs. Software coupled with the Gemini unit automatically generates reports and calculates the following: single-point BET SA, multipoint BET SA, multipoint Langmuir SA, and total pore volume. In addition, this instrument can report up to 1,000 discrete point adsorption isotherms. As many as 50 data points can be reported in the BET range and can be plotted on an X-Y recorder.

Gemini uses a flowing gas in which the analysis gas (N_2) flows simultaneously into both the sample and balance tubes. The only difference between the two tubes is the presence of the sample in one of them. The delivery rate of the gas into the sample is controlled by the rate at which the sample can adsorb the gas onto the surface; the rate of flow into the balance tube is controlled to yield the same pressure. As the sample adsorbs the gas, the pressure tends to drop in the sample tube. A rapid servo-device continuously restores the pressure balance between the tubes by admitting more gas into the sample side. The result is that the unit maintains constant pressure over the sample while varying the rate of gas delivery to match the sample adsorption rate. Surface areas as low as 0.01 m_2/g are easily determined with excellent precision using N_2 gas as the adsorbate. Software accrues the data and calculates the SA according to the various methods mentioned above.

Table 4 gives the SA measurements for the slag samples. A comparison of the SAs among slags shows that OH slag Sample 3 has a larger SA than OH Samples 2 and 4. BOF slag Sample 7 has a larger SA as compared with Samples 5, 6, and 8. BOF slag Samples 5 and 8 have approximately same SA. BOF slag Sample 6 has the least SA and thus should produce less tufa as compared with the other BOF slags. This conclusion is drawn on the hypothesis that larger SAs will lead to a more rapid reaction. However, other factors, which include pore size distribution, effective porosity, degree of weathering, and total reactive free lime present in these aggregates, need to be considered to reach an accurate conclusion.

TABLE 3 Results of X-Ray Diffraction Studies

Mineral Type	Sample Number							
	1	2	3	4	5	6	7	8
Silicates								
Larnite (B Ca_2SiO_4)[a]			P		A	A	A	A
Akermanite ($Ca_2MgSi_2O_7$)[a]	A							
Hydro-Grossular ($Ca_3Al_2(SiO_4,CO_3(OH)_3$)	P				P	P		
Glaucochroite ($(Ca,Mn)_2SiO_4$)					T	T		
Wadsleyite ($(Mg,Fe)_2Sio_4$)[a]						P		
Clinoferrosilite ($FeSiO_3$)[a]							P	P
Fayalite ($(Fe,Mg)_2SiO_4$)[a]							P	P
Nagelschmidite ($2Ca_2Sio_4.Ca_3(PO_4)_2$)[a]								P
Pyroxene (Aluminium Augite) $(Ca(Fe,Al,Mg)SiO_4)$			A					
Gehlenite ($(Ca_2Sl)Al,SiO_4$)[a]				A				
Unnamed (Fe-Mg-Al-SiO)	P		P					
Xonolite ($Ca_6Si_6O_7O_{17}(OH)_2$)				T				
Goosecreekite ($CaAl_2SiO_6.5H_2O$)						P		
Calcio-Olivine (G Ca_2SiO_4)[a]								M
Oxides and Hydroxides								
Periclase (MgO)[a]		P			P		P	
Wustite (FeO)[a]			P				P	
Hematite (Fe_2O_3)[a]		M	M					
Magnetite (Fe_3O_4)				T				T
Hausmanite ($(Mn,Mg)(Mn,Fe)_2O_4$)		T		T		M		
Portlandite ($Ca(OH)_2$)[a]		P	P	P	P	P	P	
Vernadite (Mn(OH))					T			
Pyrochroite ($Mn(OH)_2$)					T			
Srebrodolskite ($Ca_2Fe_2O_5$)[a]					A	A	A	A
Magnesioferrite ($MgFe_2O_4$)				T	T			P
Spinel ($MgAl_2O_4$)					T	P	M	
Mayenite ($Ca_{12}Al_{14}O_{33}$)		A	A					
Quartz (SiO_2)		T	M	M			M	
Moganite (SiO_2)								
Cristobilite (SiO_2)				T				
Carbonates								
Calcite ($CaCO_3$)[a]		P		P	P		P	P
Magnesite ($MgCO_3$)					P			
Ferromagnesite ($(Mg,Fe)CO_3$)		M						
Dolomite ($CaMg(CO_3)_2$)			M			T		
Ferroan Dolomite $(Ca(Mg_{0.67},Fe_{0.33})(CO_3)_2)$						T		
Ankerite ($Ca(Fe,Mg)(CO_3)_2$)						T		
Rhodochrosite ($MnCO_3$)	T							
Phosphates								
Nagelschmidite ($2Ca_2SiO_4.Ca_3(PO_4)_2$)[a]								P
Berlinite ($AlPO_4$)					P			
Sulfides								
Albandite (MnS)						T		
Hauerite (MnS_2)			T					
Pyrite (FeS_2)						T	M	
Marcasite (FeS_2)[a]							M	
Mackinawite ($(Fe,Ni)_9S_8$)		T						
Niningerite (MgS)			T					
Chlorides								
Halite (NaCl)[b]				T				

A - Abundant, P - Partial, M - Minor, T - Traces

a - Presence verified by the petrographic polarizing microscope both in the transmission and the reflection modes.

b - Verified by energy dispersions X-ray analyses (EDS) and X-ray diffraction of the laboratory (leachate) produced tufa.

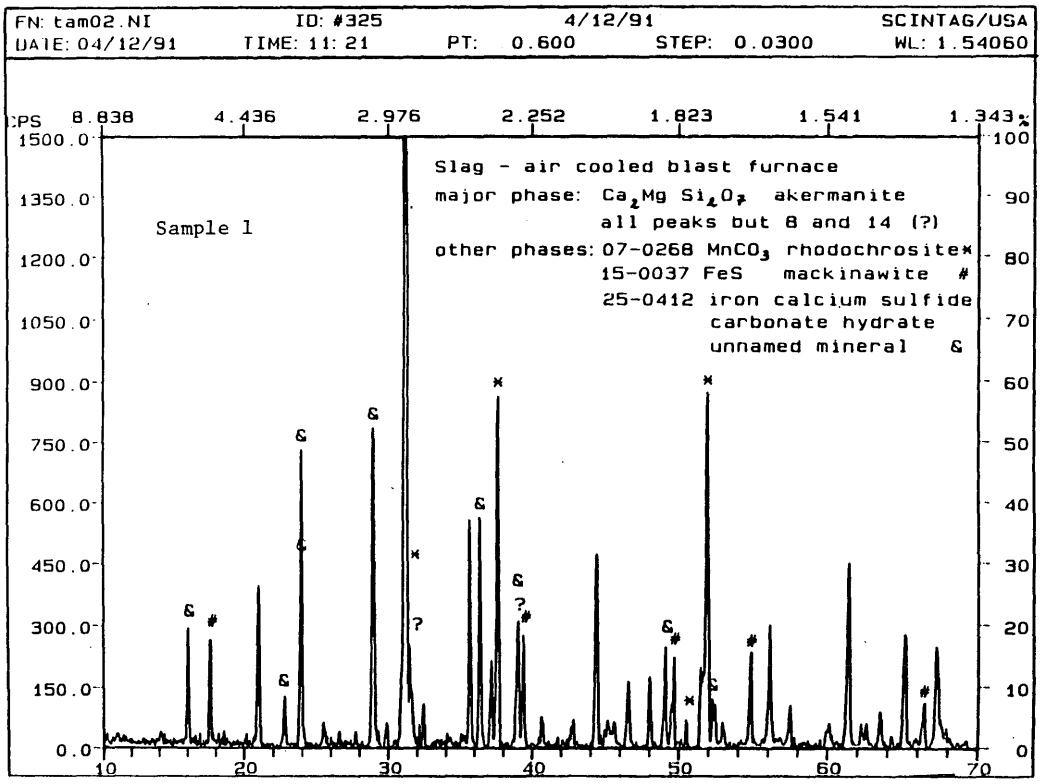

FIGURE 2 X-ray diffractogram of ACBF slag.

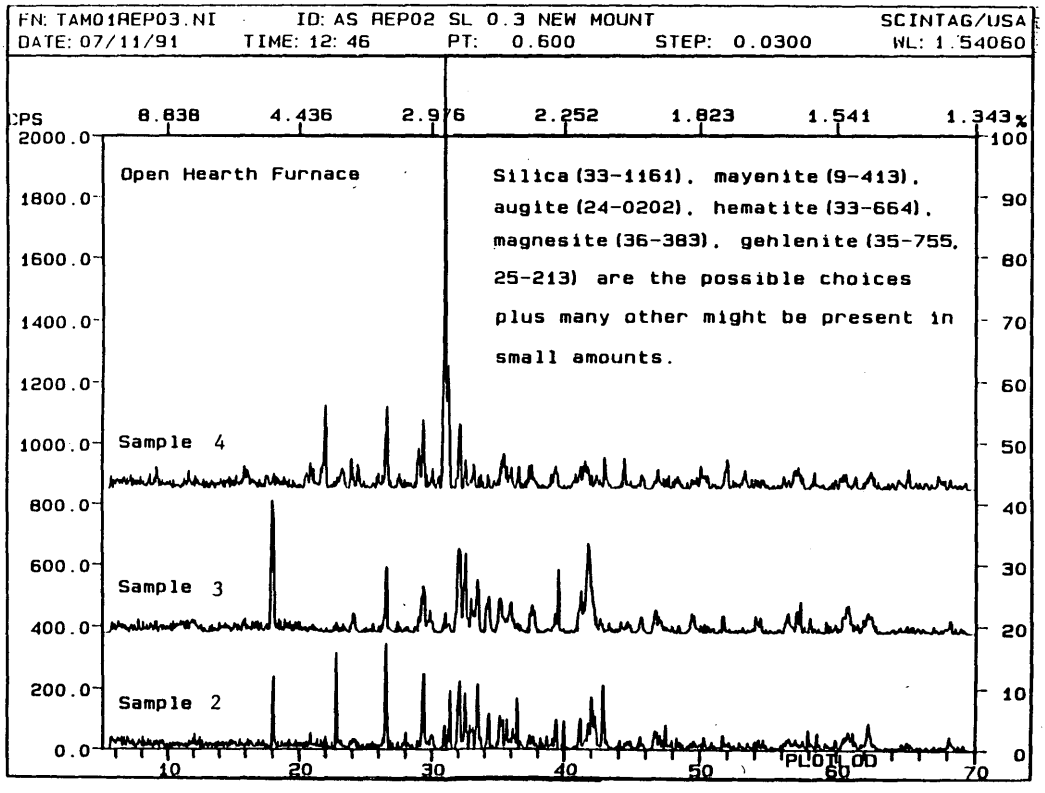

FIGURE 3 X-ray diffractograms of OH slag.

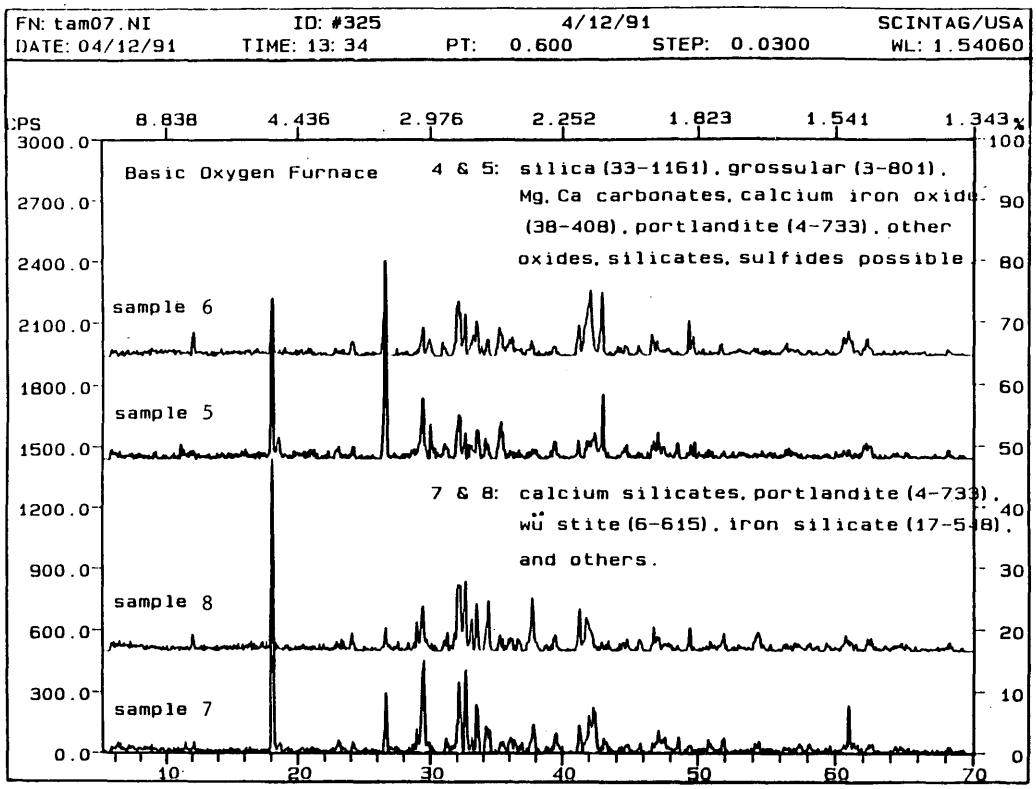

FIGURE 4 X-ray diffractograms of BOF slag.

Leachate Analysis

In a leaching process, liquid passes through solids, where some of their contents are dissolved, and appears over the surface or outlet. When porewater passes through the slags containing free lime (CaO), a chemical reaction takes place forming calcium hydroxide and eventually calcium carbonate.

A special apparatus was designed for the leachate study. Thirty cylinders 12 in. high and 6 in. in diameter with an outlet facility at the bottom to draw water for analysis were made for this study. For each leachate experiment, 3000 g of deionized water was added to 6000 g of slag in the cylinder. The pH and conductance of deionized water were recorded before adding it to the sample. The sample was kept undisturbed for 24 hr to permit the chemical reactions to occur. The pH of the leachate increased to more than 10.0 within 24 hr. Initially, the pH values increased approximately to 12 with time but after 10 days, pH values stabilized for all samples.

At the end of the fourteenth day, the leachate from each sample was collected in a beaker and filtered for the insoluble matter. The filtrate was kept in the oven until the water evaporated; no precipitate was recovered from the beaker. This result indicates that deionized water alone does not produce tufa from the slag.

TABLE 4 Surface Area Measurements for Slag Samples

Sample Number	Slag Type	Surface Area M^2/Gm		
		BET/MP/SA[a]	BET/SP/SA[b]	LANGMUIR/SA[c]
1	ACBF	4.64	4.41	6.81
2	OH	3.05	2.84	4.54
3	OH	21.15	20.59	33.14
4	OH	14.61	23.84	22.78
5	BOF - Aged	11.20	10.88	17.69
6	BOF - Unaged	3.67	3.53	5.85
7	BOF - Aged	17.96	17.62	27.90
8	BOF - Unaged	11.44	11.00	16.63

a - BET/MP/SA - Brunauer, Emmett, and Teller Multi Point Surface Area
b - BET/SP/SA - Brunauer, Emmett, and Teller Single Point Surface Area
c - LANGMUIR/SA - Langmuir Multi Point Surface Area

Another set of experiments was conducted by passing carbon dioxide through the samples to accelerate tufa precipitation. The pH and conductance were recorded after the CO_2-charged deionized water was added to the sample. Carbon dioxide at a rate of flow less than 0.2 ft^3/hr was passed through the sample. The pH of the leachate was monitored constantly, and the carbon dioxide was passed until the pH of the leachate reached the pH of the deionized water. All the leachate water from the apparatus was drained out and collected in a beaker. After filtration, the filtrate was kept in the oven until the water evaporated; this time some residue was observed in the beaker. The residue was collected from the beaker for X-ray analysis. The diffractograms of the residue indicate that the composition was similar to tufa. This initial experiment was conducted for OH slag Sample 2 and BOF slag Sample 8 as a precursory effort to show that tufa is produced by CO_2-charged waters.

X-ray diffraction analyses of all the leachate samples recorded as major phases the presence of calcite ($CaCO_3$), aragonite ($CaCO_3$), and halite (NaCl). In addition, one sample (OH-10) recorded the presence of bassanite, ($CaSO_4 \cdot {}^1/_2\ H_2O$) and two other samples (OH-3 and BOF-4) recorded the presence of magnesium carbonate hydroxide hydrate [$Mg_5(CO_3)_4(OH)_2 \cdot 4H_2O$].

Anhydrous Ethylene Glycol (Sugar Test)

Warm ethylene glycol (at 60°C to 70°C) has the property of dissolving only free lime (CaO). This property was used to determine the free lime present in the slag by titrating with 0.05 *N* HCl and with phenolphthalein as an indicator.

The results of the sugar test as percentages of free lime in the slag are as follows:

Sample	*Aggregate*	*Percent Free Lime*
1	ACBF slag	None
2	OH slag	0.237
3	OH slag	0.131
4	OH slag	0.044
5	BOF slag, aged	0.604
6	BOF slag, unaged	1.051
7	BOF slag, aged	0.691
8	BOF slag, unaged	10.64

Note that the ACBF slag possesses no free lime and therefore should not produce any tufa. The OH and BOF slags have some free lime content, and the unaged BOF slags possess more free lime than those that are aged.

A comparison of aged slag samples with the unaged slag samples indicates that the aging of slag has not helped sufficiently to reduce the free lime content because in the steel slags the residual free lime (CaO) is encapsulated by silicates. This encapsulation protects the CaO from hydration and the effect of CO_2-charged porewater.

Variation of Free Lime Content with Stockpile Depth

ODOT requires slags to be aged for 6 months before they are used as subbase aggregates. Because stockpile aging does not necessarily remove all the free lime content of the slag, slag samples from different depths (0 to 7 ft at 1-ft intervals) in a stockpile were collected by a backhoe and analyzed for their free lime content by using the sugar test. The results of the analysis are as follows:

Depth (ft)	*Percent Free Lime*
0	0.096
1	0.185
2	0.265
3	0.335
4	0.388
5	0.401
6	0.451
7	0.579

The results indicate that the percent of free lime in the slag increases with an increase in the stockpile depth. Further analysis of the tufa produced in the laboratory from aged and unaged slag samples also confirms that aging does not totally eliminate the precipitation of tufa.

FINDINGS AND CONCLUSIONS

Findings

X-ray diffraction analyses determined that the slags are composed of complex aluminosilicates, ferrites, carbonates, and oxides of calcium, magnesium, and minor amounts of sulfides. The ACBF slag was found to be inert because no free lime (CaO) was found by the sugar test and the X-ray analysis did not show the presence of portlandite or calcite. Furthermore, this ACBF slag has a low SA and is primarily composed of crystalline calcium magnesium silicate (akermanite) as indicated by X-ray analysis.

The OH slags contain larnite (β-Ca_2SiO_4). The X-ray analysis also indicated the presence of calcite and portlandite. In addition, free lime was found in these samples by the sugar test. OH slag Samples 3 and 4 show more SA and should be more reactive than OH slag Sample 2, which has a lower SA; however, the high free lime content in OH slag Sample 2 gives it a high potential for tufa formation.

Both aged and unaged BOF slags contain free lime (CaO), portlandite [$Ca(OH)_2$], and calcite ($CaCO_3$). However, the aged samples have more $CaCO_3$ because of weathering and less free lime than the unaged samples. All OH and BOF samples produced tufa in the laboratory. High SAs in connection with the free lime, $Ca(OH)_2$, and $CaCO_3$ content in all these samples should result in the formation of tufa.

The free lime content is not totally removed by stockpile aging and increases with stockpile depth as indicated by the sugar test. This is also confirmed through the tufa produced in the laboratory from aged and unaged slag samples. The amount of tufa precipitated by the slag aggregate depends on its original free lime content, SA, pore size distribution, effective porosity, and degree of weathering. The study indicates that OH and BOF slags will produce tufa, and only ACBF slag will not produce tufa.

Conclusions

On the basis of the research study, the following conclusions are drawn for the continued use of slags as subbase aggregates in highway construction:

1. The ACBF slag can be used in highway construction,
2. The hydrophilic property of the aggregates may be responsible for water retention and precipitation of tufa,

3. Range of tufa precipitation varies with the SA,
4. Carbon dioxide is needed for the precipitation of tufa,
5. Stockpile aging of slag might reduce the rate of tufa precipitation but will not completely eliminate it, and
6. OH and BOF slags will produce tufa.

A further study on aging of OH and BOF slags should be conducted to document free lime content versus aging.

ACKNOWLEDGMENTS

This study was funded by the Ohio Department of Transportation (ODOT). The authors are grateful to the agency personnel, especially Bill Edwards, John Hurd; and Stu Schwotzer, for their constructive criticism. The authors also thank Jill Posta and Sridhar Katipally for typing this paper.

REFERENCES

1. Feldman, R. M., D. J. Biros, and D. L. Middleton. Tufa Deposition Along a Highway Embankment, Cuyahoga County Ohio. *The Compass*, Vol. 57, No. 3, 1980, pp. 82–88.
2. Bates, R. L., and J. A. Jackson. *Glossary of Geology*, 2nd ed. American Geological Institute, Falls Church, Va., 1980, p. 749.
3. Feldman, R. M. *Tufa Precipitation and Its Effects on Drainage of Highways.* FHWA Report OH-81-0100. Ohio Department of Transportation, Columbus, 1981.
4. Hurd, J. O. The Effect of Slag Type on Tufa Precipitate Formation. In *Transportation Research Record 1192*, TRB, National Research Council, Washington, D.C., 1988.

The opinions and viewpoints expressed are entirely those of the authors and not necessarily those of ODOT.

Publication of this paper sponsored by Committee on Subsurface Drainage.

Determination of Original Free Lime Content of Weathered Iron and Steel Slags by Thermogravimetric Analysis

WILLIAM A. KNELLER, JIWAN GUPTA, MICHELLE LEA BORKOWSKI, AND DAVID DOLLIMORE

Iron and steel slags are often used as subbase materials in the construction of highways. Previous studies have suggested that the free lime (CaO) in these subbases is responsible for the deposition of calcium carbonate (tufa) in many highway drains. Clogging of these drains leads to the deterioration of highways. Previous work has shown that if the total original CaO in slags exceeds 1 percent, the slags will readily produce tufa. Therefore, to classify the tufa-producing potential of these slags, it is necessary to determine the total original CaO. Thermogravimetry (TG) methods were employed and most of the TG plots indicated two major changes in weight loss—dehydroxylation of $Ca(OH)_2$ and dissociation of carbonates. From these changes in weight loss the percentage of CaO was calculated. These calculated percentages of CaO from the TG plot plus the results from the "sugar test" determine the total original percentage of CaO. Five groups are recognized according to the calculated total percentage of CaO: 0 percent, 3.5 to 5 percent, 8 to 9 percent, 10 to 12 percent, and 24 to 25 percent. Air-cooled blast furnace slag (0 percent CaO) is the only slag that should be used as a subbase in highway construction, whereas all others are considered to be harmful and could lead to the formation of tufa. TG methods and the sugar test are excellent and economical ways to characterize the original CaO in slags and the susceptibility of the slags to precipitate $CaCO_3$ in subdrains of highways.

Iron and steel slags from blast, open hearth, basic oxygen, and electric arc furnaces are often used as subbase materials in the construction of highways. Previous studies (*1–3*) suggest that the free lime (CaO) present in these subbase materials is responsible for the deposition of a chemical sedimentary rock composed of calcium carbonate called *tufa*. It is formed as a precipitate by the evaporation of water rich in dissolved calcium carbonate. This precipitate has been observed clogging many drains along highways in northeastern Ohio. Because the clogging of drains leads to highway deterioration, it is necessary to devise a rapid method to determine the total original CaO in these subbase materials.

PURPOSE AND SCOPE

The purpose of this study is to (*a*) characterize the slags, (*b*) determine the amount of "original" CaO in the weathered iron and steel slags, and (*c*) classify these slags according to their tufa-producing potential. The prepared samples were taken from stockpiles exposed to weathering for various lengths of time. Thermogravimetry (TG) analyses were performed on air-cooled blast furnace, basic oxygen furnace, open hearth, and electric arc furnace slags to determine the percent calcium hydroxide [$Ca(OH)_2$] and calcium carbonate ($CaCO_3$) in the samples. These percentages were added to the results from an extraction and titration method nicknamed the "sugar test" to determine the total original CaO—the free CaO content at the time the slag was in a molten state or just poured from the ladle. After determination of the total original CaO content, the slags were clustered and classified according to the total original percentage of CaO.

W. A. Kneller, Department of Geology, University of Toledo, Ohio 43606-3390. J. Gupta, Department of Civil Engineering, University of Toledo, Ohio 43606-3390. M. L. Borkowski, Department of Geology, Michigan State University, East Lansing, Michigan 48824. D. Dollimore, Department of Chemistry, University of Toledo, Ohio 43606-3390.

IRON AND STEEL SLAGS

Slag is produced during the manufacture of iron and steel. It is formed by the combination of oxidized impurities and flux. Flux is used to purge the ores of impurities, lower the melting point of the slag, and remove sulfur from the smelted iron. The types of slags that are produced vary greatly according to the extraction or refining processes used.

Blast Furnace Slag

Blast furnace slag is a by-product of the iron industry. The process begins when iron ore, a limestone flux, and coke are heated in a blast furnace. The iron ore is a mixture of oxides of iron, silica, and alumina. Preheated air is then blown into the furnace, and the oxygen combines with the carbon from the coke to produce heat and carbon monoxide. The carbon monoxide reacts with the oxides of the iron ore to produce iron. The silica and alumina of the iron ore combine with the calcium of the limestone to form the slag. Air-cooled blast furnace (ACBF) slag is one that is allowed to solidify under normal atmospheric conditions. Water is sometimes sprayed on the slag to accelerate cooling and to induce cracks. Table 1 records the range of compositions for blast furnace slags.

Steel Furnace Slags

In the steel-producing industry three types of furnaces are used: open hearth, basic oxygen, and electric arc. The actual heating and smelting methods are very similar for each type of furnace;

TABLE 1 Range of Composition for Blast Furnace Slags (4)

Compound	Range Percent	Typical Analysis
SiO_2	33-42	36.4
Al_2O_3	10-16	12.8
CaO	36-45	41-43
MgO	3-12	5.8
FeO	0.3-2.0	0.4
Fe_2O_3	-	0.5
FeO + Fe_2O_3	0.2-1.5	1.4
Mno	-	1.3
S	1.3	-
P_3O_5	-	-

Modified from T. Segal [4]

however, there are some minor differences between the steel furnaces. In open hearth (OH) furnaces the limestone is added along with the scrap steel. The OH furnace takes about 5 to 14 hr to produce 300 tons of steel, whereas it would take the basic oxygen furnace (BOF) only 45 min to produce an equivalent amount. In the BOF, oxygen is blown onto the top of the charge at supersonic speed before the flux is added. Another steel furnace is the electric arc furnace (EAF) in which graphite electrodes are used for the heating process. Table 2 gives a range of compositions for OH, BOF, and EAF slags.

CHEMISTRY AND MINERALOGY OF SLAG SAMPLES

The chemical analyses of the slag samples used in this study are shown in Table 3. The process involved heating the slag in a crucible over an open flame until dehydration was complete. The samples were analyzed for elemental and oxide content by X-ray fluorescence (XRF) methods. These analyses were normalized to include the hydroxyl water and CO_2 data gleaned from the TG studies.

X-ray powder diffraction analysis was used to determine the gross mineralogy of the slags (5). Search-and-match routines were used against the ICPDS data base for the identification of the resulting peaks. Many minerals typical of these slags were identified, but for brevity they are not listed here. Of importance to this study, however, is the identification of $Ca(OH)_2$ and $CaCO_3$ in all the slags except the ACBF sample (No. 1). These chemical species should not be present in an unweathered slag. They would have been dissociated to CaO because of the high temperature of the original molten slag. The presence of $Ca(OH)_2$ and $CaCO_3$ in the stockpiled slags is assumed to be due to weathering. Residual CaO is present because some of it is encapsulated by silicates. This encapsulation protects the CaO from the effect of CO_2-charged porewater.

THERMAL ANALYSIS

Thermal analysis is the study of chemical and physical changes in a given material due to changes in temperature. These temperature changes are usually linear with time. The changes in enthalpy that accompany chemical and physical changes can be observed and recorded. These enthalpic changes, either exothermic (+) or endothermic (−), are caused by phase transitions such as fusion, crystalline structural inversions, boiling, sublimation, and vaporization; dehydration reactions; dissociation or decomposition reactions; oxidation and reduction reactions; destruction of crystalline structures; and other chemical reactions. Generally, phase

TABLE 2 Range of Composition for Steel Furnace Slags*

Compound	Open Hearth		BOF**	EAF**
	Range %	Typical Analysis %	Range %	Typical Analysis %
SiO_2	16-19	18.4	7.2-18.2	13.9
Al_2O_3	2-3	2.5	0.42-3.0	2.8
CaO	40-55	45.0	36-49	48.3
MgO	5-7	5.9	5-12	9.9
FeO	-	12.2	15-30	15.0
$Fe_2\hat{}O_3$	-	3.4	N/A	N/A
FeO + Fe_2O_3	10-23	15.6	N/A	N/A
MnO	5-6	8.6	N/A	N/A
S	0-1	-	0.05-0.5	0.06
P_2O_5	-	-	0.03-0.9	0.88

* *Modified from T. Segal [4] and synthesized from 50 analyses furnished by J.M. Olle, Edward C. Levy Co. 8800 Dix Ave., Detroit, MI 48209*

** *From Olle, J.M., 1991, Personal correspondence*

transitions, dehydration, reduction and some decomposition reactions produce endothermic effects, whereas crystallization, oxidation, and some decompositions produce exothermic effects. Researchers (*6–10*) since the mid-century have made important contributions to thermal analysis.

There are five basic categories or techniques of thermal analysis: thermometry, differential thermal analysis (DTA), differential scanning calorimetry (DSC), thermomechanical analysis and dilatometry (TMA), and thermogravimetry (TG). The last technique was used in this study.

THERMOGRAVIMETRY

TG analysis measures the loss or gain of weight by a substance as its temperature is raised or lowered at a constant rate. The reactions that occur during the heating process are responsible for the changes in weight. Knowing that certain reactions occur at specific temperatures enables the identification of the constituents of the sample. The data from the experiment are then recorded as a TG plot of mass versus temperature or time. From the TG plots, the composition of a sample can be determined. The physicochemical applications of thermogravimetry are given in Table 4 (*10*). Also from the TG plot, the first derivative can be calculated with respect to either time or temperature; this is called derivative thermogravimetry (DTG). The calculations can be done either by the TG thermal balance or by a computer program. The derivative is usually superimposed on the TG plot (see Figure 1). The DTG plot is set up so that temperature or time is on the abscissa, increasing from left to right, and the derivative values are on the ordinate, increasing from bottom to top. The DTG plot is used to help locate the start, peak, and end temperatures of a given reaction.

METHOD OF ANALYSIS

A high-temperature (1400°C) thermobalance was used to measure weight gain or loss during heating. The sample and operational parameters employed in this study are weight, 9 to 10 mg; grain size, +325 mesh; atmosphere-nitrogen flow rate, 30 ml/min; heating rate, 20°C/min; and water flow rate, 300 ml/min. The instrument was calibrated using melting and magnetic standards. In addition, a further check for accuracy was made by using a calcium oxalate ($CaC_2O_4 \cdot H_2O$) standard. These calibrations were repeated every 25 runs.

DISCUSSION AND RESULTS

Analysis of TG Plots

Most of the TG curves indicate two major changes in weight loss. This doublet is evidence of a two-stage reaction that is characteristic of OH, BOF, and EAF steel slags. All samples were preheated to 350°C to drive off any chemiabsorbed water. The first-stage reaction is caused by the evolution of hydroxyl water at about 400°C and ending at about 460°C. The second stage of decomposition is the evolution of carbon dioxide from the calcium carbonate in the slag, which occurs at about 490°C and ends at about 785°C. These reactions are detailed below:

$$Ca(OH)_2 + \text{heat} \rightarrow CaO + H_2O \uparrow$$

$$CaCO_3 + \text{heat} \rightarrow CaO + CO_2 \uparrow$$

The first derivative of the TG curve, DTG, was superimposed on each of the plots, excluding the ACBF sample (No. 1), for which no reactions occurred throughout the heat. In this study DTG was used to indicate the initial peak and final temperatures of the reaction of the TG plots.

The first reaction, if present, is labeled *1* at the point at which the reaction begins and *2* at the point at which the reaction ends. These numbers were determined, as mentioned before, from the first derivative. The temperature and percent weight loss for these numbers are found in the box labeled POINT TABLE on the left side of each plot. The value that is located between the numbers 1 and 2 on the curve is the extrapolated onset temperature, which is determined from the computer program.

The initial and final temperatures and the percent weight loss of the second reaction, if present, are labeled by the two-point angle. Again, these points were determined from the DTG plot.

TABLE 3 Oxide Analysis of Slags

Sample No.	Type	Al_2O_3	CaO	Fe_2O_3	MgO	Mn_2O_3	P_2O_5	K_2O	SiO_2	Na_2O	SO_3	$(H_2O)_{08}$	CO_2	Others
1	ACBF	8.52	40.09	0.85	10.80	0.71	<0.02	0.24	38.09	0.23	0.24	0.04	-	0.18
2	OH	3.50	36.02	26.57	9.84	3.31	0.26	0.01	15.19	0.06	1.70	0.42	3.13	-
3	OH	3.57	40.76	23.81	7.81	5.26	0.10	<0.01	13.73	<0.01	<0.01	0.78	1.51	1.13
4	OH	4.66	34.02	15.41	5.04	3.39	0.10	0.17	26.06	0.08	<0.01	0.57	10.49	
5	BOF	3.75	35.27	24.08	10.52	2.81	0.29	<0.01	12.77	0.08	<0.01	3.08	5.54	1.79
6	BOF	4.46	38.49	26.33	8.35	4.48	0.13	<0.01	12.41	0.07	0.01	0.61	2.11	2.54
7	BOF	2.97	48.02	15.05	9.67	3.12	0.22	<0.01	13.21	0.01	<0.01	2.65	6.06	-
8	BOF	3.01	50.81	15.62	5.32	3.56	0.30	<0.01	15.04	<0.01	0.04	2.88	3.40	-
9	EAF	Oxides Not Determined											2.36	17.02

Others, commonly include: SrO, BaO, TiO_2, Cr_2O_3, and V_2O_5
Dash (-) indicates not detected.

TABLE 4 Applications of Thermogravimetry

Physical Changes

- Sublimation
- Vaporization
- Absorption
- Adsorption
- Magnetic properties
  - Curie temperature
  - Magnetic susceptibility

Chemical changes

- $Solid \rightarrow gas$
  - Thermal decomposition of many organic and polymeric substances
  - Pyrolysis of coal, petroleum, and wood
  - Thermal oxidation degradation of polymeric materials
  - Carbon gasification with oxygen, steam, or carbon monoxide
- $Solid_1 \rightarrow solid_2 + gas$
  or
  $Solid_1 + solid_2 \rightarrow solid_3 + gas$
  - Thermal decomposition of many inorganic materials
  - Roasting and calcining of minerals
  - Determination of moisture, volatiles, and ash contents
  - Dehydration studies
  - Dehydroxylation studies
  - Decomposition of explosives
  - Development of analytical procedures
  - Kinetic studies (also applicable to solid - gas)
- $Solid_1 + gas \rightarrow solid_2$

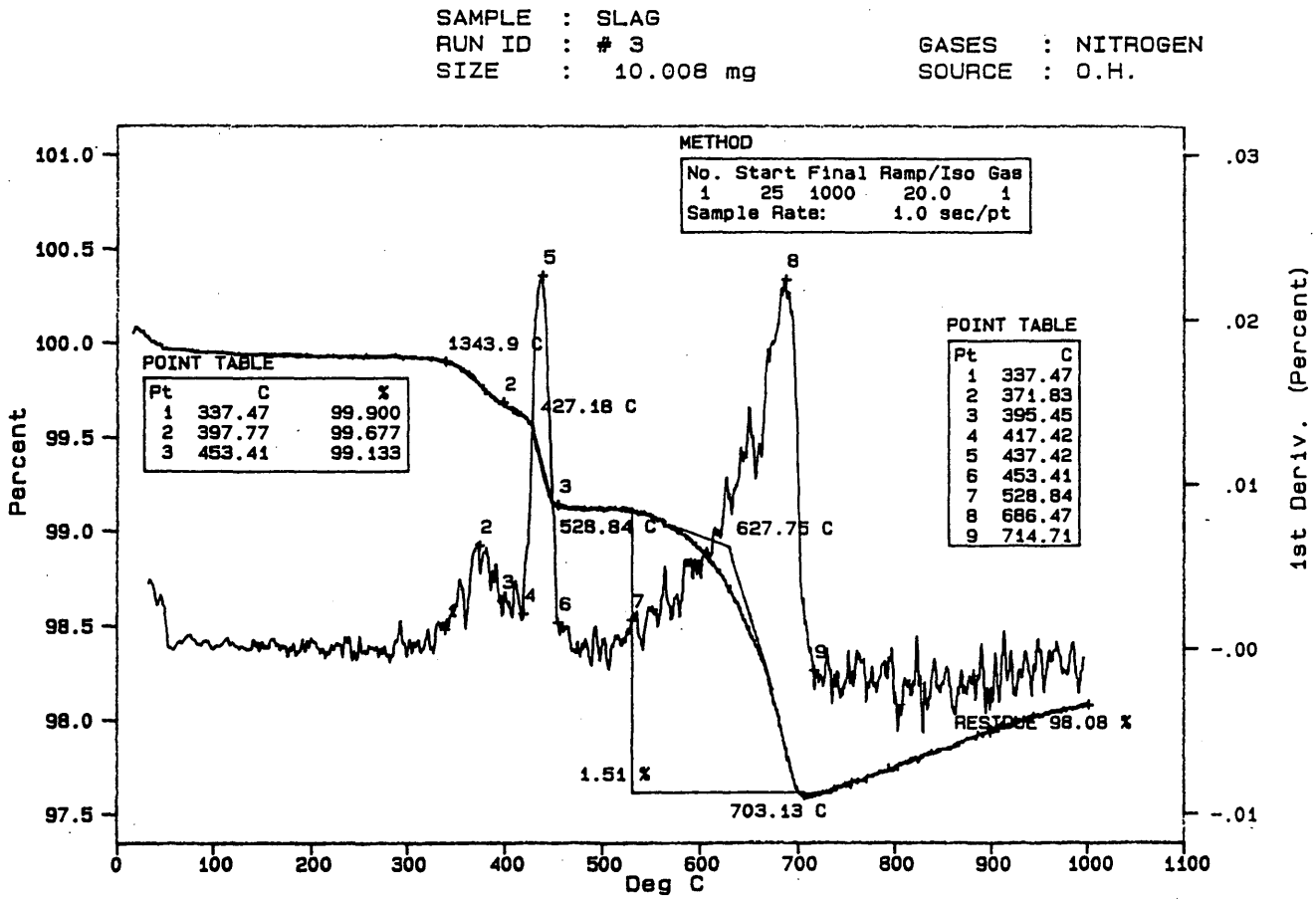

FIGURE 1 TG plot of sample No. 3, OH slag.

TABLE 5 Data from Thermogravimetric Analysis

Dehydroxylation of $Ca(OH)_2$						Dissociation of $CaCO_3$				
Sample #	I.T. [1]	O.T.[2]	P.T.[3]	F.T.[4]	% $(OH)_2$ Loss	I.T.[1]	O.T.[2]	P.T.[3]	F.T.[4]	% CO_2 Loss
1 (ACBF)		No reaction occurred					No reaction occurred			
2 (OH)	416.07	430.85	441.95	459.95	0.20	517.40	668.81	709.92	731.37	3.18
3 (OH)	397.77	427.18	437.42	453.41	0.54	528.84	627.75	689.90	703.13	1.51
4 (OH)		Reaction not measurable				674.04	712.14	743.49	766.87	6.65
5 (BOF)	408.78	441.81	448.79	464.19	0.96	509.22	658.51	708.55	734.15	5.55
6 (BOF)	402.60	418.77	430.92	453.94	0.32	549.26	648.32	686.73	705.63	2.11
7 (BOF)	404.61	435.13	446.45	462.17	0.89	487.57	655.16	709.81	737.46	6.16
8 (BOF)	408.80	430.54	443.24	460.02	0.87	543.39	660.14	703.21	723.79	3.52
9 (EAF)	424.31	448.49	452.52	466.12	0.75	561.76	708.74	763.82	783.03	17.20

1 Initial temperature. 2 Onset temperature. 3 Peak temperature. 4 Final temperature.

These temperatures and percentages were determined from the TG and DTG curves.

The extrapolated onset temperature is located to the right of the reaction. The plot for sample No. 3 is shown in Figure 1 and illustrates the double reaction, point table, and the first derivative. The TG curve in Figure 1 is labeled as mentioned above, with the residue located at the end of the curve. The peak temperatures for the two reactions are labeled on the derivative. All values for the reactions that occurred in the samples are given in Table 5, which also records the percent weight loss for $(OH)_2$ and CO_2 for the nine slag samples.

Method Used To Determine Total Original Percentage CaO

The total original percentage of CaO is calculated by addition of the results from the sugar test, calculated percentage of CaO due to dehydroxylation of $Ca(OH)_2$ (first reaction), and the calculated percentage of CaO due to dissociation of $CaCO_3$ (second reaction).

The sugar test (*11*) determined the CaO in the slag aggregates by dissolution and extraction of the CaO by hot (60 to 70°C) anhydrous ethylene glycol. The CaO is determined by titration with 0.05 *N* HCl and phenolphthalein as the indicator (see Table 6). The CaO percentages are calculated by using the values for sample No. 3 from Table 5, such as percent hydroxyl water loss, 0.54; percent CO_2 loss, 1.51; and by using the mole weights from the reaction. As stated previously, the reactions that occur are

$$Ca(OH)_2 + \text{heat} \rightarrow CaO + H_2O \uparrow$$

$$CaCO_3 + \text{heat} \rightarrow CaO + CO_2 \uparrow$$

The mole weights for each of the components are as follows:

CaO = 56.079 = 56; H_2O = 17.99 = 18; $Ca(OH)_2$ = 74.096 = 74;

$CaCO_3$ = 100.088 = 100; and CO_2 = 44.079 = 44.

TABLE 6 Total Original Percentage of CaO by TGA

Sample #	% CaO*	% $CaO_{(OH)_2}$**	% $CaO_{(CO_3)}$***	Total % CaO	Rank/ Cluster
1 (ACBF)	0	N/D	N/D	0	1
2 (OH)	0.237	0.622	4.047	4.906	2
3 (OH)	0.131	1.692	1.922	3.745	2
4 (OH)	0.044	N/D	8.464	8.508	3
5 (BOF)	0.604	2.971	7.064	10.639	4
6 (BOF)	1.051	0.992	2.685	4.728	2
7 (BOF)	0.691	2.775	7.840	11.306	4
8 (BOF)	1.064	2.700	4.480	8.244	3
9 (EAF)	0.602	2.340	21.891	24.833	5

N/D = Not Determinable
** Data derived from anhydrous ethylene glycol, 'sugar test'*
*** Calculation of % CaO due to dehydroxylation of Portlandite ($Ca(OH)_2$)*
**** Calculation of % CaO due to dissociation of carbonates*

The equations are set up as follows to calculate the percentage of CaO:

$$\frac{CaO}{56} = \frac{H_2O \text{ delta wt. loss}}{18} \quad (1)$$

$$\frac{CaO}{56} = \frac{CO_2 \text{ delta wt. loss}}{44} \quad (2)$$

Now the percentage of CaO is easily calculated, that is, using the values 0.54 and 1.51 (from Table 5 for sample No. 3) and cross-multiplying, as shown below:

$$\frac{CaO}{56} = \frac{0.54}{18} = 1.692 \text{ percent CaO} \quad (3)$$

$$\frac{CaO}{56} = \frac{1.51}{44} = 1.922 \text{ percent CaO} \quad (4)$$

The final step in determining the total original percentage of CaO is to add the three percentages of CaO together as shown in Table 6.

From the studies by Narita et al. (*12*), weathering slag is related to the amount, distribution, and characteristics of the CaO. If the unweathered slag contains less than 1 percent CaO, it should be volumetrically stable and should not produce tufa. If, however, the original amount of CaO is in excess of 1 percent, the slag should readily produce tufa in subdrains of highways. All slag samples are grouped in Table 6 according to their range of total original percent CaO. Five groups are recognized: 0 percent, 3.5 to 5 percent, 8 to 9 percent, 10 to 12 percent, and 24 to 25 percent. ACBF slag (0 percent CaO) is the only one that can be used as a subbase in highway construction; all others are considered to be harmful and could lead to the formation of tufa.

CONCLUSIONS

Previous work (*12*) has shown that if the percentage of total original CaO in a slag exceeds 1 percent, the slag could readily precipitate $CaCO_3$. The results from the TG plots showed two major changes in weight loss—dehydroxylation and dissociation of carbonates. From these changes in weight loss, the percentage of CaO can be calculated. These calculated percentages of CaO from plots plus the results from the sugar test determine the maximum *original* percentage of CaO. ACBF slag (0 percent CaO) is the only one that can be used as a subbase in highway construction; all others are considered to be potentially deleterious and could lead to pavement failure. The TG method together with the sugar test are excellent and economical ways to determine the maximum original CaO in slags and the tendency of the slags to precipitate $CaCO_3$ in the subdrains of highways.

ACKNOWLEDGMENTS

This research was funded by the Ohio Department of Transportation (ODOT). The authors are most thankful to the agency personnel, especially Bill Edwards, John O. Hurd, and Stu Schwotzer, for their guidance and constructive criticism. The opinions and views expressed are entirely those of the authors and not necessarily those of ODOT.

REFERENCES

1. Feldman, R. M. *Tufa Precipitation and Its Effects on Drainage of Highways*. Report OH-81-0100. FHWA; Ohio Department of Transportation, Columbus, 1981, 147 pp.
2. Barenberg, E. J., and M. R. Thompson. Design Construction and Performance of LFA and Slag Pavement. In *Transportation Research Record 839*, TRB, National Research Council, Washington, D.C., 1982, pp. 1–6.
3. Hurd, J. O. *The Effect of Slag Type on Tufa Precipitate Formation*. Open Report. Ohio Department of Transportation, Columbus, 1988.
4. Segal, T. Slag—Michigan's All-Purpose Construction Aggregate. In *Proc., Sixth Forum on Geology of Industrial Minerals and Rocks* (W. A. Kneller, ed.), *Miscellany No. 1*, Michigan Geological Survey, Lansing, 1970, pp. 117–126.
5. Tamirisa, R. *Study of Highway Base/Subbase Aggregates That Cause Deposition of Calcareous Tufa in Drains*. M.S. thesis. Civil Engineering Department, University of Toledo, Ohio, 1993, 154 pp.
6. Duval, C. *Inorganic Thermogravimetric Analysis*, 2nd ed. Elsevier, Amsterdam, 1963.
7. Keattch, C. *An Introduction to Thermogravimetry*. Heydon & Sons, London, 1969, pp. 1–3.
8. Ernest, C. M. The Modern Thermogravimetric Approach to the Compositional Analysis of Materials. In *Compositional Analysis by Thermogravimetry* (C.M. Ernest, ed.), American Society for Testing and Materials, Special Technical Publication 997, Philadelphia, Pa., 1989, pp. 1–18.
9. Bhatty, J. I. A Review of the Application of Thermal Analysis to Cement-Admixture Systems. *Thermochimica Acta*, Vol. 189, No. 2, 1991, pp. 313–350.
10. Dollimore, D. Thermoanalytical Instrumentation. In *Analytical Instrumentation Handbook* (G. W. Ewing, ed.), Marcel Dekker, Inc., New York, 1990, pp. 905–960.
11. Javellana, M. N., and I. Jawed. Extraction of Free Lime in Portland Cement and Clinker by Ethylene Glycol. *Cement and Concrete Research*, Vol. 12, pp. 399–403.
12. Narita, K., T. Onoye, and Z. Takata. *On the Weathering Mechanism of LD Converter Slag* (in Japanese). Kobe Steel, Ltd., Japan, 1978, p. 52.

Publication of this paper sponsored by Committee on Subsurface Drainage.

Drainability of Granular Bases for Highway Pavements

BRUCE M. MCENROE

The best measure of the drainability of a granular base is the minimum degree of saturation that can be achieved through gravity drainage in the field. The amount of water that can drain from a base course depends not only on the physical properties of the material, but also on the cross-sectional geometry of the pavement system. A fine-grained base may remain fully saturated under the largest suction that can be developed through gravity drainage. A formula for the minimum degree of saturation in the granular base is developed from Brooks and Corey's formula for water retention in unsaturated porous media. The relationship for drainable porosity in the FHWA subdrainage design manual tends to overestimate the amount of drainage from fine-grained bases and greatly underestimate the amount of drainage from coarse-grained bases. If the minimum degree of saturation for a granular base is sufficiently low, it will drain fairly quickly. The recommended method for the estimation of drainage times is a one-dimensional analysis of the saturated flow below the phreatic surface. This analysis accounts for the nonuniform spatial distribution of drainable porosity. Casagrande and Shannon's procedure, which is recommended by FHWA, tends to underestimate drainage times, particularly for base courses that are relatively thin. The recommended procedures for subdrainage analysis have been implemented in the SUBDRAIN computer program of the Kansas Department of Transportation.

Pavements with inadequate subsurface drainage deteriorate much faster than well-drained pavements. If the base course of the pavement is saturated or nearly saturated, wheel loads can cause water and base material to be pumped out through joints and cracks and at pavement edges, which eventually undermines the pavement. Because it is virtually impossible to keep water from entering pavements through joints and cracks over the long run, good drainage is essential for pavement longevity.

The AASHTO procedure for pavement design (*1*) incorporates a drainage coefficient as a key input. The value of this coefficient depends on the quality of drainage of the pavement system and the percentage of time that the road bed is exposed to moisture levels near saturation. The AASHTO design guide relates the quality of drainage to the time required for the removal of water from the base course, but it does not specify what degree of drainage or level of saturation constitutes "removal." In FHWA's computer program (*2*), the drainability of the base is measured by time required for a saturated base to drain to water content equal to 85 percent of the water content at saturation.

One measure of the drainability of a base course is its coefficient of permeability (Darcy permeability), k. The coefficient of permeability depends upon the intrinsic permeability of the granular material and the specific weight and viscosity of the fluid. The relationship is

$$k = \frac{K\gamma}{\mu} \tag{1}$$

in which K is the intrinsic permeability of the granular material and γ and μ are the specific weight and viscosity of the fluid, respectively. The coefficient of permeability, k, has dimensions of L/T (length/time). The intrinsic permeability, K, has dimensions of L^2.

Another measure of drainability is the lowest degree of saturation that can be achieved through gravity drainage in the field. The degree of saturation, s, is defined as the ratio θ/n, in which θ is the volumetric water content and n is the porosity (the volumetric water content at complete saturation). The lowest degree of saturation that can be achieved in the field through gravity drainage is denoted s_{min}. The difference between the water content at saturation and the lowest water content that can be achieved in the field through gravity drainage is termed the drainable porosity, n_d. The porosity, the drainable porosity, and s_{min} are related as follows:

$$S_{min} = 1 - \frac{n_d}{n} \tag{2}$$

In current practice, the drainable porosity of the base material is usually estimated from the coefficient of permeability by means of a relationship that appears in graphical form in FHWA's report *Highway Subdrainage Design* (*3*). The algebraic form of this relationship is

$$n_d = 0.0355k^{0.235} \tag{3}$$

for k in meters per day. The corresponding formula for the minimum degree of saturation is

$$s_{min} = 1 - \frac{0.0355}{n} k^{0.235} \tag{4}$$

for k in meters per day. Equation 3, which is strictly empirical, was fitted to measured values of the coefficient of permeability and the drainable porosity for soils of varied gradations and densities. The report states that it "should be used with caution, particularly at the extremities where data were lacking or were quite scattered." Despite this warning, FHWA's DAMP program (*2*) obtains the drainable porosity of the granular base from Equation 3 exclusively. It does not allow the user to enter another value for the drainable porosity.

Drainage times are normally estimated, directly or indirectly, from formulas published by Casagrande and Shannon (*4*) in 1951.

Department of Civil Engineering, 2006 Learned Hall, University of Kansas, Lawrence, Kans. 66045.

The methods for estimation of drainage times in FHWA's subdrainage design manual (*3*) and the DAMP program (*2*) are based on these formulas. The basic forms of Casagrande and Shannon's relationships were derived through a simplified one-dimensional analysis in which the phreatic surface (water table) was considered planar at all times. To compensate for the error introduced by this approximation, they incorporated an undetermined coefficient in their analysis as a correction factor and used experimental data to determine its values for various conditions.

This paper presents a new analysis of the drainage of a saturated granular base. Starting from basic principles of water retention and flow in porous media, this analysis leads to some new methods for the estimation of minimum degrees of saturation, drainable porosities, and drainage times. It also provides a basis for the evaluation of the current methods. Two example problems illustrate the practical application of the recommended procedures.

MINIMUM DEGREE OF SATURATION

Theory

Any granular material has a characteristic drainage curve that relates the degree of saturation to the pore-water suction head (negative pressure head), ψ. The drainage curve is best determined from measurements of the water content at equilibrium for successively larger suction heads in the laboratory. An approximate drainage curve can be computed from grain-size distribution and bulk density data (*5*). The drainage curves of most granular materials can be approximated closely by the formula of Brooks and Corey (*6*),

$$s = \begin{cases} 1 & \psi \le \psi_a \\ s_r + (1 - s_r)\left(\dfrac{\psi_a}{\psi}\right)^{\lambda} & \psi > \psi_a \end{cases} \tag{5}$$

The terms s_r, ψ_a, and λ in Equation 5 are constants for a particular material. The values of these constants are determined by fitting Equation 5 to the data that make up the drainage curve. The constant s_r is termed the residual saturation. It is the degree of saturation that is approached asymptotically at very large suction heads. The constant ψ_a is termed the air-entry head. It is the suction head below which the material remains fully saturated. The dimensionless constant λ is termed the pore-size distribution index. The more uniform the material, the larger the value of λ.

Laliberte et al. (*7*) showed that the values of s_r, ψ_a, and λ are related to the porosity and intrinsic permeability of the granular material and the specific weight, viscosity, and surface tension of the fluid according to the formula

$$\frac{(1 - s_r)\, n\, \sigma^2}{K\, \psi_a^2\, \gamma^2} \frac{\lambda}{\lambda + 2} \approx 5 \tag{6}$$

in which K is the intrinsic permeability of the granular material and γ, μ, and σ are the specific weight, viscosity, and surface tension of the fluid, respectively. The form of this relationship has a theoretical basis. The value of the constant on the right-hand side was determined experimentally.

The drainable porosity of the base course of a pavement depends not only on the physical properties of the material, but also on the cross-sectional geometry of the pavement system. The geometry of the pavement section determines the maximum pore-water suction at any point in the base. Figure 1 shows a pavement section with a granular base and edge drains. The subgrade is considered impervious. If the granular base is saturated and then allowed to drain under the force of gravity with no further inflow and no evaporation, drainage will eventually cease. In this state of static equilibrium, the suction head at any point is equal to its height above the water table in the edge drain ($\psi = w + z$) and, from Equation 5, the corresponding minimum degree of saturation at this level, $s_{\min}(z)$, is

$$s_{\min}(z) = \begin{cases} 1 & z \le \psi_a - w \\ s_r + (1 - s_r)\left(\dfrac{\psi_a}{w + z}\right)^{\lambda} & z > \psi_a - w \end{cases} \tag{7}$$

At elevations $z \le \psi_a - w$, the granular base will not drain at all. The drainable porosity at any level is the difference between the porosity and the minimum water content at that level:

$$n_d(z) = n\,[1 - s_{\min}(z)] \tag{8}$$

Equation 8 follows from Equation 2. The average minimum saturation at a distance x from the edge drain, $\bar{s}_{\min}(x)$, is the average of $s_{\min}(z)$ over the thickness of the granular base:

$$\bar{s}_{\min}(x) = \frac{1}{d} \int_{mx}^{mx+d} s_{\min}(z)\, dz \tag{9}$$

The evaluation of the right-hand side of Equation 9 leads to an algebraic formula for $\bar{s}_{\min}(x)$:

$$\bar{s}_{\min}(x) = \begin{cases} 1 & x \le x_1 \\ s_r + (1 - s_r)\left\{\dfrac{\psi_a - w - mx}{d} + \dfrac{\psi_a^{\lambda}}{d(1 - \lambda)} \cdot [(w + d + mx)^{1-\lambda} - \psi_a^{1-\lambda}]\right\} & x_1 < x \le x_2 \\ s_r + (1 - s_r)\dfrac{\psi_a^{\lambda}}{d(1 - \lambda)}[(w + d + mx)^{1-\lambda} - (w + mx)^{1-\lambda}] & x > x_2 \end{cases} \tag{10}$$

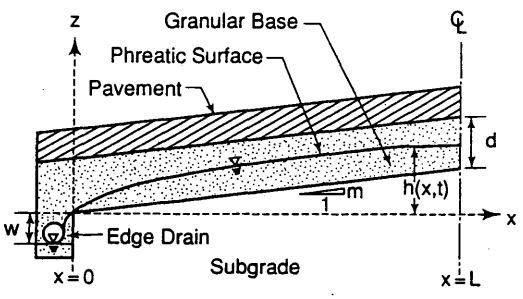

FIGURE 1 Cross section of pavement with granular base and edge drain.

in which

$$x_1 = \begin{cases} 0 & \dfrac{\psi_a - w - d}{m} < 0 \\ \dfrac{\psi_a - w - d}{m} & 0 \le \dfrac{\psi_a - w - d}{w} < L \\ L & \dfrac{\psi_a - w - d}{m} > L \end{cases} \quad (11)$$

$$x_2 = \begin{cases} 0 & \dfrac{\psi_a - w}{m} < 0 \\ \dfrac{\psi_a - w}{m} & 0 \le \dfrac{\psi_a - w}{m} < L \\ L & \dfrac{\psi_a - w}{m} > L \end{cases} \quad (12)$$

The average drainable porosity at a distance x from the edge drain, $n_d(x)$, can be determined from the porosity and the average minimum water content at this location as follows:

$$\bar{n}_d(x) = n\,[1 - \bar{s}_{\min}(x)] \quad (13)$$

The spatially averaged minimum saturation for the entire base course, $S_{\min}$, is the average of $\bar{s}_{\min}(x)$ from $x = 0$ to $x = L$:

$$S_{\min} = \frac{1}{L}\int_0^L \bar{s}_{\min}(x)\,dx \quad (14)$$

The evaluation of the right-hand side of Equation 14 leads to an algebraic formula for $S_{\min}$:

$$S_{\min} = s_r + (1 - s_r)\left\{\frac{x_1}{L} + \frac{(\psi_a - w)(x_2 - x_1)}{dL} - \frac{m(x_2^2 - x_1^2)}{2dL} - \frac{\psi_a^{\lambda}}{mdL(1-\lambda)(2-\lambda)} \cdot \left[(w + d + mL)^{2-\lambda} - (w + d + mx_1)^{2-\lambda} - (w + mL)^{2-\lambda} + (w + mx_2)^{2-\lambda}\right] - \frac{\psi_a (x_2 - x_1)}{dL(1-\lambda)}\right\} \quad (15)$$

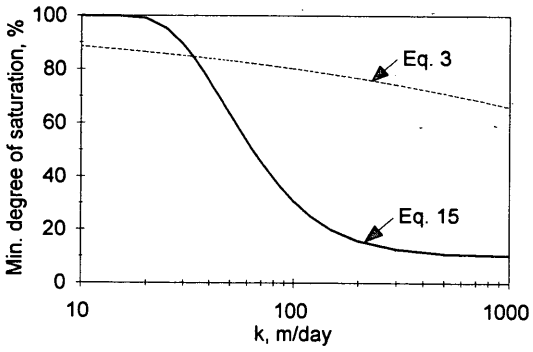

FIGURE 2 Minimum degree of saturation versus coefficient of permeability for Example 1.

The average drainable porosity for the entire base course, N_d, can be determined from the porosity and the spatially averaged minimum saturation as follows:

$$N_d = n(1 - S_{\min}) \quad (16)$$

For the base to drain at all, the air-entry head of the granular material must be less than the elevation difference between the top of the base at the crown and the water table in the edge drain ($\psi_a < w + d + mL$).

The following example illustrates the relationship between the coefficient of permeability of the base material and the minimum degree of saturation. It also provides a comparison of Equations 15 and 16 and Equation 3.

Example 1: Minimum Degree of Saturation for Typical Pavement Section

Problem: The base course of a pavement is to have a slope of 0.02 m/m, a thickness of 0.1 m (3.9 in.), and a half-width (L in Figure 1) of 7.0 m (23.0 ft). The bottom of the drainpipe is to be 0.1 m (3.9 in.) below the bottom of the base (w = 0.1 m). The base is to be constructed of a well-sorted granular material. This type of material would have a porosity of about 0.40, a residual saturation on the order of 0.1, and a pore-size distribution index on the order of 4. The objective is to determine the (spatially averaged) minimum degree of saturation of the base for materials with coefficients of permeability from 10 to 1000 m/day (33 to 3,300 ft/day).

Solution: According to Equation 15, the minimum degree of saturation of the base is determined by four geometric variables (d, w, L, and m) and three properties of the material (s_r, ψ_a, and λ). Equation 6 provides an estimate of the air-entry head based on other properties of the material and the fluid. The solid curve in Figure 2 shows $S_{\min}$ from Equation 15 for d = 0.1 m (3.9 in.), w = 0.1 m (3.9 in.), m = 0.02 m/m, L = 7.0 m (23.0 ft), s_r = 0.10, and $\psi_a = 1.333K^{-1/2}$ for ψ_a in meters and k in meters per day. The formula for ψ_a, from Equation 6, is based on n = 0.40, γ = 9810 N/m^3, μ = 0.00131 N s/m^2, and σ = 0.0742 N/m (water at 10°C).

The foregoing example demonstrates that a granular base must be fairly coarse to drain well. In this example, materials with coefficients of permeability less than 15 m/day do not drain at all because their air-entry heads are too large ($\psi_a > w + d + mL$). Materials with coefficients of permeability below 33 m/day (110 ft/day) will remain more than 85 percent saturated. A minimum saturation of 50 percent requires a coefficient of permeability of 64 m/day (210 ft/day). On the other hand, nearly all of the pore water will drain by gravity if the material is very coarse. Materials with coefficients of permeability above 150 m/day (490 ft/day) will drain to below 20 percent of saturation.

Figure 2 also shows Equation 3, the relationship incorporated in FHWA's DAMP program (*2*). This formula appears to overestimate the amount of drainage from fine-grained material and to greatly underestimate the amount of drainage from coarse-grained materials.

DYNAMICS OF DRAINAGE

One-Dimensional Analysis with Spatially Varied Drainable Porosity

Figure 1 shows the drainage of a granular base with no inflow or outflow through the pavement or subgrade. Drainage starts from

an initial condition of complete saturation at time $t = 0$. The objective of the analysis is to determine the degree of saturation of the base at times $t > 0$. The primary direction of flow is downslope parallel to top of the subgrade. The vertical distribution of pore-water pressure is essentially hydrostatic everywhere except over the edge drain and very near $x = 0$, where the vertical curvature of the streamlines is significant. Most of the flow occurs in the zone of positive pore-water pressures below the phreatic surface (the surface of atmospheric pressure).

The drainage of the base course is analyzed as a problem of one-dimensional unconfined saturated flow in the zone of positive pressures below the phreatic surface, with a spatially varied drainable porosity. The degree of saturation above the phreatic surface at a distance x from the edge drain is assumed to be $\bar{s}_{min}(x)$. The corresponding water content above the phreatic surface is $n - \bar{n}_d(x)$.

The continuity equation for the flow in the zone below the phreatic surface is

$$\bar{n}_d(x) \frac{\partial h(x,t)}{\partial t} - \frac{\partial q(x,t)}{\partial x} = 0 \tag{17}$$

in which $h(x,t)$ is the elevation of the phreatic surface and $q(x,t)$ is the discharge (per unit width) in the $-x$ direction. The equation of motion is the Dupuit discharge formula for unconfined seepage over a sloping bed:

$$q(x,t) = K\,[h(x,t) - mx] \frac{\partial h(x,t)}{\partial x} \tag{18}$$

The substitution of the right-hand side of Equation 18 for $q(x,t)$ in Equation 17 yields the governing equation with $h(x,t)$ as the dependent variable:

$$\bar{n}_d(x) \frac{\partial h(x,t)}{\partial t} - K \frac{\partial}{\partial x} \left\{ [h(x,t) - mx] \frac{\partial h(x,t)}{\partial x} \right\} = 0 \tag{19}$$

The initial condition is $h(x,0) = mx + d$, which represents complete saturation with no excess pressure. The lower boundary, $x = 0$, is the brink of the edge drain. The appropriate boundary condition at this location is a hydraulic gradient of unity (*8*). The upper boundary, $x = L$, is the crown of the road. Symmetry requires that no flow cross this boundary. This requirement is satisfied by a horizontal phreatic surface (hydraulic gradient of zero) until h becomes zero. The average degree of saturation at any time can be determined from the phreatic-surface profile:

$$S(t) = \frac{1}{L} \int_0^L \left\{ \bar{s}_{min}(x) + [1 - \bar{s}_{min}(x)] \frac{h(x,t) - mx}{d} \right\} dx \tag{20}$$

This mathematical model of the drainage process has been implemented in the SUBDRAIN computer program of the Kansas Department of Transportation. This program solves Equation 19 for the stated initial and boundary conditions by a nonlinear implicit finite-difference scheme. The program returns the average degree of saturation at the end of each time step. It also returns the time to 85 percent saturation ($S = 0.85$) and the time to 50 percent drainage ($S = S_{min} + 0.5N_d/n$).

One-Dimensional Analysis with Constant Drainable Porosity

A more approximate analysis with a constant drainable porosity leads to a simple algebraic formula for the time to 50 percent drainage. In this analysis, the spatially averaged drainable porosity, N_d, is substituted for the local drainable porosity, $\bar{n}_d(x)$, in the governing differential equation. With this simplification, the problem can be stated in terms of the dimensionless variables

$$T = \frac{Kmt}{LN_d} \tag{21}$$

$$X = \frac{x}{L} \tag{22}$$

$$H = \frac{h}{mL} \tag{23}$$

$$D = \frac{d}{mL} \tag{24}$$

The governing equation is

$$\frac{\partial H(X,T)}{\partial T} - \frac{\partial}{\partial X} \left\{ [H(X,T) - X] \frac{\partial H(X,T)}{\partial X} \right\} = 0 \tag{25}$$

and the initial condition is $H = D + X$. The boundary conditions can also be stated in terms of these dimensionless variables. $H(X,T)$ is determined entirely by D, the dimensionless thickness of the base.

The degree of drainage at any dimensionless time, U, is the fraction of drainable pore space that has been drained:

$$U = \frac{1 - S}{1 - S_{min}} \tag{26}$$

Its value at any time can be calculated from the dimensionless phreatic-surface profile:

$$U(T) = \int_0^1 [H(X,T) - X]\,dx \tag{27}$$

Because D determines $H(X,T)$, it also determines $U(T)$. Figure 3 shows the relationship between the dimensionless time to 50 percent drainage, T_{50}, and the dimensionless thickness of the base, D, as determined from numerical solutions of the governing equation for many values of D. These numerical results are fitted closely by the simple empirical formula

$$T_{50} = \frac{0.63}{D + 1.3} \tag{28}$$

In dimensional form, this formula is

$$T_{50} = 0.63 \frac{LN_d}{Km} \left(\frac{d}{mL} + 1.3 \right)^{-1} \tag{29}$$

Formulas for times to other degrees of drainage could be developed in the same way.

Simplified One-Dimensional Analysis by Casagrande and Shannon

Casagrande and Shannon's model of the drainage process (*4*) can be expressed concisely in terms of the dimensionless variables T, U, and D as

$$T = C(D) \cdot f(D, U) \tag{30}$$

in which

$$f(D, U) = \begin{cases} 2U - D \ln \dfrac{D + 2U}{D} & U \leq 0.5 \\ 1 + \ln \dfrac{2D - 2UD + 1}{(2 - 2U)(D + 1)} & \\ - D \ln \dfrac{D + 1}{D} & U > 0.5 \end{cases} \tag{31}$$

and

$$C(D) = 2.45 - 0.8D^{-1/3} \tag{32}$$

The function $f(D,U)$ is the solution for T from their simplified one-dimensional analysis with a planar phreatic surface. The function $C(D)$ is a correction factor that was introduced to better fit the results of some laboratory and field experiments. A formula for the time to 50 percent drainage can be obtained by the substitution of 0.5 for U in Equation 30. This formula is

$$T_{50} = (1.225 - 0.4D^{-1/3}) \left(1 - D \ln \frac{D + 1}{D}\right) \tag{33}$$

Equation 33 is plotted in Figure 3. For large values of D, Equation 33 closely approximates the numerical results from the complete one-dimensional analysis with a constant drainable porosity. For small values of D, Equation 33 appears to underestimate T_{50} considerably.

The following example illustrates the relationship between the coefficient of permeability of the base material and two measures of the drainage time for a typical pavement section. It also provides a comparison of three different methods for estimating these drainage times.

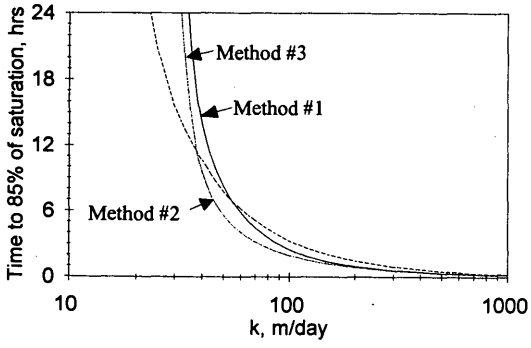

FIGURE 3 Comparison of two approximate methods for time to 50 percent drainage.

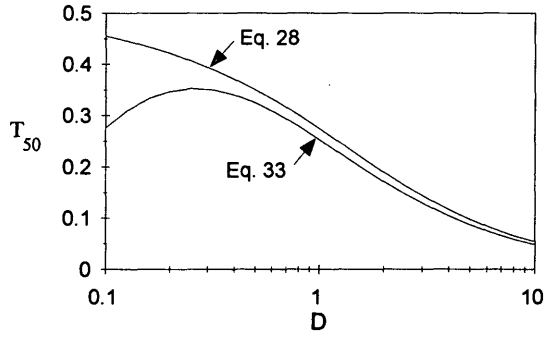

FIGURE 4 Time to 85 percent of saturation versus coefficient of permeability for Example 2.

Example 2: Drainage Times for Typical Granular Base

Problem: As in the previous example, the base course of a pavement is to have a slope of 0.02 m/m, a thickness of 0.1 m (3.9 in.), and a half-width (L in Figure 1) of 7.0 m (23.0 ft). The bottom of the drainpipe is to be 0.1 m (3.9 in.) below the bottom of the base (w = 0.1 m). The base is to be constructed of a well-sorted granular material. This type of material would have a porosity of about 0.40, a residual saturation on the order of 0.1, and a pore-size distribution index on the order of 4. The objective is to determine the times to 85 percent saturation (S = 0.85) and the times to 50 percent drainage (U = 0.50) for base materials with coefficients of permeability from 10 to 1000 m/day (33 to 3,300 ft/day).

Solution: The drainage times are estimated by three different methods:

1. Complete one-dimensional analysis with spatially varied drainable porosity from Equations 10–13 (SUBDRAIN program),
2. Complete one-dimensional analysis with a constant, spatially averaged drainable porosity from Equations 15–16 (modified SUBDRAIN program), and
3. Simplified one-dimensional analysis by Casagrande and Shannon (*4*) with constant drainable porosity from Equation 3 (DAMP program).

Figure 4 compares the results for the time to 85 percent of saturation. These results for Methods 1 and 3 do not differ greatly except for k < 40 m/day (130 ft/day). A comparison of the results for Methods 1 and 2 shows that the more approximate method yields considerably shorter estimates of drainage times for materials with permeabilities less than about 100 m/day (330 ft/day). The drainable porosity is actually larger near the centerline of the road than near the sides because of the difference in elevation. Most of the water that drains from the base must travel a distance greater than $L/2$ to reach the edge drain. This is why Method 1, which uses spatially varied drainable porosities, yields longer drainage times than Method 2, which uses a spatially averaged drainable porosity. The two methods yield nearly identical drainage times for very coarse materials because the spatial variability of drainable porosity is very small for these materials in this system.

Figure 5 compares the results for the time to 50 percent drainage. The drainage times for Method 3 are based on different drain-

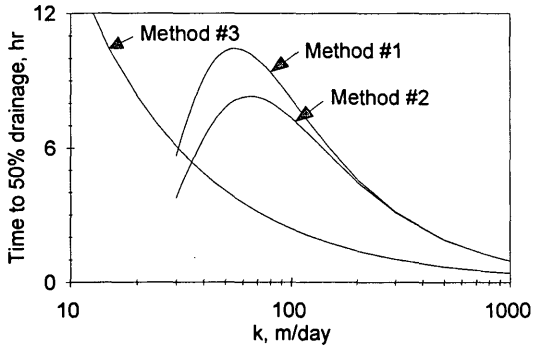

FIGURE 5 Time to 50 percent drainage versus coefficient of permeability for Example 2.

able porosities, and therefore different volumes of drainage, than the drainage times for Methods 1 and 2. Method 2 underestimates the time to 50 percent drainage for materials with permeabilities less than about 100 m/day (330 ft/day) because the spatial variability of the drainable porosity is relatively large for these materials in this system.

CONCLUSIONS

The best measure of the drainability of a granular base is the minimum degree of saturation that can be achieved through gravity drainage in the field. The amount of water that can drain from a base course depends not only on the physical properties of the material, but also on the cross-sectional geometry of the pavement system. The geometry of the pavement section limits the amount of suction that gravity can exert on the pore water. A granular base must be fairly coarse to drain adequately. A fine-grained base may remain fully saturated under the largest suction that can be developed through gravity drainage.

Equation 15 can provide a good estimate of the minimum degree of saturation for a granular base. It incorporates both the water-retention properties of the drainage material and the cross-sectional geometry of the pavement. Equation 3, which appears in FHWA's subdrainage design manual (*3*) and the DAMP computer program (*2*), tends to overestimate the amount of drainage from fine-grained bases and to greatly underestimate the amount of drainage from coarse-grained bases. Equation 3 does not account for the cross-sectional geometry of the pavement.

The recommended method for estimation of drainage times is a one-dimensional analysis of the saturated flow below the phreatic surface, with the local drainable porosities determined from Equation 10. The equation that governs the drainage process is solved numerically by a finite-difference method. If the spatial variability of the drainable porosity is neglected, drainage times are underestimated. The formulas of Casagrande and Shannon (*4*) underestimate drainage times, particularly for systems in which $d/mL << 1$.

The recommended procedures for subdrainage analysis have been implemented in the SUBDRAIN computer program of the Kansas Department of Transportation. These procedures could easily be incorporated into FHWA's DAMP program and other similar programs.

ACKNOWLEDGMENT

This project was supported by the Kansas Department of Transportation (KDOT) through the K-TRAN Cooperative Transportation Research Program. Andrew Gisi served as the project monitor for KDOT.

REFERENCES

1. *AASHTO Pavement Design Guide.* American Association of State Highway and Transportation Officials, Washington, D.C., 1986.
2. Carpenter, S. H. *Highway Subdrainage Design by Microcomputer: Drainage Analysis and Modelling Programs (DAMP).* Report FHWA-IP-90-012. FHWA, U.S. Department of Transportation, 1990.
3. Moulton, L. K. *Highway Subdrainage Design.* Report FHWA-TS-80-224. FHWA, U.S. Department of Transportation, 1980.
4. Casagrande, A., and W. L. Shannon. Base Course Drainage for Airport Pavements. *Proceedings of the American Society of Civil Engineers,* Vol. 77, Separate No. 75, 1951.
5. Arya, L. M., and J. F. Paris. A Physicoempirical Model to Predict the Soil Moisture Characteristic from Particle-Size Distribution and Bulk Density Data. *Soil Science Society of America Journal,* Vol. 45, 1981, pp. 1023–1030.
6. Brooks, R. H., and A. T. Corey. *Hydraulic Properties of Porous Media.* Hydrology Paper 3. Colorado State University, Fort Collins, 1964.
7. Laliberte, G. E., A. T. Corey, and R. H. Brooks. *Properties of Unsaturated Porous Media.* Hydrology Paper 17. Colorado State University, Fort Collins, 1966.
8. McEnroe, B. M. Maximum Saturated Depth Over a Landfill Liner. *Journal of Environmental Engineering,* Vol. 119, No. 2, Mar./Apr. 1993, pp. 262–270.

Publication of this paper sponsored by Committee on Subsurface Drainage.

Field Evaluation of Various Types of Open-Graded Drainage Layers

T. J. KAZMIEROWSKI, A. BRADBURY, AND J. HAJEK

Pavement drainage layers have been proved to be highly effective in the efficient and quick dissipation of subsurface water from a pavement structure. The Ministry of Transportation of Ontario requires a 100-mm lift of open-graded drainage layer (OGDL) directly beneath the concrete slab as part of the rigid pavement design for expressway facilities. The gradation of the OGDL consists almost entirely of coarse aggregates retained on the 4.75-mm sieve, which provides a highly permeable drainage layer. Because of this uniformly graded coarse aggregate, the drainage layer has proved difficult to construct by conventional means. In order to alleviate this problem, the OGDL is treated with 1.8 percent asphalt cement to increase the stability of the material during construction. The addition of an asphalt cement binder has been used successfully on numerous contracts. In 1990, the Ministry initiated a demonstration project to evaluate alternative methods of increasing the constructibility of the OGDL. The three types of OGDL placed on this project were (*a*) a 1-km section of portland cement-treated OGDL with various cement contents [cement-treated permeable base (CTPB)], (*b*) a 1-km section where no binder was used but the amount of fine aggregate passing the 4.75 mm was increased to improve the stability [untreated permeable base (UTPB)], and (*c*) the asphalt cement-treated permeable base (ATPB) as just mentioned. The design and construction details are elaborated on in this paper, and the OGDL sections are evaluated in terms of permeability, gradation, constructibility, and stability on the basis of falling weight deflectometer test results.

The presence of free water within a pavement structure can lead to the premature deterioration of a roadway (*1*). To prevent this from happening, a layer of permeable granular material can be placed within the pavement structure in order to facilitate the internal drainage. These drainage layers have proved to be highly effective in the efficient and quick dissipation of water from a pavement structure and are used by many state and provincial highway agencies (*1–3*).

The Ministry of Transportation of Ontario (MTO) requires a 100-mm thick lift of a permeable base and drainage layer referred to as an open-graded drainage layer (OGDL) to be placed directly beneath the concrete slab as part of the rigid pavement design for expressway facilities. Because the OGDL is 90 to 100 percent uniformly graded coarse aggregate, it has proved difficult to construct by conventional means.

In order to ensure the constructibility of the OGDL, 1.8 percent asphalt cement (A/C) is added to the aggregate, commonly referred to as an asphalt-treated permeable base (ATPB). Although this has proved to be successful, MTO decided to evaluate two additional techniques for improving the stability of the OGDL material without significantly affecting the layer's permeability: (*a*) the use of portland cement as a stabilizer, a cement-treated permeable base (CTPB), and (*b*) an increase in fine aggregate in an untreated OGDL, also referred to as an untreated permeable base (UTPB).

In this paper the design and construction details will be elaborated on, and these various OGDL materials will be evaluated in terms of permeability, gradation, constructibility, and load and deflection characteristics based on falling-weight-deflectometer (FWD) test results.

Ministry of Transportation of Ontario, 1201 Wilson Avenue, Downsview, Ontario, M3M 1J8, Canada.

BACKGROUND

In 1989, MTO developed new specifications requiring that a 100-mm layer of OGDL be placed beneath the concrete slab in all new rigid pavement designs. The gradation of the OGDL consists almost entirely of coarse aggregates retained on the 4.75-mm sieve. Although this provides a highly permeable drainage layer, the stability of the material is inadequate to support construction traffic without unacceptable distortion. To alleviate this problem, the OGDL has been treated with 1.8 percent A/C in order to increase the stability of the material during construction. The addition of an A/C binder has been used successfully on numerous contracts (*1*).

In 1990, MTO initiated a demonstration project to evaluate alternative methods of providing a constructible, stable, and permeable OGDL. Highway 115, where 13.4 km of a new portland cement concrete (PCC) pavement was being constructed, was chosen as the site for this demonstration project. The three types of OGDL placed on this project were

1. PCC-treated OGDL (CTPB) at various cement contents,
2. Untreated OGDL (UTPB) in which no binder was used but the amount of fine aggregate passing the 4.75 mm was increased to improve the stability, and
3. The A/C-treated OGDL (ATPB).

In order for the OGDL to function properly, it must be constructed in direct contact with a free-flowing collector system to ensure the efficient and quick removal of any free water. Also, there must be a filter layer between the OGDL and the subgrade material to prevent the intrusion and pumping of the subgrade material into the OGDL (*2,4*). On this project a geocomposite drainage system and a lift of dense-graded granular base material between the subgrade and the OGDL were specified as part of the overall design.

EXISTING CONDITIONS

Highway 115 is located near the city of Peterborough, approximately 100 km east of Toronto. Figure 1 shows the location of the project.

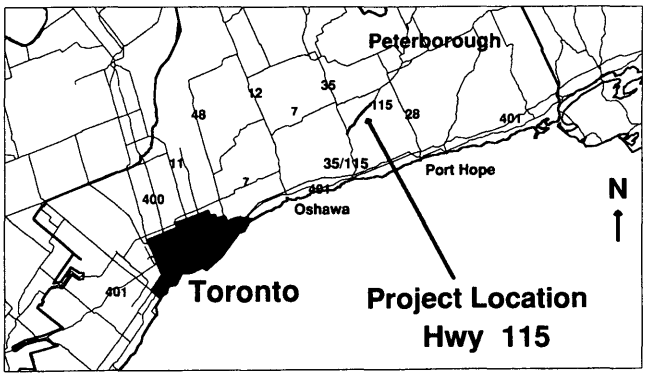

FIGURE 1 Location map.

At the time of construction, Highway 115 was a two-lane arterial highway. The new design called for the highway to be reconstructed as a four-lane divided rural freeway. The two existing lanes would become the eastbound lanes; the two westbound lanes would be new PCC pavement construction.

The annual average daily traffic (AADT) in 1991 on this section of highway was 8,800 vehicles, 8 percent of which were commercial vehicles. This represents approximately 127,000 equivalent single-axle loads (ESALs) in the design lane during 1 year.

The subgrade soils in the area consist of a fine-grained silty sand and sandy silt that is moderately to highly frost susceptible.

PAVEMENT DESIGN

The cross section of the new westbound lanes consisted of two lanes at 7.5-m width with a 0.5-m paved outside shoulder and a 1.0-m paved inside shoulder (see Figure 2 for a typical section).

The pavement structure for the new westbound lanes, shown in Figure 3, consisted of

- 200 mm jointed plain concrete pavement (JPCP) with load transfer devices;
- 100 mm OGDL, A/C treated (ATPB);
- 100 mm granular A; and
- 300 mm select subgrade material (SSM).

The purpose of the 100 mm of granular A was to act as the filter layer between the subgrade and the OGDL. Granular A is a dense-graded base course material that consists of crushed rock or gravel. The gradation for granular A is shown in Figure 4.

The SSM is a nonplastic select borrow material used to provide a uniform, non-frost-susceptible subgrade.

The existing pavement structure of Highway 115 that would become the future eastbound lanes consisted of

- 150 to 175 mm hot mix,
- 150 mm granular A, and
- 450 mm to 1.2 m sand or sandy gravel.

The 13.4-km project incorporated an ATPB throughout the project, except for a 1-km section of untreated OGDL (UTPB) and a 1-km section of CTPB. The CTPB encompassed a section 500 m long consisting of 120 kg of Type 10 portland cement/m^3 of mix and a section 500 m long with 180 kg/m^3 of mix.

The collector system designed to drain the OGDL was a premanufactured drainage system (PDS) commonly known as a geocomposite drain. The type used was a Hitek 25 manufactured by Burcan Industries. The 300-mm by 25-mm drain was placed directly in contact with the OGDL. Outlet pipes were placed every 100 m into the ditch along the edge of pavement. The typical location of the geocomposite drain within the pavement structure is shown in Figure 3.

After construction of the concrete pavement, the PDS was installed in a trench 100 mm wide excavated by a Vermeer cutter. The trench was backfilled with the compacted excavated material.

CONTRACT SPECIFICATIONS

Highlights of the construction specifications for the three OGDL materials used are as follows:

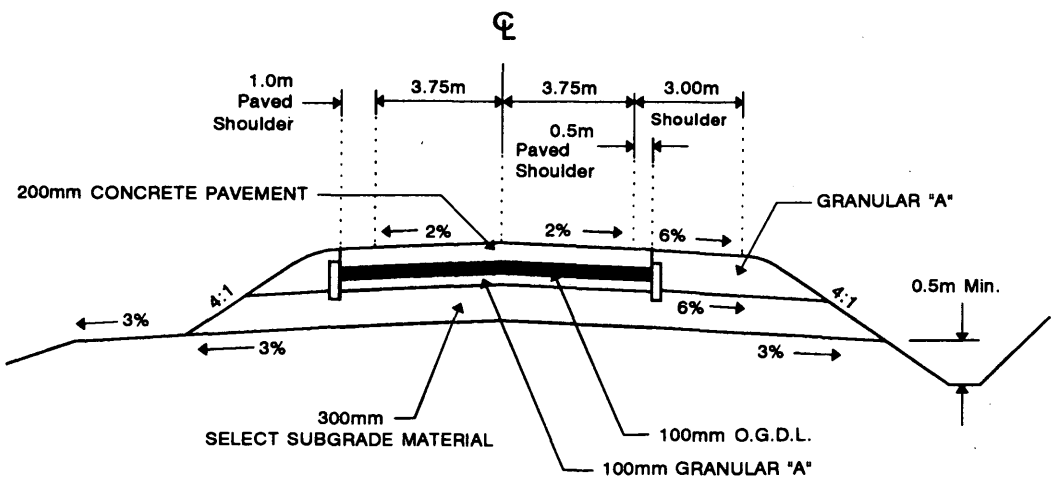

FIGURE 2 Typical cross section, Highway 115, westbound lanes.

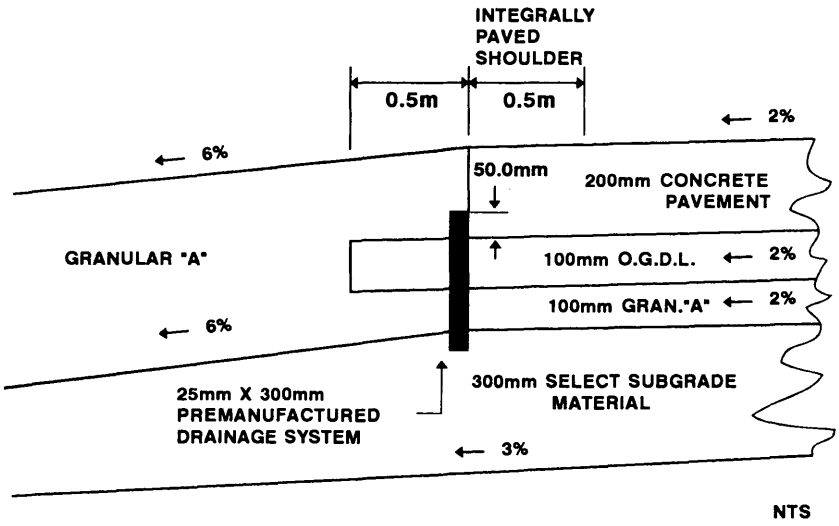

FIGURE 3 Drainage system, Highway 115.

- The aggregates should have 100 percent crushed faces produced by crushing bedrock (steel slag or reclaimed asphalt pavement should not be used).
- Construction traffic should not be permitted on the OGDL except for the paving train during placement of the overlying pavement. Haul trucks should not be allowed on the OGDL except to discharge material directly into the paver.
- The OGDL should be covered with the concrete pavement within 30 days of placement to prevent contaminations resulting from prolonged exposure. The OGDL should be protected from dirt or dust during construction.
- Compaction of the ATPB should consist of three to five passes of a class S2 roller (mass per millimeter of roll width, 4.5 kg) weighing 9 to 11 tonnes. The final compaction should be such that the OGDL can support the weight of the paving equipment. Pneumatic-tired or vibratory rollers should not be used.
- The final grade of the OGDL should not deviate more than 5 mm above or 10 mm below the specified grade and cross section. The surface of the OGDL should not deviate more than 10 mm at any place with a 3-m template. No problems were encountered during construction in meeting these tolerances.
- A Marshall mix design procedure is not required for ATPB.

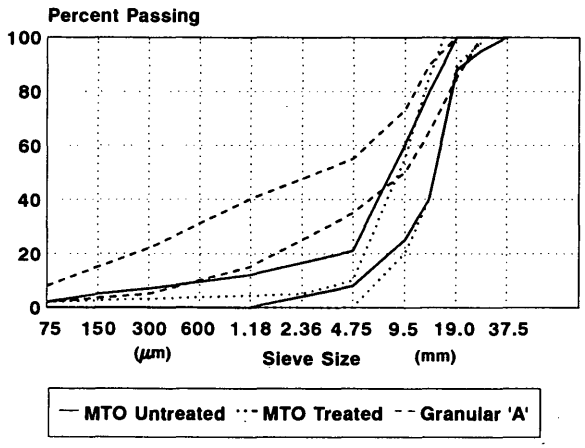

FIGURE 4 Specification limits for aggregate gradations.

CONSTRUCTION

CTPB

The contractor chose to place the CTPB with the Gamaco 3000 concrete slipform paver using a stringline for grade control. The same equipment was used to place the overlying concrete pavement (5).

A water-to-cement ratio of 0.42 to 0.43 was used for both the 120-kg/m^3 and 180-kg/m^3 mixes. Initially the lack of fines and low cement volume made it difficult to feed the material through the augers of the slipformer and caused segregation. This was solved by slowing the process down. Consolidation was achieved by activating only half the number of spud vibrators on the slipform machine. There were no noticeable differences in placing the two mixes at the two cement contents (5).

Both mixes of the CTPB appeared to be stable, well bonded, and relatively smooth after placement. There was no sloughing of the material at the edge of the pavement. During placement of the concrete pavement, minor breakdown of the surface of the OGDL was caused by the trucks carrying the concrete, especially in the section with only 120 kg/m^3; however, the section was paved last and therefore carried more accumulated truck traffic than the 180-kg/m^3 section.

Curing commenced one day after placement. It was achieved by sprinkling water from a truck-mounted tank in a fine spray every 2 hr for an 8-hr period.

ATPB

The ATPB with 1.8 percent A/C content was placed in two 50-mm lifts with a conventional hot-mix paver (Barber Green 200). It was compacted using a Dynapac CC-04 vibratory roller ballasted at 15.5

tonnes with a 2.13-m wide drum in the static mode. Although the roller used was heavier than that specified, the contractor obtained the required compaction without damaging the mat.

It is expected that stripping will occur in the ATPB over the long term, but the A/C is only a stabilizer to hold the aggregate together during construction to provide stability. It is not expected that there will be any long-term performance problems caused by stripping.

UTPB

The UTPB was placed by trucks and a grader; the final grade was achieved utilizing a profile machine. The compaction was achieved with three to five passes of a smooth drum roller. It was visually stable after compaction.

There were no problems achieving acceptable compaction levels and surface tolerances with the UTPB. Water was used sparingly to keep the dust under control and facilitate compaction.

The UTPB sloughed at the edge of the lift. This became a concern when the PDS was placed along the edge of the concrete by trenching techniques because it caused a void under the concrete slab. This void was small and is not expected to cause any short-term damage to the concrete slab, although it could result in long-term performance problems.

Cores were taken in the pavement within the UTPB section after construction, and although the profile grade of the OGDL was within specifications, the depth of the UTPB ranged from 65 to 100 mm.

EVALUATION

Laboratory Permeability Tests

At present, there is no standard laboratory test for permeability of granular materials. MTO tests the permeability of an OGDL using a Constant Head Test. The Constant Head Test (MTO Test No. LS-709) used is based on ASTM D2434 and AASHTO T-215-70 (*1*). This test utilizes proctor molds with the granular material compacted to its optimum density or a 150-mm diameter core taken in the field. The core is wrapped in paraffin wax and tested in the same manner as the proctor molds. The results from this test are useful as a relative comparison between the different granular materials, but they cannot be used as a direct comparison with the results of other permeability testing methods.

All permeability results referred to in this paper are based upon MTO's laboratory testing methodology.

TABLE 1 Average Permeability Results

	Coefficient of Permeability (cm/sec)
Untreated OGDL (UTPB) (from roadway samples)	7.5×10^{-2}
A/C-treated OGDL (ATPB) (field cores at 1.8% A/C)	8.6×10^{-2}
Cement-treated OGDL (CTPB) (field cores)	5.9×10^{-2}
Aggregate for treated OGDL (aggregate from stockpile)	6.3×10^{-2}

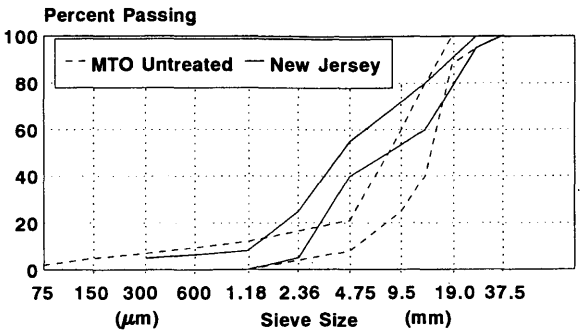

FIGURE 5 Gradations for UTPB: MTO versus New Jersey.

The average permeability test results are shown in Table 1. The ATPB had the highest permeability as determined from cores, 8.6 10^{-2} cm/sec, whereas the UTPB from roadway samples had comparative results at 7.5 10^{-2} cm/sec. Samples of the aggregate used for the CTPB and ATPB from the stockpile were also tested. The aggregate had permeability results of 6.3 10^{-2} cm/sec. The CTPB cores had the lowest permeability, 5.9 10^{-2} cm/sec.

The granular A used as a filter material has results ranging from 2 10^{-2} cm/sec to 2 10^{-6} cm/sec depending upon where the gradation falls within the allowable band for granular A (*1,2*) as shown in Figure 4.

Ideally the permeability of a granular base should be on the order of 10^{-4} cm/sec or greater (*6*). An OGDL layer should have a permeability on the order of 10^{-2} cm/sec (*6*).

The results of MTO's permeability testing are an order of magnitude less than the test results reported in FHWA-TS-80-224. The difference is due to different laboratory testing procedures. Figure 5 shows the New Jersey gradation for UTPB and Figure 6 shows the AASHTO 57 gradation for a treated OGDL; both are compared with the MTO required gradation. Figures 5 and 6 show slight differences between the gradations, indicating that the two materials would have similar permeabilities.

Extraction Tests

Extraction tests were carried out on the cores taken from the ATPB. The A/C content of the cores ranged from 1.52 to 1.73 percent. This is slightly less than the required 1.8 percent A/C, however, the specification does allow for a ± 0.2 percent deviation from this requirement.

Aggregate Gradation

Figure 4 compares the requirements of the untreated, treated, and granular A (filter layer) gradation bands. The treated and untreated bands are similar in the coarse aggregate range but differ in that the untreated allows more fine material for stability. The granular A band is much wider and much more uniformly graded than the OGDL gradation bands.

Gradation tests were completed on the aggregate samples from the stockpile used for both the ATPB and the CTPB. Tests were also carried out on the cores taken from the ATPB. For obvious

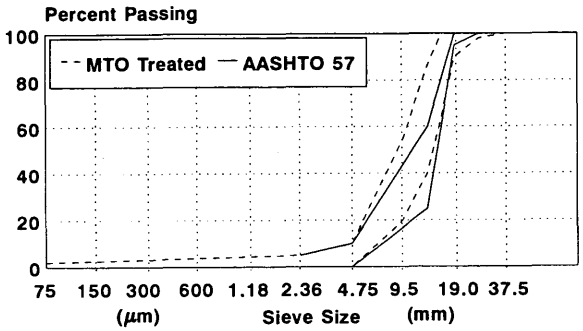

FIGURE 6 Gradations for treated OGDL: MTO versus AASHTO 57.

reasons, it was not possible to do gradation testing on the cores taken from the CTPB. Tests were also done on the UTPB aggregate from field samples. These results are shown in Table 2.

The results indicate that the aggregate gradations meet specifications except for the ATPB from cores. The 2.36 sieve is out by +0.1 percent and the 0.075 sieve is out by +0.5 percent. Both of these encroachments are minimal.

The gradation curves for the averages of all samples are shown in Figures 7 and 8.

Aggregate Quality Testing

The limestone aggregate used for both the untreated and treated OGDL was from the Buckhorn Quarry, approximately 20 km north of Peterborough. The material was specified to meet the requirements of a medium-quality hot-mix aggregate. Table 3 shows the test results for the untreated and treated aggregate. All test requirements were met. The aggregate was 100 percent crushed from bedrock. Previous test sites where OGDL was placed using a crushed gravel proved to be very unstable and difficult to compact even with the addition of A/C as a stabilizer.

Although the aggregate used for both the treated and untreated OGDL was from the same quarry, it was obtained from separate stockpiles because of the different gradations. This could be an explanation for the differences between the quality testing results.

Pavement Drainage

In addition to the laboratory testing of the OGDL materials, a full-scale field evaluation of the subdrainage system performance was conducted about a year after construction. The field evaluation was done by introducing a controlled quantity of water into the OGDL material through a core hole in the PCC pavement and observing water discharge rates at outlets. The procedure effectively engaged the OGDL (both its permeability and cross-sectional slope), permeability of granular material underneath the OGDL, interface between the OGDL and the PDS, the PDS (flow capacity and longitudinal slope), and, finally, the function of the outlet pipes.

The full-scale testing was motivated in part by a concern for the relative impermeability of the backfill material used during the PDS installation. The installation was completed using a modified Vermeer trencher and the excavated material was used as backfill. The backfill consisted of a mixture of granular A, pieces of OGDL material, and select subgrade material. The permeability results obtained previously for this mixture had a coefficient of permeability of about $1.0 + 10^{-4}$ cm/sec. The low-permeability backfill material can contaminate the interface between the OGDL and the PDS since the installation trench wall is rough. The rough surface creates a space in front of the PDS that can be filled with backfill fines.

Testing Procedure

To achieve a significant inflow rate, a hole with a diameter of 15 cm was cored through the PCC pavement and the OGDL in the right traffic lane. The results reported here are for core holes located 2.3 m from the PDS (cross-sectional distance) and about 12 m from the nearest downstream outlet (longitudinal distance). The pavement grade (longitudinal slope) ranged from 1 to 1.5 percent. The pavement elevation was about 1 m above the terrain. Only the ATPB and CTPB sections were evaluated using the above arrangement. It was not possible to establish a corresponding location for the UTPB.

The inflow rate of water poured into the core hole was maintained constant at 22 L/min throughout the main portion of the test. The system could easily accommodate the inflow rate of 22 L/min without flooding the OGDL material (i.e., the water level was well below the bottom of the concrete slab). Precautions were

TABLE 2 OGDL Aggregate Gradation

Sieve Size		Untreated, % Passing		Treated, % Passing		
Millimeters	Inches	MTO Requirements	Field Samples (n = 3)	MTO Requirements	A/C-Treated from Cores (n = 3)	Aggregate from Stockpile (n = 3)
37.5	1 1/2	100	100			
26.5	1	95–100	100	98–100	100	100
19.0	3/4	88–10	97.9	90–10	98.9	95.7
13.2	1/2	40–80	72.0	40–86	67.7	64.2
9.5	3/8	25–60	49.7	20–55	36.5	33.9
4.75	No. 4	8–21	12.7	0–10	7.9	3.0
1.18	No. 16	0–12	2.9	N/A	4.0	1.4
0.300	No. 50	0–7	1.7	N/A	3.1	1.0
0.150	No. 100	0–5	1.4	N/A	2.9	0.9
0.075	No. 200	0–2	1.0	0–2	2.55	0.8

taken to minimize erosion of the granular materials by the water poured into the hole. Overall, the field testing procedure used can objectively evaluate the performance of the whole pavement drainage system.

Results

Both the ATPB and the CTPB sections exhibited similar performance. After the inflow started, it took 25 to 27 min before water appeared at the downstream outlets and 40 to 47 min before the outflow reached a relatively steady discharge rate of 8.6 to 9.6 L/min. When the inflow rate was increased from 22 to about 25 L/min, the reaction time to the increased flow at the outlet was about 2.5 to 4 min. After the inflow was stopped, water continued to discharge for 19 to 29 min.

From the total inflow of 22 L/min, less than 50 percent of the flow was reaching the outlet pipes despite the fact that the inflow was only 12 m from an outlet (outlets were spaced at about 100-m intervals) and the longitudinal grade of the pavement was at least 1 percent. The difference in the input and output flows was draining by alternative means even though the underlying granular A has much lower permeability than the OGDL material or the geotextile covering the PDS. In general, the amount of water retained in the pavement structure depends not only on the permeability of the material below the OGDL, but also on the interface between the OGDL and the PDS.

It may be argued that the results of the full-scale testing are undesirable since more than 50 percent of the water fails to reach the outlets and penetrates the pavement structure. However, there are no comparable results for other types of subdrainage systems incorporating OGDL. To further test the influence of the interface between the OGDL and the PDS, the MTO is now installing a PDS in a trench backfilled with a manufactured sand with high permeability. The results of the full-scale performance testing of this system incorporating high-permeability backfill, as well as results from other drainage systems, would enable a better interpretation of the existing results.

FWD Testing

Deflection testing was done utilizing the FWD in order to determine the load and deflection characteristics of the OGDL. Measurements were taken at 10-m intervals in the outside wheel path of the driving lane on the granular A layer; on the surface of the CTPB, the UTPB, and ATPB; and on the surface of the concrete pavement.

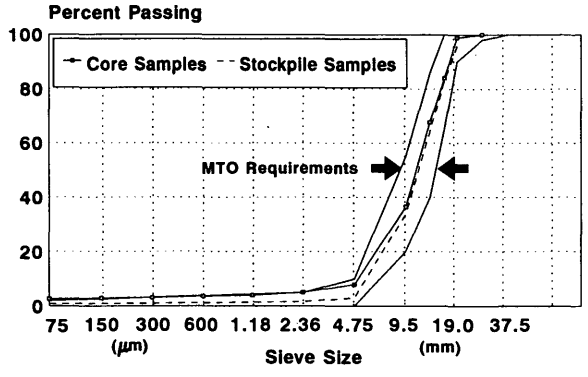

FIGURE 7 Gradation curves for treated OGDL aggregate.

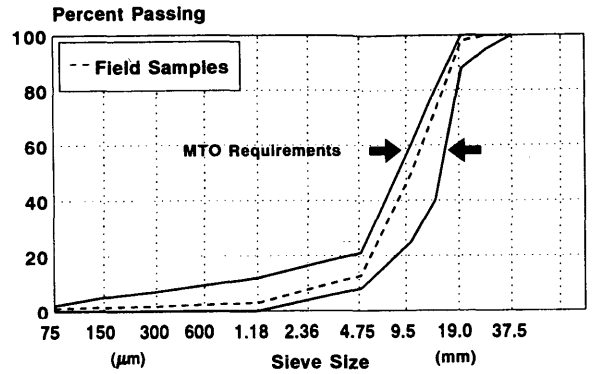

FIGURE 8 Gradation curves for UTPB aggregate.

Tests on the granular A were done using a 450-mm diameter loading plate. A 300-mm diameter loading plate was used for the various OGDL and concrete pavement layers. The deflection data are based on a normalized 40-kN dynamic load and are reported without a temperature correction factor. Tests were done from May 29, 1992, to July 19, 1992. Additional FWD testing was done on the concrete pavement on July 6, 1993. These new tests were taken in the center of every fifth slab (approximately every 20 m).

It is difficult to reliably determine the moduli of the different pavement layers from the data collected through backcalculation, because the programs available are limited in their ability to calculate the moduli of granular layers and of layers beneath a rigid concrete layer. For this reason, the results of FWD testing are reported as average peak deflections.

Shown in Figure 9 are the average peak surface deflections of the various layers for all three types of OGDLs. The deflections give an indication of the comparative strength and stability of the different layers. Because of the difference in the size of the load-

TABLE 3 OGDL Aggregate: Physical Requirements and Test Results

	MTO Lab Test No.	MTO Requirements	Untreated Aggregate	Treated Aggregate
Los Angeles abrasion, % maximum loss	LS-603	35	27	28
Magnesium sulfate soundness, 5 cycles, % maximum loss	LS-606	12	1	4
Petrographic number, maximum	LS-609	160	106	101
Flat and elongated particles, % maximum	LS-608	20	N/A	17
Freeze-thaw maximum loss %	LS-614	10	9	N/A

NOTE: N/A = not available.

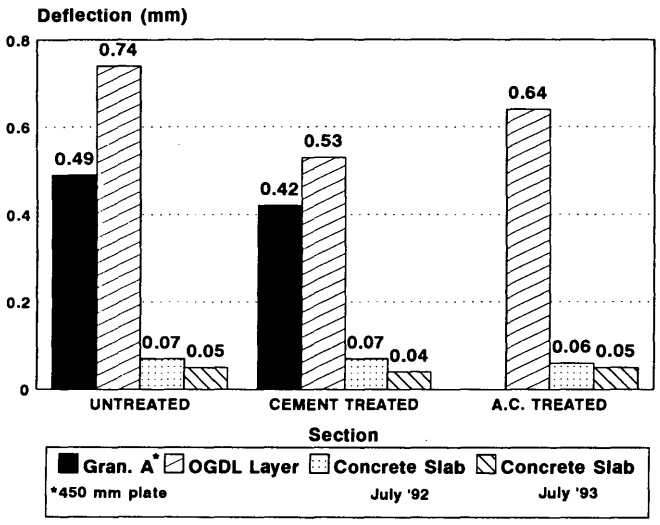

FIGURE 9 Average deflection measurements.

ing plates, the results for the granular A layer should not be compared with those shown for other material layers. The granular A results are similar under the UTPB and CTPB. The CTPB has the highest modulus with an average deflection of 0.53 mm, whereas the UTPB has the highest deflection, 0.73 mm, indicating the lowest modulus. The ATPB with a deflection of 0.64 mm is in between.

The concrete slab deflections from the June 1992 testing ranged from 0.07 to 0.06 mm for all sections. The deflections of the concrete slab taken a year later range from 0.04 to 0.05 mm. It is not expected that a 200-mm thick concrete slab would be affected by minor variation in the deflection characteristics of the various underlying OGDL layers, although the long-term performance of the concrete pavement would be influenced by an unstable or nonuniform base layer.

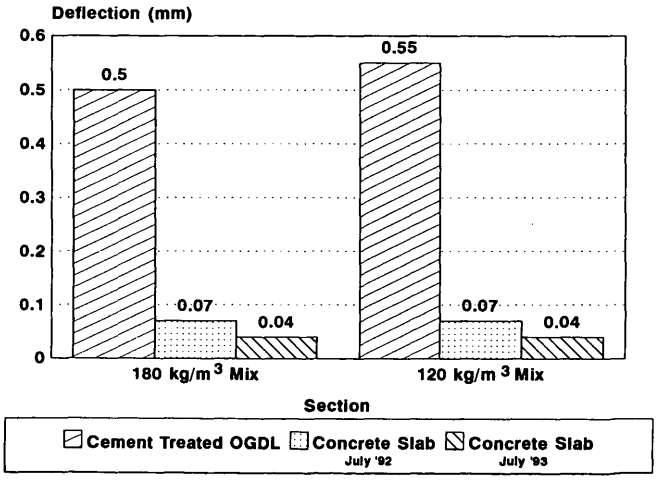

FIGURE 10 CTPB deflection measurements.

Figure 10 indicates the difference in deflections between the two CTPB mixes. As anticipated, the results indicate that the deflections for the 180-kg/m^3 mix are slightly lower than those for the 120-kg/m^3 mix based on deflection values, but both are higher than those for the UTPB or ATPB (Figure 9).

CONCLUSIONS

The following conclusions have been made:

- All three types of OGDL met the requirements for permeability and stability; that is, the OGDL mat was able to carry construction traffic without any significant damage or break-up.
- The FWD measurements indicate that the deflection of the CTPB is 17 percent less than that of the ATPB and some 28 percent less than that of the UTPB. On the basis of these values, a similar strength characteristic (modulus) relationship would exist among the three materials.
- The relative rigidity of the concrete pavement based on the FWD measurements is not expected to be affected by the type of OGDL used.
- The placement of the ATPB and CTPB layers within acceptable tolerances may require a slight adjustment to conventional construction practices but requires no specialized equipment.
- The overall performance of the pavement drainage system can be objectively evaluated by the field drainage test; however, more comparative data are required for reliable interpretation of the results.
- There is a concern with sloughing that occurs at the edges of the UTPB (at the edge of the 0.5-m paved shoulder), nonuniform thickness, as well as its somewhat lower strength characteristic as indicated by the deflection testing.
- The 1.8 percent A/C provides adequate stability to the OGDL aggregate accommodating construction practices and equipment.
- The gradations of both the untreated and treated OGDL aggregates provide excellent permeability.
- There appear to be no significant differences between the 180-kg/m^3 and 120-kg/m^3 cement-treated OGDL mixes with regard to construction, permeability, and strength characteristics.

RECOMMENDATIONS

The following recommendations are made:

- The contractor should be allowed to choose between an ATPB and a CTPB on selected projects. This would allow the contractor to choose the most economical materials and methods of construction available.
- The cement content of the CTPB should be specified as 120 kg/m^3.
- The placement and use of the UTPB need to be reviewed further. It appears that it is impractical to use this material with a collector system that is installed by a trenching operation. Preinstallation of the collector system and backfilling with a permeable filter material are required. The minimum depth of UTPB should be increased to 150 mm to address inaccuracies in placement operations.

REFERENCES

1. Marks, P., J. Hajek, H. Sturm, and T. Kazmierowski. Ontario's Experience with Pavement Drainage Layers. Presented at TAC Conference 1992, Quebec City, Sept. 1992.
2. Bathurst, R. J., and G. P. Raymond. *Stability of Open Graded Drainage Layers (Phase I) Final Report*. Royal Military College of Canada; Queen's University, Sept. 1989.
3. Baldwin, J. S. Use of Open Graded, Free Draining Layers in Pavement Systems: A National Synthesis Report. In *Transportation Research Record 1121*, TRB, National Research Council, Washington, D.C., 1987.
4. Kazmierowski, T., and A. Bradbury. Ten Year Evaluation of Experimental Concrete Pavement Sections in Ontario. In *Proceedings of the 5th Annual Conference on Concrete Pavement Design and Rehabilitation,* April 1993.
5. Weremi, A. *Construction Techniques Used in Placing Open Graded Drainage Layer*. Internal Report. Ministry of Transportation of Ontario, Quality Assurance Section, Central Region, 1992.
6. Senior, S. New Developments in Specifications for Road Base Materials in Ontario. *45th Canadian Geotechnical Conference Proceedings, Canadian Geotechnical Society,* Oct. 1992.

Publication of this paper sponsored by Committee on Subsurface Drainage.

Development and Comparison of Permeability Measurement Techniques for Jointed Concrete Pavement Bases

ANDREW BODOCSI, ISSAM A. MINKARAH, ANTHONY AMICON, AND RAJAGOPAL S. ARUDI

Prior research has shown that a well-drained base is a very important requirement for preserving the soundness of a highway pavement. Although adequate knowledge exists to guide an engineer in the design of a new pavement with good drainage characteristics, there are no established methods to estimate the quality of drainage under an existing pavement and therefore to estimate its life expectancy or to properly design its overlay. A summary is presented of research efforts aimed at investigating and adapting existing techniques from the geotechnical area for the development of methods for measuring the permeability of pavement bases. Two geotechnical methods were adapted, and one new technique was developed. The first two methods were used to conduct permeability tests near the middle of the pavement slabs, using either constant head or falling head setups. These were named the Midslab Constant Head Test Permeability Test and the Midslab Falling Head Permeability Test, respectively. The third method was designed for conducting permeability tests near the edge of a slab. This method was named the Edge-of-Slab Constant Head Permeability Test. Numerous permeability tests were conducted under a jointed reinforced concrete test pavement in Chillicothe, Ohio, using these three methods. It was found that the tests conducted near the edge of the slab held the most promise, even though the method needs further refinements. However, the results of the edge-of-slab test were quite different from those of the midslab test, partly because of the erosion of fines from the base in the edge-of-slab test. In addition, it became clear from the tests that the field test results were considerably different from laboratory test results.

A well-drained base is of utmost importance for highway pavements. Cedergren (*1*) in 1978 estimated that the lack of proper drainage of infiltrated water from the nation's highway pavements would cost U.S. taxpayers more than $200 billion in just 15 years. The AASHTO design guide (*2*) recognizes the importance of pavement drainage in its thickness design procedures by accounting for the quality of drainage and for the period of time during which the pavement section is exposed to moisture. However, the design guide does not help the engineer with criteria to establish what good quality drainage entails, especially when the rehabilitation of an existing pavement is in question. Nonetheless, engineering judgment points to the permeability of the base as one of the most important factors in pavement drainage.

The literature survey on the permeability of bases found several articles and references on the subject. Moulton and Seals (*3,4*) presented permeability testing methods applicable to the field measurement of permeability of newly placed bases and subbases before the pavement is placed on them. They designed a special permeameter device that is placed on (or driven into) the surface portion of the base or subbase. The method is not applicable to existing pavements.

There is also FHWA Demonstration Project 87 (*5*), which was designed to assist highway agencies in using new techniques in their design of permeable bases for concrete pavements.

The literature survey did not reveal accepted field procedures for finding the in-field permeability of existing base courses under concrete pavements. Therefore, concurrent with other research on a test pavement in Chillicothe, Ohio (*6*), a great deal of effort was spent on the development of appropriate in-field test procedures for finding the permeability of the base. Three different methods were tried and their results compared.

The test pavement on which permeability tests were conducted was built by the Ohio Department of Transportation in 1972 (*7*). It is a 983-m (3,225-ft) jointed portland cement concrete (JPCC) section in the southbound roadway on Route 23 in Chillicothe, Ohio. The pavement consists of two lanes 3.7 m (12 ft) wide separated by a longitudinal joint. The test section has 100 transverse joints. All slabs are 229 mm (9.0 in.) thick, and, except for a short segment, they are reinforced with wire mesh. The pavement is underlain by an embankment approximately 6.1 m (20 ft) high. Several variables were incorporated in the pavement: various joint spacings, type of base, type of dowel bar, and configuration of the saw cut. Table 1 gives details on the various sections of the pavement. The concrete slabs were supported on either a 191-mm (7.5-in.) thick granular base (Grade A, 310 material) or a 102-mm (4.0-in.) thick, Item 301 Bituminous Aggregate Base (ATB). Researchers at the University of Cincinnati studied the pavement between 1972 and 1980 and again between 1989 and 1992. Permeability tests were conducted only in the second phase of the study.

Although the test pavement was not designed for the purpose of evaluating the parameters that affect pavement drainage, the researchers undertook the task of investigating the as-is drainage characteristics of the portion of the pavement that was supported on granular base. From construction plans and field exploration, it was found that the test pavement had an edge collector drain consisting of one trench for the southbound two lanes, filled with pea gravel, and a drainpipe at the bottom.

In the permeability phase of the study, measurements were made on the granular base and the embankment subgrade material. The granular base was studied in both the laboratory and the field, whereas the embankment material was only tested in the laboratory. The permeability tests on the embankment were conducted

A. Bodocsi, I. A. Minkarah, and R. S. Arudi, Department of Civil and Environmental Engineering, University of Cincinnati, ML 0071, Cincinnati, Ohio 54221-0071. A. Amicon, H. C. Nutting Co., Cincinnati, Ohio.

TABLE 1 Details of Sections with Type of Joints, Base, and Dowel Bars

Section	Joint #	Number of Slabs	Slab Length m(feet)	Type of Base	Type of Dowels	Type of Joint (Depth & Type of Sawcut)
1	1 to 7	7	12.2(40)	Granular	Standard	3.2mm(1/8") Bevel
2	8 to 16	8	12.2(40)	Granular	Standard	6.4mm(1/4") Standard
3	17 to 24	8	6.4(21)	Stabilized	Standard	6.4mm(1/4") Standard
4	25 to 34	10	12.2(40)	Stabilized	Standard	6.4mm(1/4") Standard
5	35 to 44	11	5.2(17)	Stabilized	None	6.4mm(1/4") Standard
6	45 to 53	9	6.4(21)	Granular	Plastic Coated	6.4mm(1/4") Standard
7	54 to 63	10	12.2(40)	Granular	Plastic Coated	6.4mm(1/4") Standard
8	64 to 73	10	12.2(40)	Granular	Standard	12.7(1/2") Standard
9	74 to 84	10	12.2(40)	Granular	Standard	6.4mm(1/4") Standard
10	85 to 94	10	6.4(21)	Granular	Standard	6.4mm(1/4") Standard
11	95 to 96	2	12.2(40)	Granular	3M Coated	6.4mm(1/4") Standard
12	97 to 100	4	12.2(40)	Granular	Standard	6.4mm(1/4") Standard

Note: 1 m = 3.281 ft
1 mm = 0.0394 inch

to ascertain that it was much less pervious than the base, ensuring that water would flow only in the base during field tests.

The testing program started with in-field density tests and sampling of the base and subgrade materials for classification and Modified Proctor density tests. Laboratory permeability specimens were prepared, and permeability tests were run. Concurrently, field permeability tests were conducted on the ase at nine different locations along both lanes of the test pavement.

Pertinent details of the laboratory and field tests on the base and subgrade materials are presented in this paper, and the permeability test methods that were tried are evaluated.

MATERIALS AND METHODS

Field Sampling and Density Testing

A number of field samples were taken to conduct laboratory index, maximum density, and permeability tests. The base samples were taken at the edge of the pavement from locations directly under a joint or a crack. The sample locations are given in Table 2.

Two subgrade (embankment) samples were taken. Subgrade Sample 1 was taken from an area immediately below the pavement base near the location of Base Sample 7. Subgrade Sample 2 was obtained from a depth between 0.61 to 1.22 m (2.0 to 4.0 ft) below the surface of an area within the median adjacent to the shoulder at Joint 50.

In-place density determinations were made by a nuclear density meter on the base and the subgrade near the location of Base Sample 7.

Laboratory Soil Testing

Grain Size Distribution

Grain size distribution tests on the base and subgrade materials were performed in accordance with ASTM D-422. The sieve analysis results were used to obtain the percentages of gravel, sand, and fines (silt and clay) in each sample using Ohio Department of Transportation Classification Standards.

Modified Proctor Moisture-Density Tests

The Modified Proctor moisture-density relationship was determined for each of the base and subgrade samples according to ASTM D-698 standard procedures.

TABLE 2 Base Sample Designations and Locations

Sample #	Joint Location	Lane
1	14	Passing
2	45-1*	Passing
3	52	Driving
4	59	Driving
5	81	Passing
6	82	Passing
7	95-1*	Passing

Note: * indicates that the sample was taken at the first pavement crack south of the indicated joint, like Joint 45 or 95.

Laboratory Permeability

Laboratory permeability tests were performed on the base and subgrade samples. The test specimens were compacted in a 102-mm (4.0-in.) diameter Proctor test mold at optimum moisture content. The actual densities of the samples ranged between 91 and 99 percent of their Modified Proctor density. The permeability tests were conducted after the complete saturation of the samples in a falling head permeability test apparatus using deaired water. Each specimen was tested until its equilibrium permeability was reached.

Field Permeability Testing

Field permeability tests were conducted at nine selected locations in the test pavement. Specifically, tests were conducted under the pavement approximately midway between the following joints: 11 and 12, 46 and 47, 52 and 53, 56 and 57, 59 and 60, 80 and 81, 81 and 82, 94 and 95, and 95 and 96 (see Table 1 to identify the type of slab under which each test was conducted). As seen, these locations covered the length of the test pavement on granular base. All field permeability tests were conducted under segments that were in good to very good condition. Even though some of the slabs tested had shrinkage cracks, all permeability tests were conducted away from these cracks. Namely, if a test was run on a slab that was cracked, such as the slabs between joints 11 and 12, 56 and 57, 80 and 81, and 95 and 96, the test site was located midway between a crack and the joint or between two adjacent cracks.

Three different field test methods were used. The first two were designed to conduct permeability tests near the middle of the pavement slabs. They were named the Midslab Constant Head Permeability Test and the Midslab Falling Head Permeability Test, respectively. The third method was designed to test the permeability near the edge of the pavement. This method was named the Edge-of-Slab Constant Head Permeability Test.

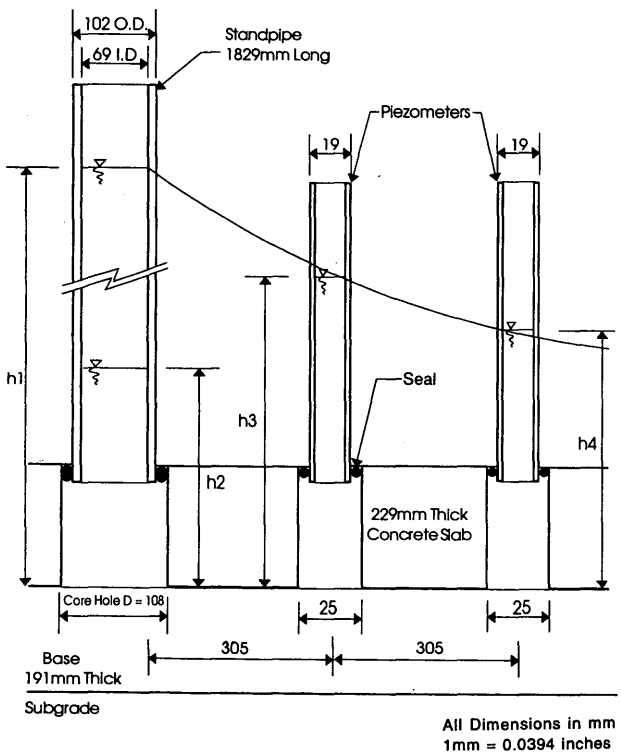

FIGURE 1 Side view of the midslab permeability test setup.

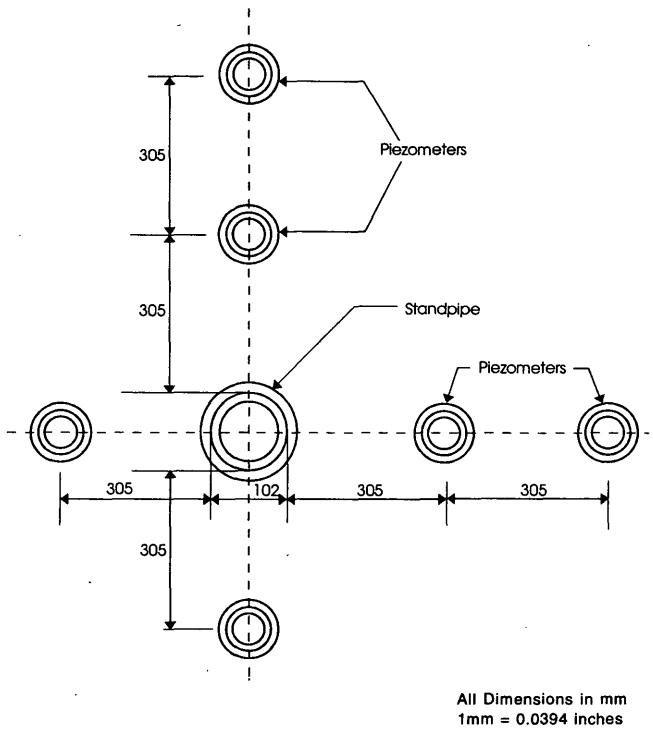

FIGURE 2 Plan view of midslab permeability test setup.

To initiate a Midslab Constant Head Permeability Test at a selected location, a 108-mm (4.25-in.) diameter hole was cored through the slab, and six 25-mm (1.0-in.) diameter holes were drilled through the slab adjacent to the core hole as shown in Figures 1 and 2. The holes were carefully cleaned of loose dirt. Into the core hole a 102-mm (4.0-in.) O.D. and 69-mm (2.719-in.) I.D., 1.83-m (6.0-ft) long acrylic tube was inserted. Acrylic tubes 19 mm (0.75 in.) O.D. and 0.6 m (2.0 ft) long were inserted in the 25-mm (1.0-in.) holes. The 102-mm (4.0-in.) tube served as a standpipe, and the 19-mm (0.75-in.) tubes were used as piezometers. The annular space between the tubes and the pavement was carefully sealed with rubber rings to prevent loss of water.

The tap water for running the tests was provided by Ohio Department of Transportation personnel from a 1.14-m^3 (300-gal) truck-mounted tank. The water was hosed by gravity into 3.8-L (1-gal) containers and then slowly poured into the 102-mm (4.0-in.) standpipe, carefully maintaining a constant head.

To find the permeability of the base material, the following formula was used:

$$k = Q(L)/dh(A)(t)$$

where

k = permeability of the base,
dh = average head drop between the inner and outer set of standpipes,

Q = measured quantity of outflow during time t,
A = cylindrical area of base section through which flow occurs between two sets of standpipes, and
L = radial distance between standpipes, typically 0.305 m (12 in.), as seen in Figures 1 and 2.

The tests at each location were conducted with two different standpipe heads. For each head, trial runs were conducted until the permeability reached equilibrium. The equilibrium water levels in the piezometers were recorded, together with the time it took to pour 1 gal of water into the standpipe.

The second field test, the Midslab Falling Head Permeability Test, was conducted with a falling water head in the standpipe. The equipment and technique were almost identical to those of the first method (see Figures 1 and 2) except that after the standpipe was filled, the time was measured for a selected drop in the water level in the tube and no attention was paid to the water level in the piezometers.

The permeability of the base was computed from the formula by Hvorslev (*8*), as presented by Daniel (*9*):

$$k = 3.14d^2 (\ln h_1 - \ln h_2)/11(D)(t)$$

where

d = inside diameter of the tube,
D = diameter of core hole in pavement slab,
h_1, h_2 = head levels in standpipe at beginning and end of test, respectively, and
t = time duration of measurement (see Figures 1 and 2).

The third field test method, the Edge-of-Slab Constant Head Permeability Test, was conducted near the edge of the pavement slab. In this method, three standpipes were installed on a line approximately 0.91 m (3.0 ft) away from the pavement edge in holes cored through the concrete pavement and spaced at 0.61 m (2.0 ft) center to center. Each standpipe was an acrylic tube with 102-mm (4.0-in.) O.D., 69-mm (2.72-in.) I.D., and 1.83 m (6.0 ft) long. At the edge of the pavement, the shoulder was excavated and a filter fabric was placed on the exposed vertical face of the base. Against the fabric, an outflow collection box was installed. Figures 3 and 4 show the position of the tubes and the collection box. The permeability measurements were made by filling the three pipes to a predetermined elevation and then maintaining this level and observing the time required for a specific quantity of outflow at the edge of the pavement. The outflow was measured in the middle 152 mm (6.0 in.) of the 0.457-m (18-in.) wide outflow collection box. The role of the water from the outer two standpipes was to laterally confine and channel the flow from the center tube toward the edge of the pavement and into the 152-mm (6.0-in.) center portion of the outflow collection box. Part of the outflow from the side tubes was collected in the two side segments of the outflow box.

The permeability of the base was computed by the following formula:

$$k = Q(L)/dh(A)(t)$$

where

Q = outflow into collection box over selected time t,
L = distance between edge of pavement slab and center of three standpipes,

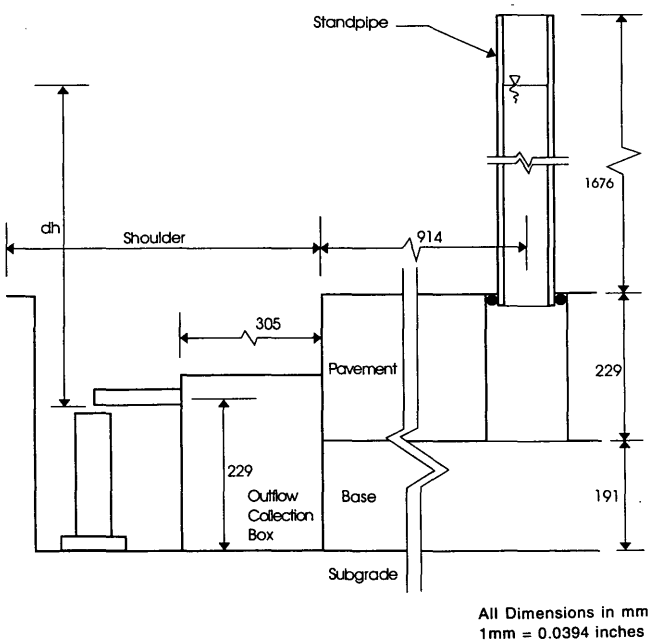

FIGURE 3 Side view of the edge-of slab permeability test setup.

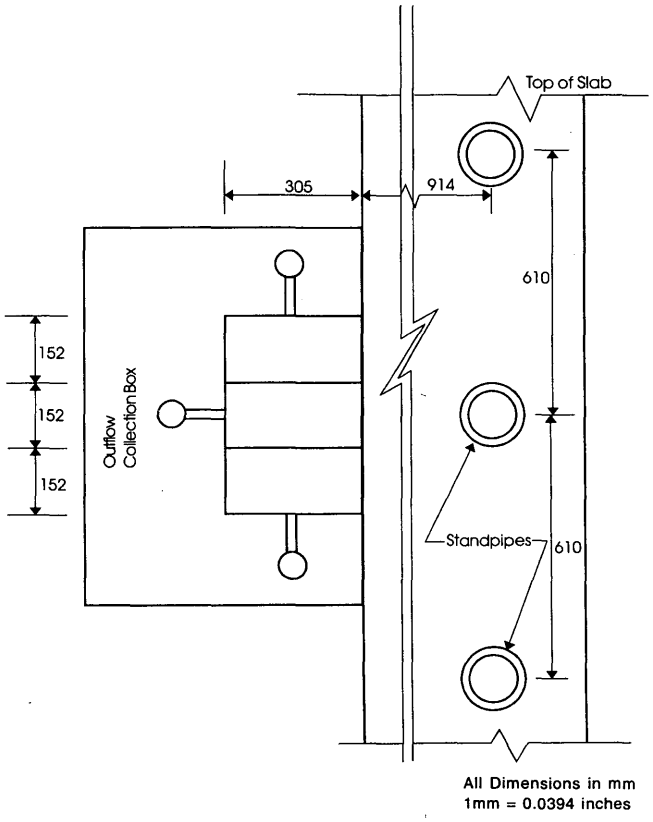

FIGURE 4 Top view of the edge-of slab permeability test setup.

A = cross-sectional area of monitored flow channel, typically 152 mm (6.0 in.) wide by 229 mm (9.0 in.) high, and
dh = difference in head between water levels in tubes and outflow box.

In all three test procedures, it was assumed that water would flow down the standpipe tube or tubes, through the core hole, and then turn to spread out horizontally in the base material between the bottom of the concrete slab and the top of the subgrade. Since the subgrade had a permeability three orders lower than that of the base, it was assumed that it practically provided an impervious bottom boundary to the flow.

In every case, numerous trials were conducted. The reported values were from test results in which the permeability had equilibrated.

RESULTS

In-Field Density Tests

Two tests were performed in both the base and the subgrade. The average in-place dry density of the base material was 20.56 kN/m^3 (130.8 pcf), with a natural moisture content of 7.9 percent. The average subgrade dry density was 20.22 kN/m^3 (128.6 pcf), with a natural moisture content of 7.6 percent.

Index Test Results

From the grain size distribution data on seven base samples and using the Unified Soil Classification System, the base material can be described either as sand with silt and gravel or as silty sand with gravel. The fines content (silt and clay) ranged between 7 and 15 percent.

The subgrade soil samples (embankment soil) contained more silt and clay particles than the base material. The two samples had 16 and 27 percent silt and clay size particles, respectively. According to the Unified Soil Classification System, the samples may be described as silty sand with gravel.

The average maximum dry density of the base was found to be 21.20 kN/m^3 (134.9 pcf) with an average optimum moisture content of 7.1 percent. On the basis of the in-place density measurement near Base Sample 7, the pavement base was compacted to approximately 97 percent of its maximum Modified Proctor density.

Laboratory Permeability Test Results

The laboratory permeability tests on the subgrade soil gave values that ranged between 6.9×10^{-8} and 3.5×10^{-6} cm/sec (6.9×10^{-10} and 3.5×10^{-8} m/sec or 2.0×10^{-4} and 0.9×10^{-2} ft/day), with an average value of 2.6×10^{-7} cm/sec (2.6×10^{-9} m/sec or 0.74×10^{-3} ft/day). This indicated that the subgrade is quite impervious and capable of confining the drainage to the base course.

The laboratory permeability tests on the base material gave a wide variation in values. The probable reasons for this may have been the air trapped in the samples and, potentially, variations in the percentage of fines in the base material. The permeability values varied from 1.8×10^{-6} to 5.6×10^{-4} cm/sec (1.8×10^{-8} to 5.6×10^{-6} m/sec or 5.1×10^{-3} to 1.6 ft/day). The mean permeability value for the base samples was found to be 0.74×10^{-4} cm/sec (0.74×10^{-6} m/sec or 2.1×10^{-1} ft/day) when the material was compacted to between 97 and 100 percent Modified Proctor density.

Field Permeability Test Results

The results from the Midslab Constant Head Permeability Test are given in Table 3. These data show that the permeability of the base is surprisingly uniform over the full extent of the test pavement. With an average permeability value of 3.9×10^{-3} cm/sec, the maimum deviation was found to be only 1.8×10^{-3} cm/sec (1.8×10^{-5} m/sec or 5.1 ft/day). Also note that the use of two different heads gave practically identical permeability values.

The field permeability results for the base by the Midslab Falling Head Permeability Test are given in Table 4. The average permeability was found to be 3.9×10^{-3} cm/sec (3.9×10^{-5} m/sec or 11.1 ft/day), which is identical to the average permeability test results found from the constant head test. Similarly, the maimum deviation from the average was only 2.2×10^{-3} cm/sec (2.2×10^{-5} m/sec or 6.2 ft/day). Also, the two test sets with different heads gave very similar results.

It is important to note that the above two midslab permeability tests gave practically identical results that were fairly uniform along the full length of the test pavement.

The location and results of the four edge-of-slab constant head tests are given in Table 5. It is seen that the edge-of-slab permeability test results are about two orders of magnitude higher than those from the midslab tests. However, the edge-of-slab test results from different locations on the test pavement were again consistent, with a maximum deviation of only 1.6×10^{-1} cm/sec (1.6×10^{-3} m/sec or 4.5×10^{2} ft/day) from the average.

TABLE 3 Base Permeabilities from Midslab Constant Head Test

Location (between the joints given below)	Permeability with Head A, (cm/s)	Permeability with Head B, (cm/s)
11-12	2.1×10^{-3}	1.7×10^{-3}
46-47	3.6×10^{-3}	-
56-57	4.4×10^{-3}	-
80-81	5.7×10^{-3}	5.7×10^{-3}
Average (all joints):	3.9×10^{-3} (11.1 ft/day)	

Note: 1 cm/s = 0.01 m/s = 2.835×10^{3} ft/day

TABLE 4 Base Permeabilities from Midslab Falling Head Test

Location (between the joints given below)	Permeability with Head A, (cm/s)	Permeability with Head B, (cm/s)
11-12	2.3×10^{-3}	1.7×10^{-3}
46-47	4.4×10^{-3}	-
56-57	3.9×10^{-3}	-
80-81	5.7×10^{-3}	5.7×10^{-3}
95-96	3.0×10^{-3}	-
Average (all joints):	3.9×10^{-3} (11.1 ft/day)	

ANALYSIS

Both midslab test results show a remarkable consistency along the full length of the test pavement. Also, there was good consistency between the results from tests with two different heads. Comparison of the results from the midslab constant head and falling head permeability tests revealed that the average values from the two were identical at 3.9×10^{-3} cm/sec (3.9×10^{-5} m/sec or 11.1 ft/day).

The edge-of-slab test was designed to simplify the flow pattern in the base and to increase the accuracy of the permeability test. This was achieved by the simple geometry of flow with well-defined boundaries. The method gave consistent values along the length of the test pavement, but the values were considerably higher than those from the midslab tests. Namely, the edge-of-slab test gave an average permeability of 2.0×10^{-1} cm/sec (2.0×10^{-3} m/sec or 5.7×10^{2} ft/day), versus the midslab test average of 3.9×10^{-3} cm/sec (3.9×10^{-5} m/sec or 11.1 ft/day). There may be several reasons for this difference. The edge-of-slab permeability may have been higher than the midslab permeability because of observed erosion of the finer particles from the base near the edge and the potential slumping of the base material under the pavement edge during the test. Conversely, it is possible that the permeability of the base at midslab is lower than that at the edge because of deposits of fines in this area from infiltrating rainwater and its slow flow. The low quantity of flow near the midslab may also result in a state of partial saturation with entrapped air, thus in lower permeability. This state of partial saturation may have prevailed during field testing, even though close to 1.14 m^3 (300 gal) of water was used for a typical test. At this time it is difficult to reconcile the difference between test results from the two methods. Most probably the true base permeability lies between the results from the two tests, and perhaps both types of tests should be run routinely.

It is believed that the edge-of slab test holds great promise, but more field research is needed to refine it. One aspect of the test that needs improvement is the leakproofing of the contact surface between the outflow collection box and the base material to increase the accuracy of outflow measurement. Also, a well-designed filter fabric should be used on the contact surface to minimize the erosion of fines. Another way of improving the method would be to make the outflow collection box very sturdy and to drive it firmly into the base at the edge of the pavement slab. This would ensure a tight fit between the box and the base that would eliminate slumping. Measuring the outflow while maintaining an equilibrium water level in the three sections of the box was difficult. Specifically, the water levels had to be kept constant and at the same elevation to prevent crossflow among the three sections.

In general, there is a need to consider a less destructive approach for the field tests. Drilling smaller holes through the pavement and using smaller-diameter standpipes may be one way of achieving this.

The laboratory permeability results yielded values that were considerably lower than those of the three types of field tests. One cause may have been that in the laboratory samples, air was trapped in the voids that blocked the flow. Another explanation may be that the laboratory samples were taken from an area near the joints where the base material may have contained more fines than the area under the slab, resulting in lower permeability. Yet another reason may be the existence of flow channels between the base and the bottom of the pavement, causing the higher field permeability. In a similar vein, another reason for higher field permeability may be the separation between the pavement slab

TABLE 5 Base Permeabilities from Edge-of-Slab Constant Head Test

Location (between joints given below)	Permeability (cm/s)
52-53	3.6×10^{-1}
59-60	2.6×10^{-1}
81-81	0.8×10^{-1}
94-95	$1.1 \times ^{-1}$
Average (all joints):	2.0×10^{-1} cm/s (5.7×10^{2} ft/day)

Note: 1 cm/s = 0.01 m/s = 2.835×10^{3} ft/day)

and the base during curling caused by temperature gradients. This could have caused sheet flow just below the slab, especially near the midslab at midday, at which point and time most of the field permeability tests were conducted.

The above differences point to the necessity of field tests. Even if laboratory tests are conducted on carefully obtained samples, the tests just cannot simulate the in situ conditions, such as air content, accumulation of fines, and flow channels.

CONCLUSIONS

No established field methods are currently available to determine the in situ permeability of the base under an existing pavement. This research made moderate progress in identifying and testing some of the promising field methods that may be used for base permeability tests.

The use of the methods that were investigated is limited to cases in which the base has a considerably higher permeability than the underlying subgrade. This condition is necessary in order to confine the flow to the base.

In principle, both midslab and edge-of-slab tests should measure the permeability of the base to an acceptable level of accuracy. Yet there was a large difference in the permeabilities found at midslab and at the edge of the pavement. As described in the analysis section, this difference may be caused by entrapped air or flow under the middle of the slab or by erosion of fines and slumping of the base at the edge of the slab and the consequent increase in flow rate. Through engineering judgment, it is estimated that the field permeability of the base tested lies between the values obtained from the two test methods (midslab and edge-of-slab). However, it is recommended that for design purposes the more critical midslab permeability value be used.

In the authors' opinion, the edge-of-slab constant head test needs further investigation and refinement. It would be the favored method since the geometry and mechanism of flow are relatively simple and fully tractable. It is recommended that the contact area between the outflow collection box and the base material be provided with a well-designed filter fabric to minimize the erosion of fines from the base. Also, the use of a small water head is recommended for the same reason. In addition, the collection box could be made sturdier and driven into the base at the edge of the pavement slab to ensure minimum disturbance to the base and provide a tight outflow surface. Furthermore, smaller standpipes should be used to reduce the size of the cored holes in the pavement and the resulting damage.

It will be necessary to narrow the difference between laboratory and field permeability test results. Ways to do this may include increased care in sampling and careful preparation of permeability samples, such as compacting them under water to ensure complete saturation. It is recommended that companion testing be done on the base material in each area (midslab and edge-of-slab) by both field and laboratory methods. It is also recommended that laboratory samples be taken from the area to be tested before and after the field tests to observe any changes in their fines content and, potentially, to run laboratory permeability tests on both types of samples.

This research produced some interesting findings, but it also showed considerable discrepancies in the results between the two main field methods, as well as between field and laboratory testing. It also emphasized the fact that laboratory tests are not adequate in characterizing the base material and that field permeability tests are necessary. The results indicate that further research should be conducted to improve the consistency between the two main methods of field testing (midslab and edge-of-slab) and to attempt to narrow the difference between the laboratory and field permeability data.

ACKNOWLEDGMENTS

The funding for this project was provided by the Ohio Department of Transportation (ODOT). The authors gratefully acknowledge the assistance of William F. Edwards, Engineer of Research and Development at ODOT, for his support throughout this project. Thanks are also due the staff of ODOT's District 4 for their able assistance in the field.

REFERENCES

1. Cedergren, H. R. Poor Pavement Drainage Could Cost $15 Billion Yearly. *Engineering News Record*, June 8, 1978.
2. *AASHTO Guide for Design of Pavement Structures.* American Association of State Highway and Transportation Officials, Washington, D.C., 1992.
3. Moulton, L. K., and R. K. Seals. *In Situ Determination of Permeability of Bases and Subbases, Phase 1, Interim Report.* Report FHWA-RD-78-21. FHWA, U.S. Department of Transportation, 1977.
4. Moulton, L. K., and R. K. Seals. *Determination of the In Situ Permeability of Base and Subbase Courses, Phase 2, Final Report.* Report FHWA-RD-79-88. FHWA, U.S. Department of Transportation, 1979.
5. *Drainable Pavement Systems.* Participant Notebook, Demonstration Project 87. Publication FHWA-SA-92-008, FHWA, U.S. Department of Transportation, March 1992.
6. Minkarah, I. A., A. Bodocsi, R. A. Miller, and R. Arudi. *Final Evaluation of the Field Performance of ROS 23 Experimental Concrete Pavement.* Draft Final Report. Ohio Department of Transportation, Columbus, Dec. 1992.
7. Minkarah, I. A., J. P. Cook, and J. F. McDonough. *Determination of Importance of Various Parameters on Performance of Rigid Pavement Joints.* Final Report. Ohio Department of Transportation, Columbus, Aug. 1981.
8. Hvorslev, M. J. *Time Lag in the Observation of Ground-Water Levels and Pressures.* U.S. Army Engineer Waterways Experiment Station, Vicksburg, Miss., 1949.
9. Daniel, D. E. In Situ Hydraulic Conductivity Tests for Compacted Clay. *Journal of Geotechnical Engineering,* ASCE, Vol. 115, No. 9, 1989, pp. 1205–1226.

Publication of this paper sponsored by Committee on Subsurface Drainage.

PART 2

Soil-Fluid Interface Phenomena

Accelerated Groundwater Transport Studies Using a Geotechnical Centrifuge

THOMAS F. ZIMMIE, ANIRBAN DE, AND MAHADZER B. MAHMUD

The use of a geotechnical centrifuge permits the simulation of long-term groundwater flow conditions through tests on scale models. In a centrifuge, relatively large soil samples can be tested under the same stress conditions as in the prototype. This allows for a more realistic representation of field conditions than is possible in small-scale laboratory experiments. In cases of contaminant migration through relatively impermeable soils, the times of interest span decades and even centuries. The scaling relations can be utilized in solving specific problems of groundwater flow through saturated soil and also to calibrate numerical models that can then be used for prediction purposes. The scaling relationships are established and the results are illustrated through an experiment in modeling of models. Two case studies simulating long-term contaminant migration through soil are presented. In the first, the transport of radioactive contaminants through groundwater was modeled. Geiger-Mueller detectors were used to observe the migration of the radionuclides. This is a nonintrusive method of observation that does not interfere with the normal flow of water through the soil medium. The second case study deals with the behavior of different types of landfill cover materials. Specifically the long-term behavior of paper sludge as a cover material was studied. Thirty years of prototype behavior was simulated in centrifuge tests on two types of paper sludges and on a clay cover used as a control material.

Conventional field and laboratory testing procedures are often found to be inadequate for cases of long-term flow of groundwater through relatively impermeable soil layers. Also, the stress levels existing in test samples are often only a fraction of what exists in the field. In addition, the small size of laboratory samples excludes most of the heterogeneity of in situ soil conditions.

Geotechnical centrifuges can be used to perform tests on models that represent full-scale prototypes under normal field conditions. A $1/N$ scale model tested at centrifugal acceleration N times the earth's gravity experiences stress conditions identical with those in the prototype. Processes of groundwater flow through saturated soil—for example, in cases of consolidation and diffusionoccur N^2 times faster in a centrifuge model. This scaling permits modeling of phenomena that last extremely long prototype times. Prototype times on the order of several decades to several centuries are of interest in various problems of contaminant migration, for example, sanitary landfills and low- or medium-level radioactive waste disposal. Many geotechnical centrifuges in use today are capable of simulating more than 100 years of prototype flow by means of model tests lasting only 24 hr.

In the following sections, the concept of scaling groundwater flow processes is presented. The relationship is later utilized in two case studies related to contaminant migration through soil.

Department of Civil and Environmental Engineering, Rensselaer Polytechnic Institute, Troy, N.Y. 12180.

CENTRIFUGE SCALING RELATIONS

Laminar flow of fluid through a saturated porous medium is governed by Darcy's law as follows:

$$v = ki \tag{1}$$

where

v = approach velocity,
k = Darcy's coefficient of permeability, and
i = hydraulic gradient.

In a centrifuge, stress conditions that are identical with those at corresponding points in the prototype are simulated in a $1/N$ model subjected to N g's when the model and the prototype have the same geometric and material properties and boundary conditions.

To understand the scaling of seepage velocity and time of flow, a conventional laboratory $1/N$ scale model at 1 g environment is considered. This model experiences the same acceleration field (namely 1 g) as the prototype but has all the linear dimensions reduced by a factor of N. This means that in the case of groundwater flow problems, the size of the flow paths as well as the water levels in the model will be $1/N$ times that of the prototype. The shape of flow nets will, of course, be the same as that in the prototype. Also, since both the model and the prototype are subjected to the same 1 g acceleration field, the velocity of flow in the two cases will be the same.

Since the length of flow paths has been scaled as $1/N$ in the model, the same velocity (as that of the prototype) will cause the time taken by the flow to be N times shorter than that in the model, that is,

$$\frac{t_m}{t_p} = \frac{l_m}{l_p} = \frac{1}{N} \tag{2}$$

where subscripts m and p refer to model and prototype, respectively. It should be noted that since no use has been made of Darcy's law (Equation 1) so far, Equation 2 is independent of flow conditions (laminar or turbulent).

Next, the model is considered to be subjected to an acceleration field that is N times the 1 g acceleration on the earth. The high g-field causes the velocity of flow to be N times the velocity at the 1 g field, that is,

$$v_m = Nv_p \tag{3}$$

Using Equation 1 to express the condition with a $1/N$ model at N g-field,

$$v_m = Nki \tag{4}$$

Although it is easily demonstrated that the velocity scales by the same factor as the centrifugal acceleration, it is an arbitrary choice whether to consider this as due to an increase in Darcy's coefficient of permeability (k) or an increase in the hydraulic gradient (i) from the prototype to the model. Pokrovsky and Fyodorov (*1*) and Cargill and Ko (*2*) have considered the expression for coefficient of permeability,

$$k = \frac{Kg}{\nu} \tag{5}$$

where

K = intrinsic permeability,
g = acceleration due to gravity at earth's surface, and
n = kinematic viscosity of the fluid.

Thus they considered k to vary in direct proportion to g. In this case the hydraulic gradient, i, is considered constant from the model to the prototype. Schofield (*3*) and Goodings (*4*), on the other hand, consider the hydraulic gradient to change since a model experiences a drop in the full prototype head over a reduced (model) seepage path. Here the coefficient of permeability, k, is considered a material property that remains constant from prototype to model.

Tan and Scott (*5*) have suggested treating the term g in Equation 5 as a constant of magnitude equal to the usual value on the earth's surface and multiplying the whole right-hand side of Equation 1 by a necessary scaling factor when cases at g levels other than normal are considered. The other suggestion put forth by Tan and Scott (*5*) is to express Darcy's law in a pressure gradient form using the intrinsic permeability and viscosity.

Following from Equations 2 and 3 for a case in which a reduced scale model is subjected to a higher acceleration, the ratio of time in the model to time in the prototype can be written as follows:

$$\frac{t_m}{t_p} = \frac{1}{N^2} \tag{6}$$

Equation 6 represents the scaling law for time in cases of laminar fluid flow through a saturated medium.

MODELING OF MODELS AT VARIOUS g-LEVELS

The validity of scaling relations, as well as the performance of models at different high g-environments, can be verified by a methodology commonly referred to as modeling of models. Equation 6 was derived for a case in which where the model has a linear scale $1/N$ times that of the prototype and is subjected to an acceleration N times that of the prototype. When modeling-of-models experiments are performed, there may actually be no prototype since the same model is subjected to different acceleration levels on the centrifuge. Making the necessary modification to Equation 6 (i.e., $l_m = l_p$), the required scaling relation in this case is

$$\frac{t_m}{t_p} = \frac{1}{N} \tag{7}$$

The experimental setup shown in Figure 1 was utilized for the modeling of models. A sheetpile was embedded in the soil and the flow of water through saturated soil from one side (at higher head) to the other was observed. Ottawa sand was used as the soil medium. Colored dyes were injected on the upstream side to observe the flow lines. Three flow lines—A, B, and C—are shown. The model consisted of a 406-mm by 229-mm by 76-mm Plexiglas box containing sand to a height of 152 mm. A 100-mm long sheetpile was introduced, with 40 mm embedded in the soil.

Experiments were conducted at accelerations of 1, 20, 25, and 30 g. Water levels at upstream and downstream sides were maintained constant during the course of each experiment. The geometry of the flow paths and the time of flow were monitored during the tests.

According to Equation 7, the time for flow is inversely proportional to the acceleration during the test. So in modeling-of-model tests run at different accelerations, the time for flow to

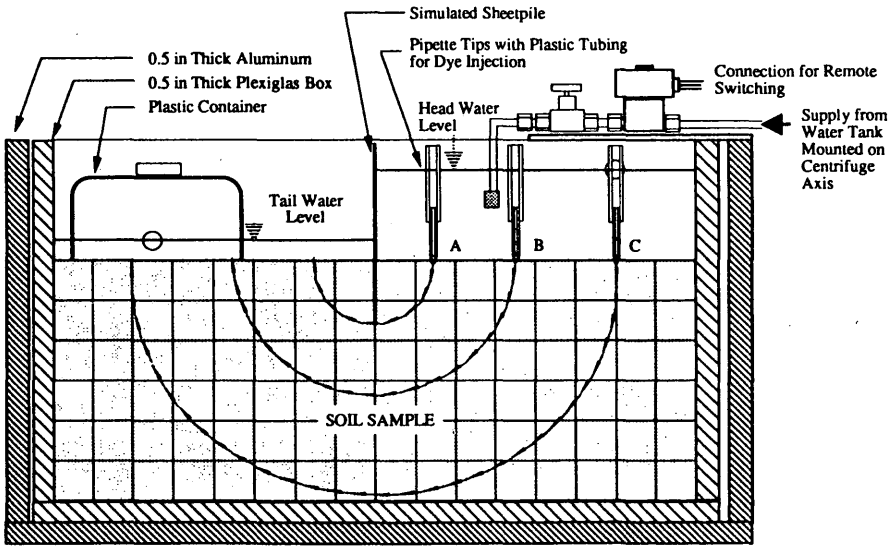

FIGURE 1 Experimental setup of model tests on simulated sheetpile.

occur will be an inverse ratio of the accelerations. That is,

$$\frac{t_2}{t_1} = \frac{N_1}{N_2} \tag{8}$$

where the subscripts indicate Tests 1 and 2. It should be noted that the same model is used in both experiments, and the time of flow between the same two points is measured in both cases. The condition of laminar flow is obeyed in both cases.

Figure 2 is a graph of the modeling validation presented above. The ratio of acceleration levels (N_1/N_2) and the inverse ratio of the time of flow (t_2/t_1) are plotted on a logarithmic scale. The points represent the ratios measured from tests with colored dyes along paths A and B at various g-levels. The theoretical line shown in Figure 2 is the plot of Equation 8.

It may be noted that although most points lie on or near the theoretical line, there is some deviation in the case of points representing times of travel for dye on Line A at higher N_1/N_2 ratios. These points represent the ratios from tests at higher g-levels (20, 25, and 30) with those from 1 g. The deviation may be attributed to a higher percentage of error in measuring the travel time of Line A than that of Line B. Line A is the shorter of the two lines, and at higher g levels the time of travel was reduced to about 1 min. The fact that the flow was observed visually and that the dye dispersed slightly in the direction normal to the flow path led to some error in the observed time of flow. Flow Line B was longer than Line A, and consequentially had a lower percentage error. This can be seen in Figure 2, where the points for Line B are seen to lie on or close to the theoretical curve.

The above application of modeling of models confirmed the scaling laws for seepage, which could then be utilized in more complex tests. Two different case studies using accelerated physical modeling will be presented here.

APPLICATION TO CONTAMINANT TRANSPORT PROBLEMS

The scaling relations for the time of seepage as the square of the scale factor (and the g-level) expressed in Equation 6 can be utilized to observe fluid transport phenomena that normally occur over long periods of time. Equation 6 can be used to show that a 1-day experiment on a 1/200 model at 200 g can model over 100 years of prototype behavior, since

$t_p = N^2 t_m$ (from Equation 6)

$= 200^2 \times 1$ days (where $N = 200$)

$= 40{,}000$ days

≈ 109.6 years

Time spans of such magnitude are commonly of interest in cases of the migration of contaminants through soils with relatively low coefficients of permeability.

Two case studies, for which experiments were performed, will be presented here. The first deals with the migration of radioactive waste materials in groundwater following a repository leakage. The second studies the long-term consolidation and seepage behavior of different types of landfill cover materials. Both experiments were performed on the 100 Gton geotechnical centrifuge at Rensselaer Polytechnic Institute.

Radioactive Waste Migration Through Soil

Much time and effort has been devoted to developing methodologies for radioactive waste disposal. Often radioactive wastes are disposed of by burial either in land-based engineered trenches or

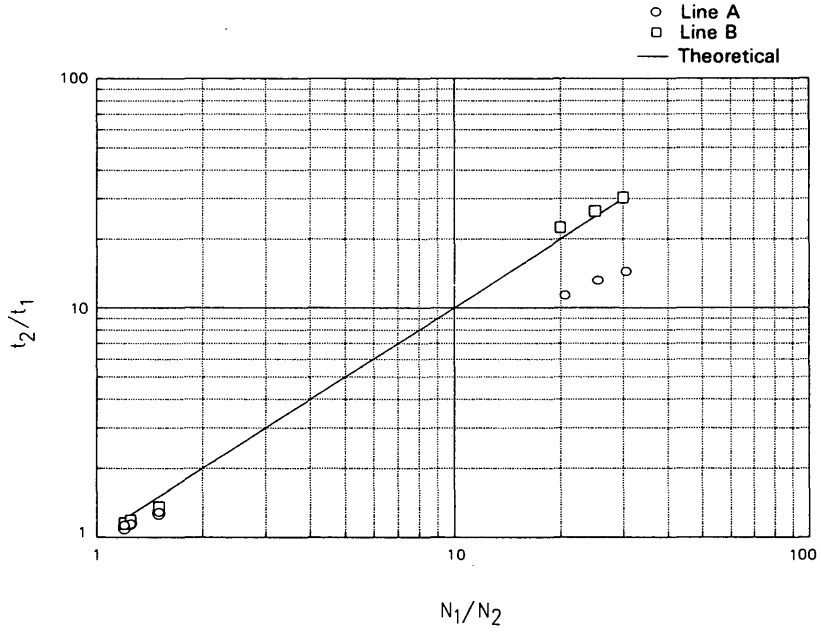

FIGURE 2 Graph showing modeling of seepage at different g-levels on centrifuge.

in deep ocean bed sediments (*6*). In either case, the repositories are best located in geologic deposits of low permeability. Besides the containment units, which are designed to prevent leakage, the low-permeability soil layers surrounding the repositories act as a series of barriers to the release of radionuclides into the environment.

Many radioactive waste species contain elements with very long half-lives and thus remain potentially hazardous over extended periods of time. The transport of the hazardous waste through the soil following a repository leakage is extremely slow because of the very low permeabilities of the soils surrounding the sites. Migrations of this nature can take several centuries to occur and hence make physical site observations impossible. A geotechnical centrifuge provides a suitable means for observing such long-term prototype behavior via accelerated physical modeling.

The experiments presented here were performed on a small-scale two-dimensional flow model as a pilot study to observe the technique of accelerated migration of radioactive materials in groundwater.

In the tests, radioactive species Iodine 131 (I^{131}) was allowed to migrate under a constant head through saturated silt soil that had a coefficient of permeability of approximately 5.6×10^{-6} cm/sec. The migration of I^{131} was detected using an array of nine end-window type Geiger-Mueller (G-M) tubes located on the outer side of the model box.

Figure 3 [from Zimmie et al. (*7*)] shows the cross-sectional view of the general setup of the model in a rectangular box. A two-dimensional flow condition was simulated, with the migrating species injected on the top center of the soil layer and drainage provided at the two bottom extremities. To ensure two-dimensional flow, the drains had sand cores running normal to the flow direction. Tests were run at 60 *g* for 5 hr, simulating prototype times of more than 2 years.

Besides the tests performed actually using the radioactive tracer, the flow pattern was verified visually in a separate test using potassium permanganate ($KMnO_4$) tracer as a colored dye. Figure 4 shows the flow pattern in this test and the location of the nine G-M tubes.

The G-M tubes used were of the end window type, TGM N205, with a 12.7-mm diameter thin mica window and a thickness of approximately 2 to 3 mg/cm^2. The 15-mm diameter by 41.9-mm length of completely sealed tube is filled with neon and halogen gases and is suitable for the detection of alpha, beta, and gamma radiation. This type of detector lacks the ability to provide information about the energy and type of radiation (*8*). Thus, known sources of radiation must be used as tracers. The advantages of this type of detector include insensitivity to small fluctuations in applied voltage, durability, and low cost, which make it particularly suitable for use in centrifuge experiments.

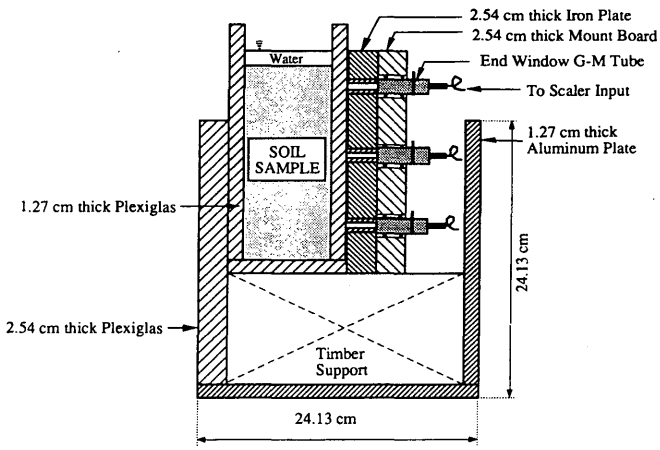

FIGURE 3 Experimental setup for tests on migration of radioactive contaminants (*7*).

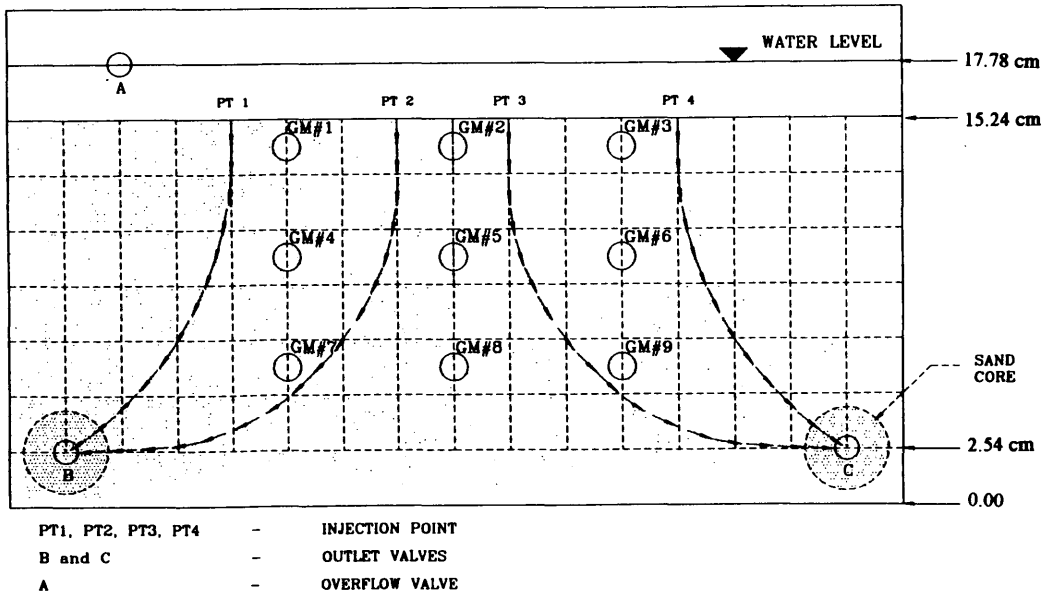

FIGURE 4 Observed flow paths of dye with respect to injection Points 1, 2, 3, and 4. Tests performed on the two-dimensional flow model at 60 *g*.

The low-voltage signals from the G-M tubes were monitored using scalers and an oscilloscope. The total counts from the tubes relative to the initial activities of the radioactive sources were plotted versus time as migration occurred. Figure 5 is a plot of the relative count with time for GM-2 and GM-7. The two points, 2 and 7, lie on the line PT 2 to B in Figure 4. The time of travel between the two points is given by the time between peaks for G-M tubes 2 and 7.

The plots in Figure 5 show some scattering. This is primarily due to the low radioactive dosage used in the study, which resulted in poor counting statistics. An initial activity of a few thousand counts per second is most desirable. However, as the counts increase, the danger from the radioactivity increases, and safety must be a consideration. Since these were pilot tests, it was not deemed necessary to use high levels of radioactivity. In spite of the low counts, the trends shown in the plots were as expected and were used to study the migration pattern of the radioactive tracer.

Good agreement between the travel times for radioactive tracer and colored dye tracers indicates insignificant sorption or attenuation of the radioactive species in the soil. A detailed description of the test process as well as discussions of the results have been presented by Mahmud (*9*).

The use of a geotechnical centrifuge in the study of contaminant migration allows the observation of behavior that spans long prototype times. Computer models used to analytically solve contaminant migration problems can be calibrated and validated using results from such experiments. The use of radioactive tracers and Geiger-Mueller detectors to observe the migration provides a means of observation that does not interfere with the natural flow pattern in the model. Such nonintrusive observation methods can be adopted for use in other studies as well. For example, to study the migration of nonradioactive contaminants, a radioactive tracer can be used to spike the pollutant of interest. After proper calibration, the measurements of tracer radioactivity can be used to determine the concentration of the migrating species. This can be done while the model is in flight, during a centrifuge test, without requiring either sample collection or chemical analyses. It is difficult to do in-flight chemical analyses.

Long-Term Behavior of Landfill Cover Materials

The long-term behavior of cover materials (impermeable barriers) for landfills was simulated in a series of experiments. The materials tested included clay, which is commonly used as the impermeable barrier layer in covers, and two different types of paper sludge, which are potential candidates for the same use.

Each test was performed at 105 *g* for a 24-hr period and, according to the scaling relations expressed in Equation 6, simulated 30 years of prototype cover behavior related to consolidation and leachate transport. The tests were conducted in a sample box 914 mm by 610 mm by 356 mm in size.

Figure 6 shows a schematic diagram of the experimental setup. The test sample consisted of a 76-mm thick layer of the cover material (clay or paper sludge) laid over a 152-mm layer of clean sand and separated from the sand by a layer of geotextile. The sand layer was compacted to nearly its maximum density and was designed to hold the leachate flowing through the cover material during the course of the experiment. The geotextile was used to prevent the clay and sludge from entering into the sand layer and clogging it. During each test, 76 mm of water was impounded on top of the cover material.

As stated previously in Equation 2, the ratio of the lengths of prototype to model is equal to the centrifugal acceleration. Accordingly, to model a typical prototype landfill cover that is 60 cm in thickness at 105 *g*, it would be necessary to build model covers about 60/105 and about 0.5 cm thick. This is not a practical thickness considering workability during model building, and the chance of leakage during the test is very high for such a thin layer. Also several liters of leachate were required to do the necessary chemical analyses. The appropriate cover thickness used in the models was selected on the basis of these criteria.

The consolidation characteristics of a soil are not functions of the thickness of the test sample. Hence in the tests performed, the coefficients of consolidation, compressibility, and volume change are not dependent on the proper scaling of cover thickness for the prototype to model.

The instrumentation on the sample consisted of linear variable differential transformers (LVDTs) on the surface of the cover and pore pressure transducers to measure the pore-water pressures at the mid-depth of the cover. The change in water level on top of the sample cover was monitored using a float mechanism attached to an LVDT. Typical settlement versus time curves (on a log scale) for the three cover materials at 105 *g* are shown in Figure 7. The spikes in two of the curves were caused when the centrifuge was stopped to add water or to correct machine imbalance, causing the surface to rebound. Once the centrifuge restarted and the model returned to 105 *g*, the settlement proceeded as a continuation of the previous curve, as can be seen in Figure 7. In case of Sludge 2, the centrifuge acceleration was reduced and maintained below 105 *g* in an attempt to reduce the machine imbalance. Following this, the machine was stopped. This explains the apparent discontinuity in the curve for Sludge 2 before and after the stoppage.

In Figure 7 the settlement reading at the beginning of the experiment at 105 *g* is taken as the initial value, and all subsequent settlements are obtained by subtracting this initial reading. This convention was followed in all the tests. As expected, the two sludges are found to be more compressible than the clay. The values of pore-water pressures at the center of the cover are plotted in Figure 8. As in Figure 7, the spikes in the curves indicate

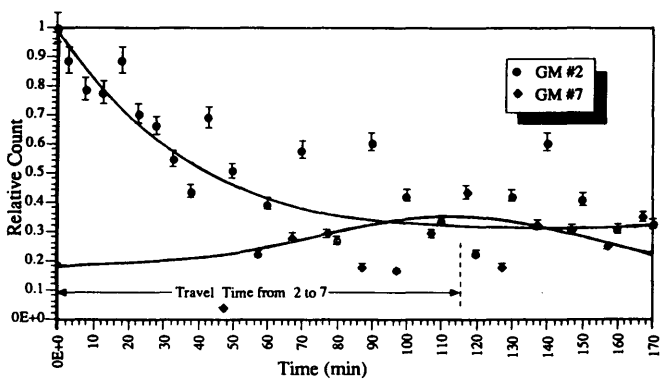

FIGURE 5 Plot of the relative counts for G-M 2 and G-M 7: distance from peak to peak denotes travel time between Point 2 and Point 7 along Flow Line 2-B; error bars represent standard deviations.

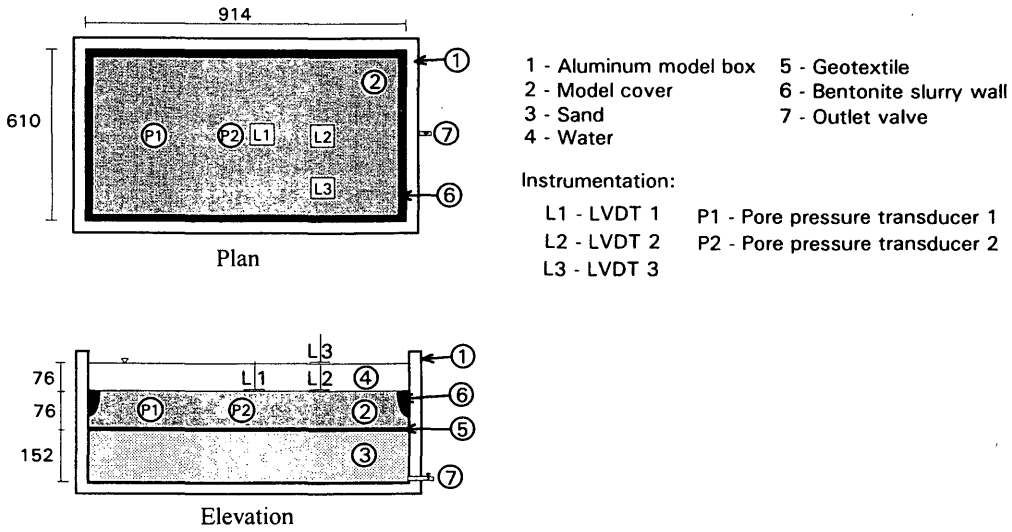

FIGURE 6 Experimental setup for tests on landfill covers.

times when the centrifuge was stopped and, consequently, the pore pressures reduced.

The change in water level on top of the cover with time indicated the rate at which water infiltrated through each of the cover materials. Some water was also lost to evaporation (since the sample rotated at about 184 rpm during the experiment). A separate test was run with only water in the box, and the drop in water level with time due to evaporation alone was measured.

Figure 9 shows changes in water level versus time, corrected for evaporation, for all three cover materials. Results from only the first 6 hr are shown.

Figure 9 may be considered indicative of the seepage characteristic of the three cover materials under identical conditions (compaction, thickness, and head of water). The clay cover is found to be the least permeable, with a coefficient of permeability of 4×10^{-8} cm/sec at 1 *g*. The plot in Figure 9 for the clay cover has an almost constant slope, indicating a constant value of permeability throughout the test. This is as expected, since there is little settlement in the clay, hence little change in void ratio.

The slopes of the curves for the two sludges shown in Figure 9 vary with time. It can be seen that at the beginning of the tests the curves for the two sludges have steeper slopes, corresponding to higher coefficients of permeability ($6\ 10^{-7}$ cm/sec for Sludge 1 and 2.5×10^{-6} cm/sec for Sludge 2). At the end of the tests the coefficients of permeability (as obtained from the slopes of the curves) are found to be 2×10^{-7} cm/sec for Sludge 1 and 4.7×10^{-7} cm/sec for Sludge 2. This demonstrates that although in the case of clay the permeability of the cover remains almost

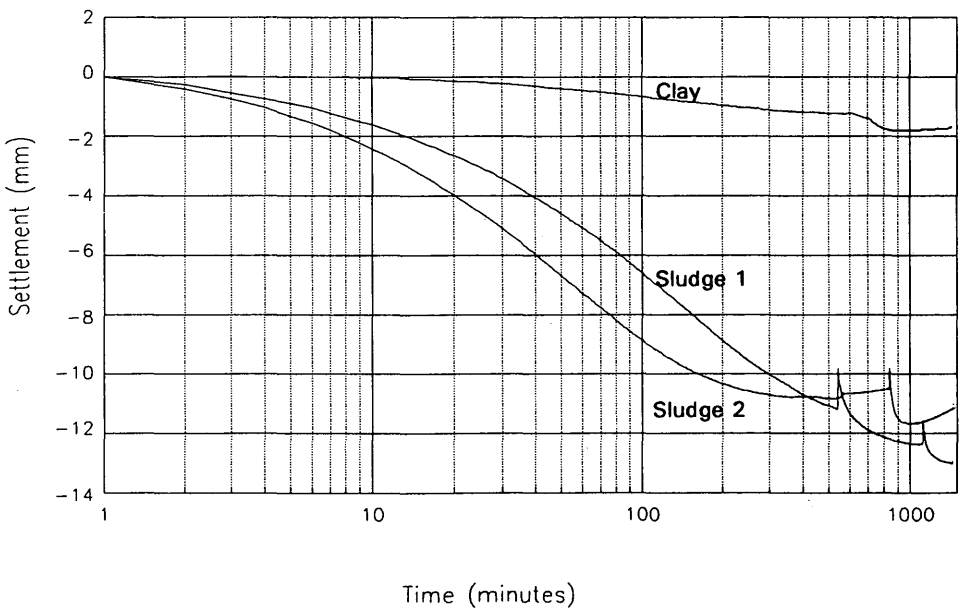

FIGURE 7 Settlement (log scale) versus time at the center of cover at 105 *g*.

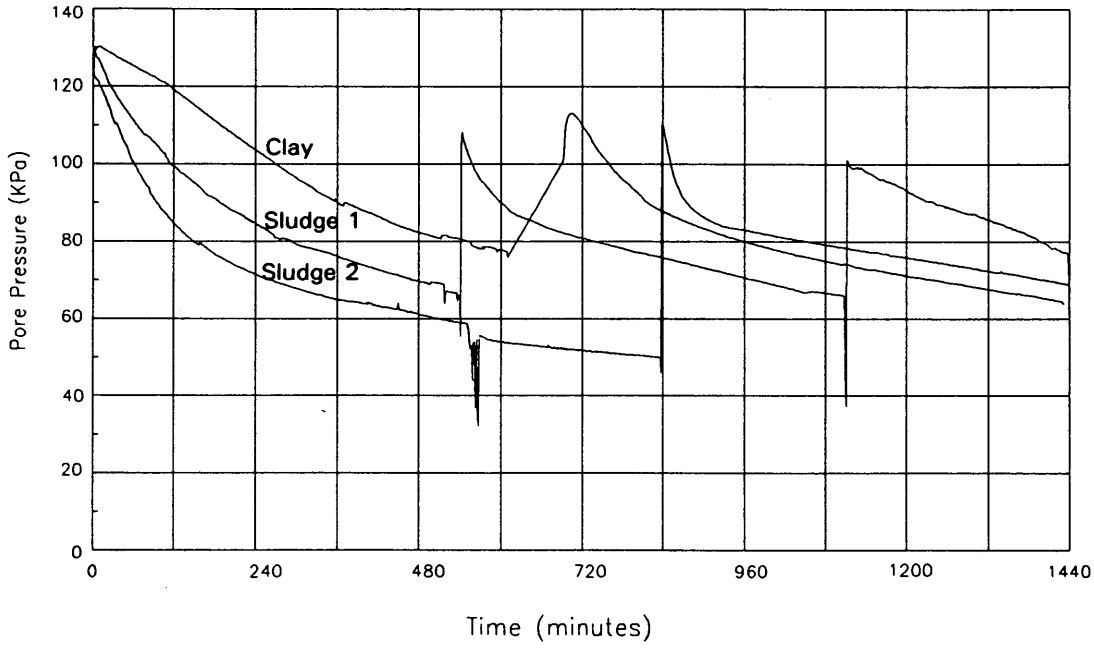

FIGURE 8 Pore-water pressure versus time at the center of cover at 105 *g*.

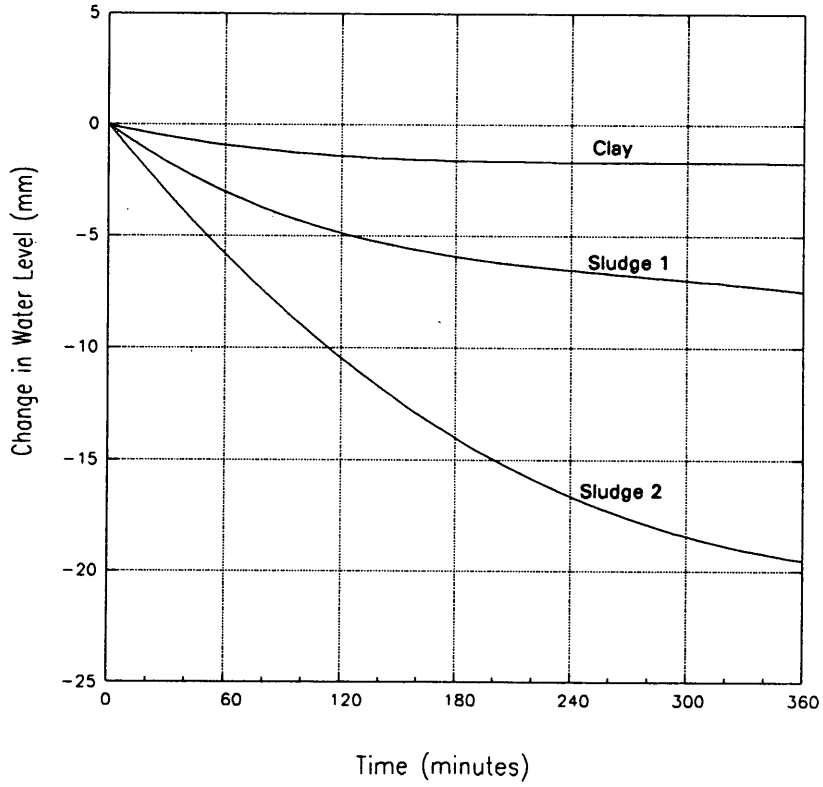

FIGURE 9 Change in water level (corrected for evaporation) (results from first 6 hr).

constant at the initial value, the coefficients of permeability for paper sludge covers tend to decrease considerably with time because of the high compressibility of the sludge, which results in large decreases in void ratio.

The biodegradation that occurs in the sludge over a period of 30 years cannot be modeled in a 24-hr test on the centrifuge. However, biodegradation causes the percentage of organics in the sludge to decrease and the paper sludge to become more soil-like in character. Because of these effects, the coefficient of permeability of the sludge decreases with the progress of biodegradation (*10*). Thus, the tests presented here are useful since they yield conservative permeability values; that is, the in situ permeabilities after 30 years are expected to be lower than those measured in the centrifuge tests.

In order to properly model flow through a saturated porous medium, it is necessary to ensure that the values for the dimensionless Reynold's and Peclet numbers are both less than 1 (*11*). In the experiments described in this paper, the values were found to be much lower than 1, and hence proper modeling of the flow was obtained.

CONCLUSIONS

The study of groundwater flow phenomena by means of accelerated physical modeling was presented in this paper. The scaling relations involved were derived and validated through the use of modeling of models. The use of the geotechnical centrifuge as a valid tool to simulate long-term contaminant migration through saturated soil and related soil behavior was demonstrated through two case studies.

In the first case study, nonintrusive Geiger-Mueller tubes were used to observe contaminant migration without interfering with the natural pattern of groundwater flow. Experiments to study the use of this method for other types of contaminants are recommended.

In the second case study, long-term tests on a relatively large landfill cover model were performed. It was possible to simulate larger prototype dimensions and to model relatively heterogeneous in situ soil. These uses can further be broadened to validate numerical and computer models, which can then be used with greater confidence in practical design.

REFERENCES

1. Pokrovsky, G. I., and I. S. Fyodorov. *Studies of Soil Pressures and Deformations by Means of a Centrifuge,* Vol. 1 (in translation). Building Research Establishment, U.K., 1968.
2. Cargill, K. W., and H-Y. Ko. Centrifugal Modeling of Transient Water Flow. *Journal of Geotechnical Engineering*, ASCE, Vol. 109, No. 4, April 1983, pp. 536–555.
3. Schofield, A. N. Twentieth Rankine Lecture: Cambridge Geotechnical Centrifuge Operations. *Geotechnique*, Vol. 30, 1980, pp. 227–268.
4. Goodings, D. J. Relationships for Modelling Water Effects in Geotechnical Centrifuge Models. In *Application of Centrifuge Modelling to Geotechnical Design* (W.H. Craig, ed.), A. A. Balkema, Rotterdam, 1984, pp. 1–24.
5. Tan, T.-S., and R. F. Scott. Centrifuge Scaling Considerations for Fluid-Particle Systems. *Geotechnique*, Vol. 35, No. 4, 1985, pp. 461–470.
6. EOS, Arctic Contamination Poses Potential Danger. *Transactions, American Geophysical Union*, Vol. 74, No. 27, July 6, 1993, p. 298.
7. Zimmie, T. F., M. B. Mahmud, and A. De. Application of Centrifuge Modeling to Contaminant Migration in Seabed Waste Disposal. *Proc., 4th Canadian Conference on Marine Geotechnical Engineering,* Vol. 2, 1993, pp. 610–624.
8. Ehmann, W. D., and D. E. Vance. *Radiochemistry and Nuclear Methods of Analysis.* John Wiley and Sons, New York, 1991.
9. Mahmud, M. B. *Geotechnical Centrifuge Modeling of Contaminant and Radioactive Waste Migration in Soil.* M. S. Thesis. Rensselaer Polytechnic Institute, Troy, N.Y., May 1993.
10. Zimmie, T. F., H. K. Moo-Young, Jr., and K. LaPlante. 1993. The Use of Waste Paper Sludge for Landfill Cover Material. *Proceedings of Green '93: Waste Disposal by Landfill Symposium,* Bolton Institute, Bolton, U.K., Vol. 2, pp. 11–19.
11. Arulanandan, K., P. Y. Thompson, B. L. Kutter, N. J. Meegoda, K. K. Muraleetharan, and C. Yogachandran. Centrifuge Modeling of Transport Processes for Pollutants in Soils. *Journal of Geotechnical Engineering,* ASCE, Vol. 114, No. 2, pp. 185–205.

Publication of this paper sponsored by Committee on Physicochemical Phenomena in Soils.

Molding Water Content and Hydraulic Conductivity of Compacted Soils Subjected to Freeze/Thaw

JOHN J. BOWDERS AND MAJDI A. OTHMAN

Independent researchers have shown that when compacted clays are subjected to freeze/thaw, they can undergo increases in hydraulic conductivity of one to three orders of magnitude. Existing data have shown that these changes are highly dependent on the initial (before freezing) hydraulic conductivity but not on the plasticity of the soil. The number of freeze/thaw cycles, state of stress, and rate of freezing have the greatest effect on the hydraulic conductivity. It has also been indicated that the availability of water during freezing is critical. In this study, it is shown for closed systems (those with no external water source) that the severity of damage to the soil during freeze/thaw correlates with the volume of water contained in the soil pores and with changes in the hydraulic conductivity. Soils compacted dry of optimum water content can be expected to undergo less than one order of magnitude change in hydraulic conductivity because of freeze/thaw, whereas those compacted wet of optimum can be expected to change by two or more orders. This difference in the magnitude of change suggests that to maintain hydraulic conductivities in compacted soils subjected to freeze/thaw, it may be necessary to compact them dry of optimum—a condition contrary to the practice of constructing low hydraulic conductivity barriers.

Compaction of fine-grained soils can yield materials having low hydraulic conductivities, which are typically utilized in seepage containment applications (*1–3*). In some applications, such as pavement subgrades, landfill liners and covers, and waterproofing for subsurface structures, the soil may be exposed to freeze/thaw conditions. It has been shown that compacted soils subjected to these conditions can undergo changes resulting in order-of-magnitude increases in the hydraulic conductivity of the soil (*4–9*). The conditions of the soil during freeze/thaw promote such changes, which are addressed in this paper.

Factors that significantly affect the resulting hydraulic conductivity include the rate of freezing, number of freeze/thaw cycles, and status of stress on the soil. Secondary factors include the ultimate or minimum temperature of the frozen specimen, the dimensionality of freezing (three-dimensional versus one-dimensional), and the availability of water. These factors have been studied by several investigators and documented in a state-of-the-art paper by Othman and Benson (*5*). It is not the intent to evaluate each of them again. Rather, a second analysis of the available data affords opportunity to highlight factors that appear to be controlling the changes in the hydraulic conductivity of the soils.

Analysis of the data in light of the factors that might correlate with the changes in hydraulic conductivity was performed. The water available within the soil during the time of freeze/thaw was the main parameter studied. Since all the specimens were tested in a closed system, the only water available during freezing was that contained within the soil pores.

J. J. Bowders, Department of Civil Engineering, West Virginia University, Morgantown, W.Va. 26506-6101. M. A. Othman, Geosyntec Consultants, 5775 Peachtree Dunwoody Road, Suite 200F, Atlanta, Ga. 30342.

BACKGROUND

Numerous investigators have shown that freeze/thaw conditions can have deleterious effect on the hydraulic conductivity of compacted soils (*4–9*). Data shown in Figure 1 exhibit increases in hydraulic conductivities of up to three orders of magnitude. It is hypothesized that a process by which the pore size or effective porosity is increasing is occurring in the soil, since the largest pores in a fine-grained soil govern the hydraulic flow through that medium (*10*).

Hunsicker (*11*) used scanning electron microscopy (SEM) to delineate small cracks (0.005 mm) in the microstructure of thawed soil. Chamberlain et al. (*12*) used thin-section analysis to photograph macroscale cracking patterns in soils that had undergone freeze/thaw. Kim and Daniel (*6*) used tracer studies to compare effective porosities (volume of fluid-conducting pores divided by the total volume of the soil) of specimens having undergone freeze/thaw and those for control specimens. They found that effective porosities of freeze/thaw specimens (compacted slightly wet of optimum) increased from 10 to 80 percent above those of the unfrozen specimens (*6*). In each of these investigations, it was the porosity or effective porosity that was altered in the soil specimens, indicating that a change in hydraulic conductivity could be anticipated.

The increase in effective porosity (referred to here as "damage") results from several phenomena, some or all of which may occur for a given specimen. The first simply involves expansion of the water (about 9 percent by volume) in the pores as it turns to ice. The second phenomenon is the growth of segregated ice as water migrates to the freezing zone and increases the volume and size of an ice lens within the soil. The final phenomenon is the potential shrinkage of soil, specifically the clay fraction, as water migrates from the soil and joins the growing ice lens. Taken in sum, these processes result in increasing the sizes and interconnectedness of the pores in the subsequently thawed soil. The result can be a soil with a hydraulic conductivity much greater than that before it underwent freezing. In summary, a factor in predicting the degree of damage that may occur to soils is knowledge of the water availability during freeze/thaw.

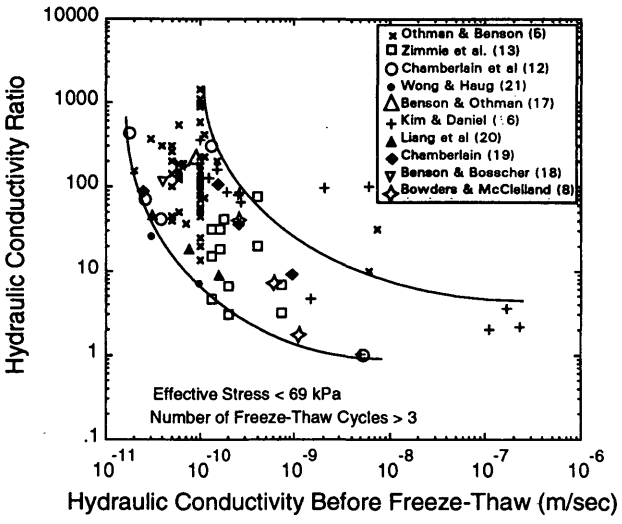

FIGURE 1 Hydraulic conductivity ratio versus hydraulic conductivity before freeze/thaw (*7*).

DATA

Data from three sources (*6–8*) have been compiled and analyzed. A total of six soils are included. The geotechnical and index properties of the soils are provided in Table 1. The soils represented cover a range in material properties expected of seepage containment applications. The data represented in this analysis include only those in which standard Proctor energy was used. Four specimens were subjected to one-dimensional freezing. All of the others were subjected to three-dimensional freezing.

The data included in this study are provided in Tables 2 through 4. The dry densities (γ_{dmax}) and water contents are those of the specimen during specimen molding. The delta water content ($\Delta w\%$) yis the difference between the molding water content and the optimum water content (w_{opt}). K_{ratio} is the ratio of the hydraulic conductivity after a specimen has been subjected to freeze/thaw to the hydraulic conductivity of the specimen (or a similar one) before it has been subjected to freeze/thaw. Only specimens subjected to five or more freeze/thaw cycles are included in the data set. It has previously been shown that the most significant damage occurs within the first five freeze/thaw cycles (*5,12,13*). In addition, the relative magnitude of the effective stress on the specimen during the time that the hydraulic conductivity was measured is reported for each hydraulic conductivity ratio. The significance of the applied effective stress on the measured hydraulic conductivity has been demonstrated previously (*7,8,14*).

TABLE 1 Geotechnical and Index Properties of Soils Subjected to Freeze/Thaw and Permeated

			Soil No. and Type of Soil[a]							
			1 and 2, Kaol	3, Wetzel	4, Mon	5, Wisconsin A	6, Wisconsin B	7, Wisconsin C	8, Wisconsin A	Range
γ_{dmax}	(kN/m^3)		13.5	19.1	15.2	18.0	16.8	14.7	18.2	13.5–19.1
w_{opt}	(%)		31	11	23	16	18.5	26	15	11.0–31.0
P_{200}	(%)		90	50	65	85	99	71	88	50.0–99.0
LL	(%)		58	33	60	34	42	84	36	33.0–84.0
PI	(%)		24	9	30	16	19	60	19	9.0–60.0
e		at γ_{dmax}	0.88	0.38	0.72	0.54	0.53	0.81	—	0.38–0.88
n	(%)	and	47	28	42	35	35	45	—	28.0–47.0
S_R	(%)	w_{opt}	91	78	86	82	95	87	—	78.0–95.0

NOTE: γ_{dmax} = maximum dry density; w_{opt} = gravimetric water content at γ_{dmax}; P_{200} = percent passing No. 200 sieve; *LL* = liquid limit; *PI* = plasticity index; *e* = void ratio; *n* = porosity; S_R = degree of saturation.

[a]Investigators: Soil Nos. 1–4, Bowders and McClelland (*8*); Nos. 5–7, Othman et al. (*7*); No. 8, Kim and Daniel (*6*).

TABLE 2 Molding Conditions, Effective Stress, Pre-Freeze/Thaw Hydraulic Conductivity, and K_{ratio} for Soil Specimens (*8*)

Soil and Soil No.	γ_d (kN/m^3)	$w\%$	Δw	$K_{initial} \times 10^{-8}$ (cm/sec)	K_{ratio} σ (kPa) ≤25	25–42	63–70	115–210
Kaol, 1	13.5	32.5	1.5	5 to 8	4.6	1.6	2.4	1.2
Kaol, 2	13.5	32.5	1.5	4 to 8	43	—	1.4	1.0
Wetzel, 3	19.1	12.5	1.5	9 to 10	1.8	2.1	—	1.2
Mon, 4	15.2	24.5	1.5	1.0	49	23	15	7.4

NOTE: Data for each soil in this table represent the average values of four specimens tested under these conditions. Soil No. refers to soils listed in Table 1. γ_d = dry density (kN/m^3); $w\%$ = molding water content (%); Δw = difference between molding and optimum water contents; σ = effective stress in soil during permeability test (kPa); K_{ratio} = hydraulic conductivity ratio (i.e., hydraulic conductivity post-freeze/thaw divided by that prior to freeze/thaw).

TABLE 3 Molding Conditions, Effective Stress, Pre-Freeze/Thaw Hydraulic Conductivity, and K_{ratio} for Soil Specimens (7)

Soil No. and Spec. No.	γ_d (kN/m^3)	w%	Δw	$K_{initial}$ (cm/sec)	K_{ratio} σ (kPa) ≤25	25–42	63–70	115–210
Othman Soil A, 5								
PV 55/51	18.0	15.9	−0.1	2.7E-7	3.7			
50/49	18.3	16.1	0.0	4.0E-8	22			
34/7	18.2	16.9	0.9	1.1E-8	418			
40/7	18.2	17.4	1.4	1.1E-8	73			
44/11	17.6	18.8	2.8	1.1E-8	73			
66/23	17.4	19.8	3.8	1.1E-8	109			
67/23	17.5	19.8	3.8	1.1E-8	64			
18/20	17.1	20.2	4.2	1.5E-8	200			
22/20	17.0	20.5	4.5	1.5E-8	167			
Othman Soil B, 6								
VT 13/10	17.3	17.0	−1.5	7.5E-7	56			
45/43	17.4	19.2	0.7	4.2E-8	13			
7/8	17.4	19.9	1.4	1.0E-8	130	—	37[a]	2.2[b]
26/28	16.5	22.4	3.9	1.0E-8	150			
Othman Soil C, 7								
SC 9/8	14.8	25.7	−0.3	6.0E-7	10			
42/4	14.9	28.4	2.4	2.5E-8	8.8			
45/4	14.2	28.4	2.4	2.5E-8	52			
103/101	14.7	30.3	4.3	6.0E-9	600			

NOTE: Soil No. refers to soils listed in Table 1. Spec. No. (PV#, VT#, and SC#) is the test specimen number. γ_d = dry density (kN/m^3); w% = molding water content (%); Δw = difference between molding and optimum water contents; σ = effective stress in soil during permeability test (kPa); K_{ratio} = hydraulic conductivity ratio (i.e., hydraulic conductivity post-freeze/thaw divided by that prior to freeze/thaw).
[a]K pre-freeze was 7.0E-9 cm/sec.
[b]K pre-freeze was 5.0E-9 cm/sec.

ANALYSES AND DISCUSSION

The data examined in this analysis were tested under closed-system conditions during freeze/thaw. Under such conditions, there is no source of water during freezing except for that already contained in the soil pores. Thus, any ice lenses that might form are limited in size to the volume of pore water available in the specimen. On the basis of this condition, the hypothesis here is that the severity of damage to the soil is directly related to the volume of water contained in the soil pores. Thus, it follows that changes in the hydraulic conductivity should also directly relate to the volume of water in the soil.

The hydraulic conductivity ratios versus molding water content for the six soils are shown in Figure 2. The relative effective stress on the specimens is indicated. Although there is scatter in the data, there is evidence that increased effective stress on the soil results in less damage or increase in hydraulic conductivities due to the action of freeze-thaw.

The data by Kim and Daniel (6) showed two orders of magnitude difference in hydraulic conductivity ratio for soils compacted wet of optimum compared with those compacted dry of optimum water content. Thus, merely recording the molding water content does not provide enough information about the availability of water in the specimens. For instance, if a specimen is compacted at 15 percent water content but the optimum water content is 20 percent, the soil will be well dry of optimum and soil pores will contain a larger percentage of air than when compacted wet of optimum. Given a closed system for freezing, it is likely that the soil that is dry of optimum will sustain less relative freeze/thaw damage.

Shown in Figure 3 is the hydraulic conductivity ratio versus the difference between the molding and optimum water contents.

TABLE 4 Molding Conditions, Effective Stress, Pre-Freeze/Thaw Hydraulic Conductivity, and K_{ratio} for Soil Specimens (6)

Soil No. and Spec. No.	γ_d (kN/m^3)	w%	Δw	$K_{initial}$ (cm/sec)	K_{ratio} σ (kPa) ≤25
Soil No. 8					
1	17.6	11	−4.1	1.1E-5	2
2	18.2	13.2	−1.9	1.7E-5	3.5
3	18.6	15.1	0.0	2.1E-7	95
4	18.4	16.4	1.4	1.5E-8	160
5	17.6	19.5	4.4	1.2E-8	125
6	16.5	22.1	7.0	2.6E-8	85

NOTE: Soil No. refers to soils listed in Table 1. Spec. No. is the test specimen number. γ_d = dry density (kN/m^3); w% = molding water content (%); Δw = difference between molding and optimum water contents; σ = effective stress in soil during permeability test (kPa); K_{ratio} = hydraulic conductivity ratio (i.e., hydraulic conductivity post-freeze/thaw divided by that prior to freeze/thaw).

Only data for low effective stress (<25 kPa) are displayed. Although degree of saturation (ratio of volume of water in the soil pores to total volume of pores) would have been a good measure to use, the authors had insufficient information to make this determination for all of the data; however, knowing the molding water content relative to the optimum water content for the soil provides an indication of the relative degree of saturation of the soil (*15*). Data points lying to the left of the zero on the horizontal axis indicate soils compacted dry of optimum. Degrees of saturation are low. The soils contain significant quantities of air in their pores; therefore, less water is available for the formation of ice when the soils are subjected to freezing temperatures. For soils lying to the left of zero, one expects less damage and smaller hydraulic conductivity ratios. Points lying to the right of the null value are soils compacted wet of optimum. As soils become increasingly wet of optimum, they obtain higher degrees of saturation and in a closed system, more water is available for ice formation. Thus, one would expect more damage or increased magnitude of the hydraulic conductivity ratios. Indeed, the data shown in Figure 3 indicate such a behavior.

A linear regression including the data for all six soils, at effective stresses below 25 kPa, is shown in Figure 4. Molding water contents for the specimens shown span from approximately 4 percent dry of optimum to 7 percent wet of optimum. For soils well dry of optimum, it is clearly evident that for soils dry of optimum, the hydraulic conductivity ratio decreases rapidly as one moves away from the optimum water content. Also evident is the increasing hydraulic conductivity ratio as soils become increasingly wet of optimum. There are two data points, K_{ratio} 418 and 600, that shift the linear regression curve. Although the integrity of these points is not in question, they have been deleted from the analysis for the sake of examining the resulting regression curve as shown in Figure 5. The curve shifts down but does not appreciably change slope.

The data shown in Figures 4 and 5 support the hypothesis that increased water availability during freezing results in increased damage to the soil and higher hydraulic conductivity ratios. Othman at al. (*7*) found that hydraulic conductivity ratios increased as the hydraulic conductivity of the unfrozen soil decreased. Typically, hydraulic conductivity of a cohesive soil can be decreased by compacting it at a water content wet of optimum. This is a common practice and often specified for soils being used in containment applications (*3*). When soils are compacted wet of optimum and subjected to several cycles of freeze-thaw, the resulting hydraulic conductivity of the thawed soil is likely to be increased above that of the unfrozen soil.

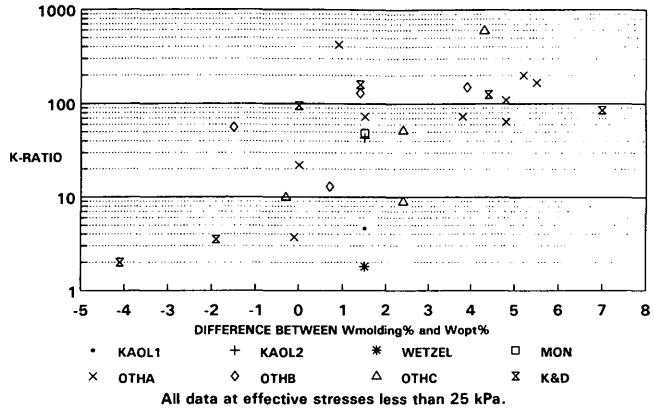

FIGURE 3 ***K*-ratio versus *w*% deviation from w_{opt}%: data.**

A point that must not be ignored is illustrated in Figure 6. This is the impact of effective stress on the final hydraulic conductivity of soil subjected to freezing and thawing. As the effective stress in the soil is increased, the hydraulic conductivity ratio (or final hydraulic conductivity) is decreased. In fact, for stresses greater than about 70 kPa (10 psi) the damage due to freeze/thaw action may be completely nullified. This behavior is in agreement with that reported by LaPlante and Zimmie (*4*) for soils subjected to freeze/thaw and by Boynton and Daniel (*14*) for soils subjected to damage by desiccation cracking.

CONCLUSIONS

Data on the hydraulic conductivity of compacted soils having undergone freeze/thaw exposure have been compiled and analyzed. Six different soils were examined. The findings, in agreement with those of previous investigators, are as follows:

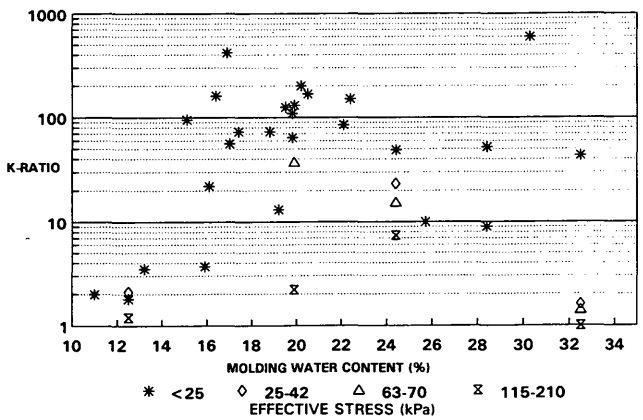

FIGURE 2 ***K*-ratio at various effective stresses versus molding water content.**

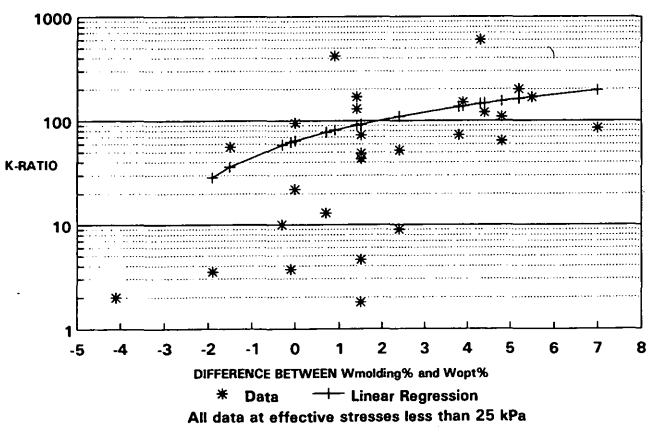

FIGURE 4 ***K*-ratio versus *w*% deviation from w_{opt}%: linear regression.**

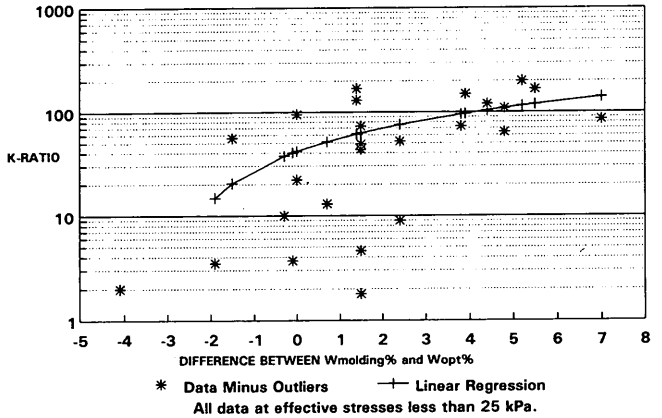

FIGURE 5 ***K*-ratio versus *w*% deviation from w_{opt}%: data minus outliers.**

1. All soil specimens exhibited an increase in hydraulic conductivity after being subjected to freeze/thaw conditions.
2. The availability of water during freezing strongly correlated with the magnitude of the increase in post-freeze/thaw hydraulic conductivity.
3. Soils compacted dry of optimum water content underwent (on the average) less than one order of magnitude increase in hydraulic conductivity, whereas soils compacted wet of optimum underwent (on mean) two orders of magnitude increase in hydraulic conductivity.
4. Increased effective stress in the soil specimens resulted in decreased magnitude of change in the post-freeze/thaw hydraulic conductivity. For effective stresses above approximately 70 kPa, the changes in hydraulic conductivity induced by the freezing action were nearly nullified.

The hypothesis that the severity of damage to the soil should correlate with the volume of water contained in the soil pores is supported by the data analyzed. All of the specimens were tested under closed-system conditions; that is, there was no source of water during freezing except for that already contained in the soil pores. Soils compacted wet of optimum, indicating a high degree of saturation, contained more water available during freezing, and the data show a marked increase in the subsequent hydraulic conductivity. Soils compacted dry of optimum, indicating less water available during freezing, showed smaller changes in post-freeze/thaw hydraulic conductivity.

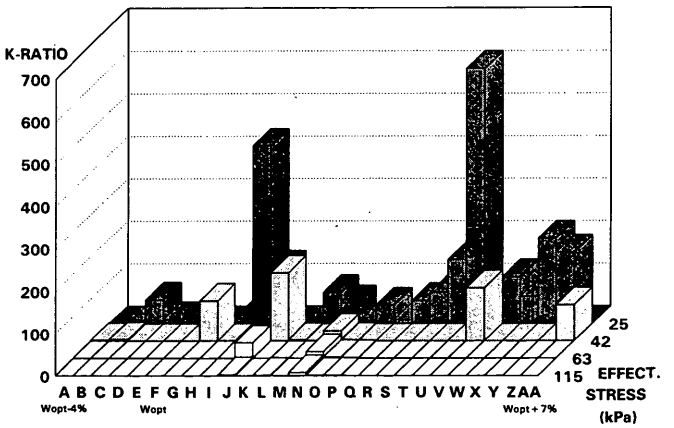

FIGURE 6 ***K*-ratio versus *w*% deviation from w_{opt}%: w_{opt} = *F*.**

In conclusion, when there is no other source of water, soils compacted dry of optimum may not be subject to significant freeze/thaw damage. This is especially likely in cases where an appreciable effective stress exists in the soil. However, in seepage containment applications, soils are most often compacted wet of optimum to minimize the hydraulic conductivity (*1,2,16*). It is in this state that damage due to freezing action is most pronounced. Thus, in situations where freezing conditions may develop, application of large confining stresses and compaction dry of optimum (while continuing to meet minimum hydraulic conductivity requirements) may help to safeguard against significant changes in hydraulic conductivity due to freezing action.

ACKNOWLEDGMENT

The authors wish to express their appreciation to their colleagues who have supplied data and helpful discussions on material reported here.

REFERENCES

1. Lambe, T. W. *The Permeability of Compacted Fine Grained Soils.* Special Technical Publication 163. ASTM, Philadelphia, Pa., 1955.
2. Mitchell, J. K. *Fundamentals of Soil Behavior*, 2nd ed. John Wiley and Sons, New York, 1993, p. 437.
3. Benson, C. H., and D. E. Daniel. Influence of Clods on Hydraulic Conductivity of Compacted Clay. *Journal of Geotechnical Engineering*, ASCE, Vol. 116, No. 8, 1990, pp. 1231–1248.
4. LaPlante, C. M., and T. F. Zimmie. Freeze/Thaw Effects on the Hydraulic Conductivity of Compacted Clays. In *Transportation Research Record 1369,* TRB, National Research Council, Washington, D.C., 1992, pp. 126–129.
5. Othman, M. A., and C. H. Benson. Effect of Freeze/Thaw on the Hydraulic Conductivity of Three Compacted Clays from Wisconson. In *Transportation Research Record 1369,* TRB, National Research Council, Washington, D.C., 1992, pp. 118–125.
6. Kim, W. H., and D. E. Daniel. Effects of Freezing on the Hydraulic Conductivity of Compacted Clay. *Journal of Geotechnical Engineering*, ASCE, Vol. 118, No. 7, 1992, pp. 1083–1097.
7. Othman M. A., C. H. Benson, E. J. Chamberlain, and T. F. Zimmie. Laboratory Testing to Evaluate Changes in Hydraulic Conductivity of Compacted Clays Caused by Freeze-Thaw: State of the Art. In *Hydraulic Conductivity and Waste Contaminant Transport in Soils,* Special Technical Publication 1142, ASTM, Philadelphia, Pa., 1993.
8. Bowders, J. J., and S. McClelland. The Effects of Freeze/Thaw Cycles on the Permeability of Three Compacted Soils. In *Hydraulic Conductivity and Waste Contaminant Transport in Soils,* Special Technical Publication 1142, ASTM, Philadelphia, Pa., 1993.
9. Chamberlain, E. J., and A. J. Gow. Effects of Freezing and Thawing on the Permeability and Structure of Soils. *Engineering Geology*, Vol. 13, 1979, pp. 73–92.
10. Olsen, H. W. Hydraulic FLow Through Saturated Clays. *Proc., 9th National Conference on Clays and Clays Minerals,* 1962, pp. 131–161.
11. Hunsicker, S. E. The Effects of Freeze-Thaw Cycles on the Permeability and Marco Structure of Fort Edwards Clay. M.E. Thesis. Thayer School of Engineering, Dartmouth College, Hanover, N.H., 1987, 186 pp.
12. Chamberlain, E. J., I. Iskander, and S. E. Hunsicker. Effect of Freeze-Thaw Cycles on the Permeability and Macrostructure of Soils. In *Proc., International Symposium on Frozen Soil Impacts on Agricul-*

ture, Range, and Forest Lands, CRREL Special Report 90-1, U.S. Army Corps of Engineers Cold Regions Research and Engineering Laboratory, Hanover, N.H., 1990, pp. 145–155.
13. Zimmie, T. F., and C. M. LaPlante. The Effects of Freeze-Thaw Cycles on the Permeability of a Fined-Grain Soil. In Proc., 22nd Mid-Atlantic Industrial Waste Conference, Drexel University, Philadelphia, Pa., 1990, pp. 580–593.
14. Boynton, S. S., and D. E. Daniel. Hydraulic Conductivity Tests on Compacted Clay. *Journal of Geotechnical Engineering,* ASCE, Vol. 111, No. 4, 1985, pp. 465–478.
15. Fredlund, D. G., and H. Rahardjo. *Soil Mechanics for Unsaturated Soils.* John Wiley and Sons, Inc., New York, 1993, 517 pp.
16. Daniel, D. E. Summary Review of Construction Quality Control for Compacted Soil Liners. In *Waste Containment Systems: Construction, Regulation and Performance* (R. Bonaparte, ed.), ASCE, New York, pp. 175–189.
17. Benson, C. H., and M. A. Othman. Hydraulic and Mechanical Characteristics of a Compacted Municipal Solid Waste Compost. *Waste Management and Research,* Vol. 11, 1993, pp. 127–142.
18. Benson, C. H., and P. J. Bosscher. Effect of Winter Exposure on the Hydraulic Conductivity of a Test Pad. *Environmental Geotechnics Report,* No. 92-8, Department of Civil and Environmental Engineering, University of Wisconsin, Madison, 1992.
19. Chamberlain, E. J. *Freeze-Thaw Effects on the Permeability of Shakopee and Rosemont II Soils.* CRREL Final Report. U.S. Army Cold Regions Research and Engineering Laboratory, Hanover, N.H., 1992, 9 pp.
20. Liang, W., X. Bomeng, and W. Zhijin. Properties of Frozen and Thawed Soil and Earth Dam Construction in Winter. In *Proc., 4th International Conference on Permafrost,* 1983, pp. 1366–1371.
21. Wong, L. C., and M. D. Haug. Cyclical Closed-System Freeze-Thaw Permeability Testing of Soil Liner and Cover Materials. *Canadian Geotechnical Journal,* Vol. 28, 1991, pp. 784–793.

Publication of this paper sponsored by Committee on Physicochemical Phenomena in Soils.

Some Physical Factors Affecting Contaminant Hydrology in Cold Environments

S. A. GRANT

Some of the physical effects of cold temperatures that should be considered when developing a contaminant-transport model are surveyed in this paper. The discussion begins with the following working definition of the term *cold region* for the purpose of contaminant hydrology modeling: an area with appreciable frozen ground and a substantial fraction of the annual precipitation as snow. Models that estimate the liquid water content and hydraulic conductivity of frozen ground are discussed.

Lexically, the adjective "cold" refers to an environment in which the ambient temperature is noticeably below body temperature. A cold region is one in which lower temperatures have significant effects on natural environments or human activities. Although moderate temperatures may be perceived as cold, cold regions have been typically defined by the intervals in which ambient temperatures are below the freezing point of water, because it is at these temperatures that the effects of cold temperatures are most pronounced. Among the criteria that have been used to delineate cold regions are (*1*)

1. Air temperatures below 0°C (32°F) or −18°C (0°F) that have a 50 percent likelihood of being observed annually,
2. Mean annual snow depth,
3. Ice cover on navigable rivers, and
4. Isolines based on permanence, depth, and continuity of frozen ground.

Traditionally, the maps made from plotting isograms based on these criteria delineate the changes in human activities due to cold. For example, isograms based on frozen ground delineate changes in the construction requirements for building footings. Isograms based on ice cover indicate the navigability of the waters during some portion of the year.

The purpose of this paper is to discuss how cold temperatures affect contaminant-transport modeling. Accordingly, cold regions should be delineated by the phenomena necessary to make the model a valid representation of the pertinent chemical, physical, and microbiological processes that determine the fate of contaminants in the cold environment. Low temperatures affect the physics of contaminant transport by freezing the water in the ground (sometimes to great depths) and by blanketing the ground (seasonally or permanently) with snow. Since no maps have been drawn delineating cold regions' effects on contaminant hydrology, the natural delineations would be those for snow covers and the extent of ground freezing.

Cold Regions Research and Engineering Laboratory, Hanover, N.H. 03755-1290.

EXTENT OF COLD REGIONS

In comparing the hydrologic systems of cold regions with those of warmer areas, two factors distinguish the former systems:

1. Some of the annual precipitation occurs as snow, which completes its role in the hydrologic cycle for a comparatively brief period during snowmelt.
2. The ground freezes to some depth. Ground freezing reduces the soil's permeability and its water-storage capacity. Accordingly, freezing of the ground dramatically decreases the soil's infiltration rate and just as dramatically increases soil runoff due to rain and snowmelt.

To be hydrologically important, a cold region must receive an appreciable proportion of its precipitation as snow, and its ground must be frozen so that the infiltration of the melting snow is limited. In the Northem Hemisphere, these two criteria can be applied to delineate the extent of cold regions for the purposes of contaminant-transport modeling.

Snow Cover

Maps with isograms of various annual snow depths have been developed (*1*) (Figure 1). Much of the United States has average maximum snow depths of 0.3 m (12 in.) or more. This includes all or part of the following states: Alaska, California, Connecticut, Idaho, Illinois, Indiana, Maine, Massachusetts, Michigan, Minnesota, Missouri, Montana, Nebraska, Nevada, New Hampshire, New Jersey, New York, North Dakota, Ohio, Pennsylvania, South Dakota, Utah, Vermont, Washington, Wisconsin, and Wyoming. The isogram in Figure 1 indicates the annual quantity, but not annual fraction, of precipitation that typically arrives as snow and therefore does not indicate the relative importance of snow to a region's hydrology. Accordingly the isogram in Figure 1 may not adequately delineate snow-affected areas in drier regions.

Frozen Ground

Three major classes of frozen ground are recognized: seasonally frozen ground, discontinuous permafrost, and permafrost.

Seasonally Frozen Ground

The potential inadequacy of snow-depth isograms to delineate cold, dry areas is borne out by the map of permafrost and frost-

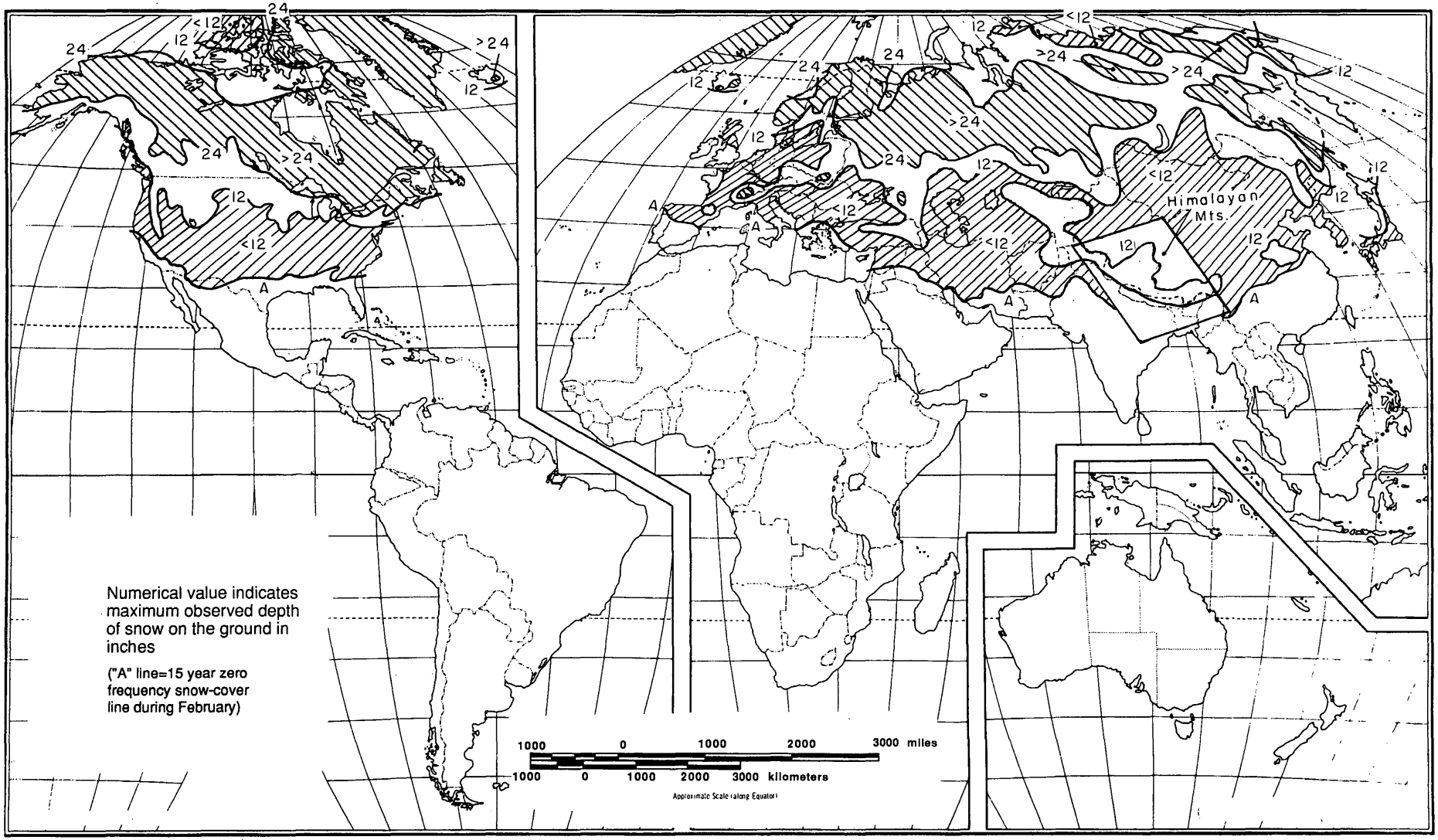

FIGURE 1 Cold-regions boundaries as determined by snow depths (*1*).

affected areas presented here in Figure 2 (*1*). Understandably, the southernmost isogram, that for frost penetration, is similar to that for snow cover. However, several areas (mostly in the western United States) with low rates of annual precipitation are now included. These areas are all or parts of Arizona, Colorado, Kansas, Maryland, Missouri, New Mexico, and Rhode Island.

Discontinuous Permafrost

In the United States, discontinuous permafrost is found only in Alaska. Discontinuous permafrost or permafrost is found under most of the land surface of the state.

Permafrost

Areas of permafrost, in which no seasonally thawed land occurs, are found in the northernmost parts of Alaska.

Importance to Contaminant-Transport Modeling

A model is a mathematical expression of the developer's understanding of the system being simulated. Accordingly, contaminant-transport models valid for cold regions differ from those appropriate for warmer climates because the system being described is conspicuously different. Below is a list of modeling aspects that differentiate contaminant-transport models valid in cold regions:

1. Much of what is understood about the hydrology of cold regions is qualitative. Because there have been comparatively few studies in cold regions, the physical, chemical, and biological processes that determine contaminant hydrology of cold regions are not completely understood. This lack of quantitative knowledge hinders the development of physically based contaminant-transport models valid for cold regions. Much basic research is needed to support the development of simulation models that are appropriate for these regions.
2. The flow of heat and aqueous-solution phase transitions must be included explicitly in the development of solute transport models.
3. In unfrozen porous media, liquid water moves largely in response to hydrostatic gradients. In frozen porous media, liquid water movement in response to osmotic or thermal gradients may be dominant.
4. The physical chemistry of electrolyte solutions in natural porous media above freezing temperatures is well understood, and models describing them are generally available. For systems below 0°C, there are comparatively few physical chemical data (aside from freezing-point depression determinations) for even simple electrolyte solutions.
5. Much of the groundwater in areas with permafrost is brackish and impotable. Contamination of currently exploited aquifers that are potable can effectively deprive communities of potable subterranean water supplies.

How these effects are incorporated in mathematical models of contaminant transport can be outlined with the differential equations that form the basis of many of these models. Water in a porous medium flows in a linearly proportional response to the hydrostatic gradient across that medium. This observation has been formalized as Darcy's law, the vector form of which is

$$\mathbf{v} = -\frac{\mathbf{k}}{\nu} + (\nabla p - \rho g \nabla z) = -\mathbf{K} \cdot \nabla h \qquad (1)$$

where

$\mathbf{v}$ = Darcian flow velocity vector (m sec^{-1});
$\mathbf{k}$ = permeability tensor (m^2);
ν = viscosity of the fluid (Pa · sec);
p = fluid pressure (Pa);
ρ = fluid density (kg m^{-3});
z = vertical distance above datum (m);
g = acceleration due to gravity (m · sec^{-2});
$\mathbf{K}$ = hydraulic conductivity tensor, which in this treatment will be assigned dimensions of square meters per pascal second; and
h = total head (Pa).

[The formulas presented here are from Mangold and Tsang (*2*).] As will be discussed in later sections, low temperatures dramatically affect three of the parameters in Equation 1: ν, p, and $\mathbf{K}$. The viscosity of the aqueous solution in freezing soils is affected directly by lowering temperatures, which cause the viscosity of pure water to increase by an order of magnitude (an effect presented in Figure 3), and by solutes excluded from ice forming in the soil solution, which cause the viscosity of the remaining liquid-water solution to be increased still further (an effect presented in Figure 4). The pressure of vicinal water in frozen porous media is controversial and an active area of basic research (*4*). It is clear that the liquid-pressure gradients accompanying differences in temperature may be much more important than pressure gradients due to elevation or water content [see, for example, Perfect et al. (*5*)]. Finally, because ice occupies some of the pore space, the conductivity of the porous material is reduced.

Once the flow of water is established, the more challenging problem of solute flows through porous media can be addressed. In many cases, the appropriate partial differential equation to describe the transport of the solute j is

$$\nabla \cdot (\mathbf{v}c_j) - \nabla \cdot (\mathbf{D} \cdot \nabla c_j) = \Phi \frac{\partial c_j}{\partial t} + Q_{c_j} \qquad (2)$$

where

c_j = aqueous concentration of the jth solute (mol m^{-3}),
$\mathbf{D}$ = dispersivity tensor (m^2 sec^{-1}),
Φ = porosity of the porous medium (L), and
Q_{c_j} = source-sink term for jth solute (mol m^{-3} sec^{-1}).

As would be expected, most of the geochemical reactions that contribute to the term Q_{c_j} are affected by temperature. The most pronounced of these effects are on the chemical-thermodynamic state of the solutes and consequently their solubility, miscibility, speciation, and reactivity.

PHYSICS OF FROZEN POROUS MEDIA

Moderately cool temperatures affect the physical-chemical state of water and its propensity to flow through porous media. For

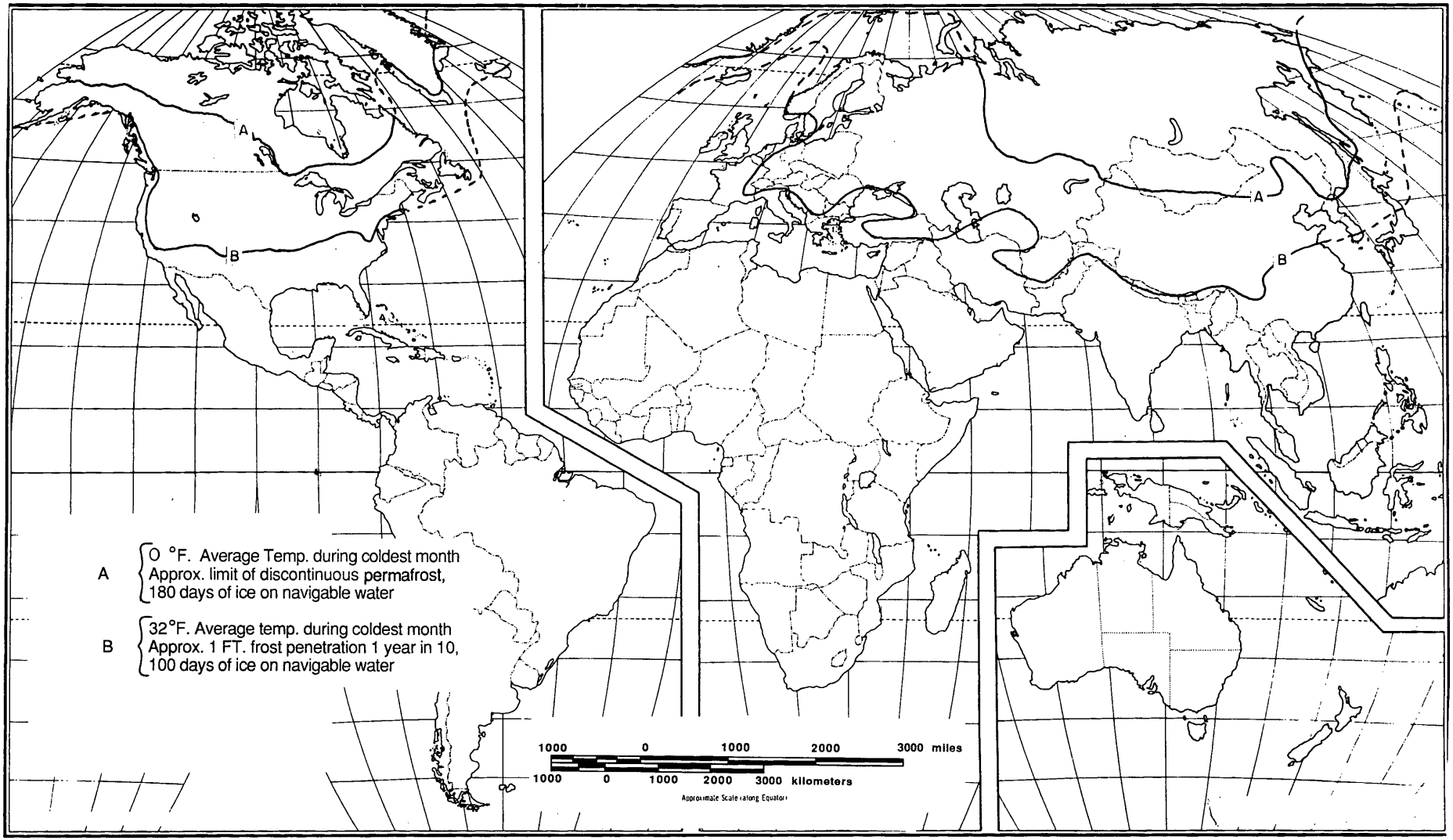

FIGURE 2 Cold-regions boundaries as determined by frozen ground (*1*).

contaminant transport, changing temperatures affect the chemical potentials of the solvents and solutes in the pore solutions and therefore the solubility and reactivity of the solutes. These changes in the physical properties of the solvent and chemical properties of the solutes can dramatically affect the mobility of contaminants in cold regions.

At low temperatures, at which surficial, vadose, and aquifer waters freeze, the nature of flow changes dramatically. First, at a macroscopic level, because the effective volume of voids is reduced, the ground has a much lower permeability when frozen. This affects the basin-scale hydrology in cold regions in sometimes unpredictable ways. Second, although frozen ground is less permeable, it is not impermeable. The mathematical description of transport of solutes through frozen ground is inherently more complex than that for unfrozen ground for the following reasons:

1. The solvent, water, is partitioned into two phases, liquid water and ice, which are intimately comingled in the pores of the ground.
2. As the ice forms, the solutes (including the contaminants) are largely excluded from the ice, concentrating the remaining liquid-water solutions in a thin film at the colloid surfaces. The chemical potentials of the solutes in these solutions, used to estimate the effects of solute-solute and solute-surface interactions, are not understood well enough to be modeled accurately.
3. In unfrozen coarse-grained soils, the movement of solutes is controlled by the Darcian flow of water in response to gravitational and pressure gradients. In frozen ground, solutes may also move appreciably in response to thermal and osmotic gradients—transport mechanisms that are less well understood and more difficult to parameterize than flow in response to gravitational and pressure gradients.

Darcy's Law

An alternative form of Darcy's law, with which water flows in porous media can be described, can be stated as follows:

$$q \equiv \frac{Q}{A} = -\left(\frac{k}{\nu}\right)\frac{(p_2 - p_1 + \rho g h)}{h} \qquad (3)$$

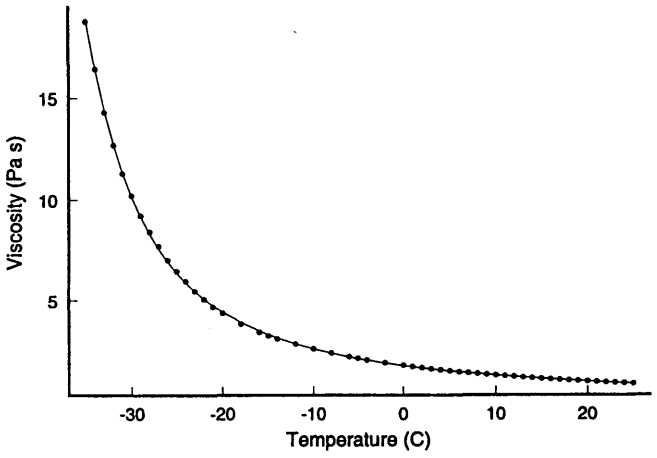

FIGURE 3 Viscosity of supercooled water [data from Osipov et al. (3)].

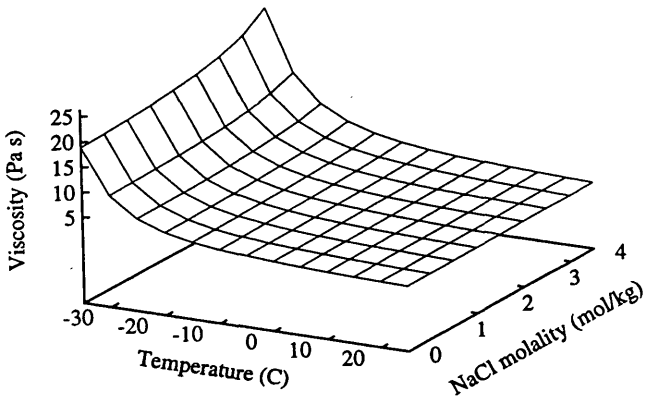

FIGURE 4 Predicted viscosity of aqueous NaCl solutions as affected by temperature and solution concentration.

which states simply that a length h of a porous medium, over which a hydrostatic gradient [equal to $(p_2 - p_1 + \rho g h)$] is posed, will transmit water at a rate that is directly proportional to its permeability k and its cross-sectional area A and inversely proportional to the viscosity of the fluid, ν . Low temperatures reduce water flows through porous media. As has been discussed, low temperatures increase the viscosity of water. Freezing reduces the permeability of soils and ground dramatically. Geochemical solutions do not freeze uniformly at 0°C. The equilibrium freezing temperature of pore water is a function of pore geometry, freezing-point depressing effects of solutes, and the charge behavior of the porous matrix (*6*). The quantitative description of these effects, which is discussed below, is an active research area.

Soil-Water Retention Curve

The permeability of a frozen porous medium is affected by its liquid water content. Accordingly, a discussion of the physics of unsaturated porous media is appropriate.

Matric Potential

Two factors have been identified in determining the relationship between matric potential and water content in unsaturated soils. The first is the pressure difference between the soil atmosphere and the liquid water bound to soil particles. The second factor is the work required to expand the liquid water-air interface as soil-water content decreases. When a stable interface is established, these two factors are balanced and the water content is stable. For a given matric potential, any environmental event that changes one of these balanced factors relative to the other can be expected to cause the water content to change.

Effect of Temperature

An obvious, and pertinent, example is temperature, which decreases the interfacial tension of water against air. The effect of temperature on the soil-water retention curve may be estimated

via

$$\left(\frac{\partial\theta}{\partial t}\right)_{\Psi} = -\left(\frac{\partial\theta}{\partial\Psi}\right)_{t}\left(\frac{\partial\Psi}{\partial t}\right)_{\theta} \tag{4}$$

where θ is the volumetric water content of the porous medium in liters, and Ψ is the matric potential of the water in the porous medium in pascals.

For a given pore radius, the relationship between capillary pressure and interfacial tension is direct:

$$\Psi = -\frac{2\gamma^{wa}\cos\phi)}{r} \tag{5}$$

where r is the pore radius in meters and ϕ is contact angle of the water-air interface with the solid in radians.

The interfacial tension of water against air (in newtons per meter) from the triple-point of water (0.01°C) to the critical point of water (374.15°C) has been fitted to

$$\gamma^{wa} = \gamma_0\left(\frac{T_\ell - T}{T_\ell}\right)^{u}\left(1 - v\frac{T_\ell - T}{T_\ell}\right) \tag{6}$$

in which the parameters have the following recommended values: $\gamma_0 = 0.2358$, $T_\ell = 647.15$, $u = 1.256$, and $v = 0.625$. Although there have been few reported measurements of γ^{wa} below 0°C, these data indicate that Equation 6 is approximately valid to at least −8°C (*7*). The complexity of Equation 6 belies the fact that the interfacial tension of water against its vapor is virtually linear from −10°C to 50°C, as can be seen in Figure 5. Accordingly, one would expect that the following relationship would hold exactly:

$$\frac{[\partial\Psi(t,\theta)/\partial t]}{[\partial\gamma^{wa}(t)/\partial t]} = \frac{\Psi(t,\theta)}{\gamma^{wa}(t)} \tag{7}$$

In fact it does not, requiring the definition of an empirical variable $[G(\theta)]$ introduced by Nimmo and Miller (*8*) to account for the discrepancy:

$$G(\theta) = \frac{\dfrac{\Psi(t_2,\theta)}{\Psi(t_1,\theta)} - 1}{\dfrac{\gamma^{wa}(t_2)}{\gamma^{wa}(t_1)} - 1} \tag{8}$$

where $t_2 > t_1$.

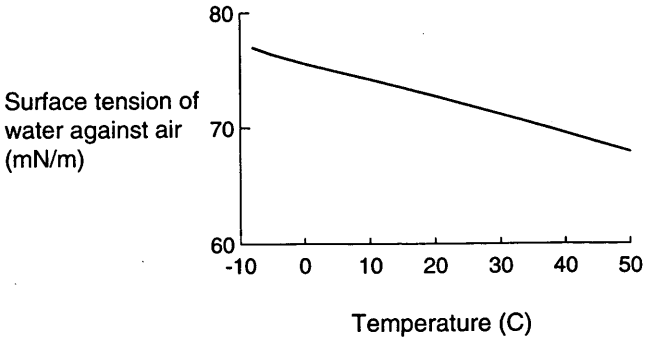

FIGURE 5 Measured values of interfacial tension of water against its vapor at a range of temperatures.

Soil Freezing Characteristic Curve

Liquid water (albeit generally very small amounts) exists in frozen soil at temperatures significantly below 0°C. For water-saturated frozen soils, an approximation of the liquid-water content can be calculated from the soil-water retention curve, if known. The physics of the two situations are similar: in the unsaturated, unfrozen soil, the liquid-water content is determined by balancing the pressure difference across the interface between the soil water and the soil atmosphere with the work necessary to deform this interface against the interfacial tension of water against air. The validity of this hypothetical mechanism for controlling the soil-water retention curve is supported by the observation that, for a given matric potential, the quantity of water held by the soil decreases as the temperature increases; that is, as interfacial tension decreases with increasing temperatures, less work is required to deform the water-air interface.

In frozen, water-saturated soils, there is a water-ice interface between the liquid water surrounding the soil particles and the ice. This situation is qualitatively similar to the water-air interface in unsaturated soils. A schematic displaying these parallel physical systems is presented in Figure 6. For a single soil sample of unaltered internal structure, liquid water contents in a frozen, unsaturated state should be a function of the pressure gradient across the water-ice interface. This function should be similar to the empirical equation that describes the soil-water retention curve.

Clapeyron Equation

For two phases at equilibrium (e.g., water and ice), the following expression applies:

$$\Delta_s^l H_m^* = T^{l+s}\Delta_s^l S_m^* \tag{9}$$

where

$\Delta_s^l H_m^*$ = molar enthalpy of fusion (J mol^{-1}),
$\Delta_s^l S_m^*$ = the molar entropy of fusion (J K^{-1} mol^{-1}), and
T^{l+s} = melting temperature (K) (*9*).

When the Gibbs-Duhem equation is applied to Equation 9, the following relation is obtained:

$$\frac{dp^{l+s}}{dT} = \frac{\Delta_s^l H_m^*}{T^{l+s}V_m^{*l}} \tag{10}$$

where p^{l+s} is the pressure at which the solid and liquid phases coexist (in pascals) and V_m^{*l} is the molar volume of the liquid phase. Equation 10 is known generally as the *Clapeyron equation*.

Following the suggestion of Koopmans and Miller (*10*), the Clapeyron equation has been applied to soil systems to estimate the matric potential of the liquid-water fraction of frozen soils.

This argument begins with the standard definition of capillary pressure (in pascals):

$$p_c = p(\text{liquid soil water}) - p(\text{ambient atmospheric pressure}) \tag{11}$$

which is related to matric potential by (*11*)

$$\Psi = \frac{p_c}{\rho g} \tag{12}$$

A similar pressure, p_i, may be defined for frozen ground to express the pressure gradient across the water-ice interface in frozen ground:

$$p_i = p(\text{liquid soil water}) - p(\text{ice}) \quad (13)$$

A term similar to matric potential can be defined for the pressure gradient across the water-ice interface in frozen ground:

$$\Psi_i = \frac{p_i}{\rho g} \quad (14)$$

If the volumetric content of soils for a given matric or supercooling potential is assumed to be dependent solely on the ratios of pressure gradients to interfacial tensions,

$$\theta\left(\frac{\Psi}{\gamma^{wa}}\right) = \theta\left(\frac{\Psi_i}{\gamma^{wi}}\right) \quad (15)$$

Then moisture-release and soil-freezing curves should be related by

$$\theta(\Psi) = \theta\left(\frac{\gamma^{wa}}{\gamma^{wi}}\frac{p_i}{\rho^{l}_{H_2O} g}\right) \quad (16)$$

The value of p_i as a function of temperature can be estimated by Equations 10 and 16 if it is assumed that $p_i = dp^{l+s}$ and $t - 0 = dT$. The necessary data are (*12,7*)

$\gamma^{wa}(p = 0.1\ \text{MPa}, t = 0.01°\text{C}) = 0.7564\ \text{N m}^{-1}$

$\gamma^{wi}(p = 0.1\ \text{Mpa}, t = 0°\text{C}) = 0.033\ \text{N m}^{-1}$

$\Delta^{l}_{s}H^{*}_{m} = 6007.0\ \text{J mol}^{-1}$

$V^{*l}_{m} = 18.018\ \text{cm}^3\ \text{mol}^{-1}$

$V^{*s}_{m} = 19.650\ \text{cm}^3\ \text{mol}^{-1}$

This implies that the pressure gradient across the water-ice interface changes with temperature according to

$$\frac{dp^{l+s}}{dT} = 1.221\ \text{MPa K}^{-1} \equiv 1.221\ \text{MPa°C}^{-1} \quad (17)$$

Making the proper substitutions into Equation 16,

$$\theta(\Psi) \approx \theta\left(-\frac{\gamma^{wa}}{\gamma^{wi}}\frac{\Delta^{l}_{s}H^{*}_{m}}{T_{fus}V^{*l}_{m}}\frac{t}{\rho^{l}_{H_2O} g}\right) \quad (18)$$

the following equation is derived:

$$\theta(\Psi) \approx \theta(ft) \quad (19)$$

where f is a constant approximately equal to 285.3 m H_2O °C^{-1}.

Changes in Hydraulic Conductivity with Soil-Water Content

The relative-hydraulic-conductivity model proposed by van Genuchten (*13*) has been adopted by many investigators. With some changes in notation, van Genuchten's model represents reduced water content, Θ (in liters), as a function of soil-water matric potential by

$$\Theta = \left[\frac{1}{(\Psi\alpha)^{\lambda} + 1}\right]^{\frac{\lambda-1}{\lambda}} \quad (20)$$

where α (m^{-1}) and λ (L) are empirical parameters. The reduced water content is defined by

$$\Theta = \frac{(\theta - \theta_r)}{(\theta_s - \theta_r)} \quad (21)$$

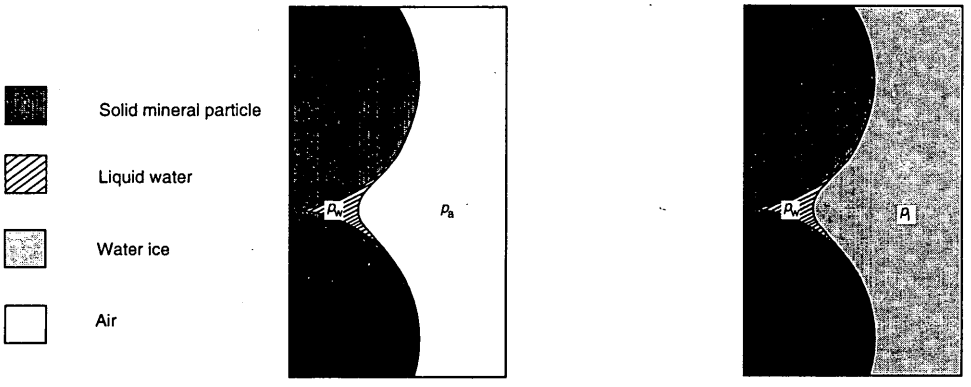

FIGURE 6 Schematic drawing showing the hypothetical similarity between water contents of unsaturated, unfrozen soils and of saturated, frozen soils.

where θ is the volumetric water content (L), and θ_s and θ_r are the the saturated and residual volumetric water content (L). The resulting empirical equations for volumetric water content are as follows; for unsaturated, unfrozen soils:

$$\theta = \theta_r + (\theta_s - \theta_r)\left[\frac{1}{(\Psi\alpha)^{\lambda} + 1}\right]^{\frac{\lambda-1}{\lambda}} \tag{22}$$

and, by extension, for frozen, saturated soils:

$$\theta = \theta_r + (\theta_s - \theta_r)\left[\frac{1}{(ft\alpha)^{\lambda} + 1}\right]^{\frac{\lambda-1}{\lambda}} \tag{23}$$

Similarly, the van Genuchten model proposed the following equations to calculate changes in relative permeability; for unsaturated, unfrozen soils:

$$K_r(\Psi) = \frac{\left\{1 - \dfrac{(\alpha\Psi)^{\lambda-1}}{[1 + (\alpha\Psi)^{\lambda}]^{\frac{\lambda-1}{\lambda}}}\right\}^2}{[1 + (\alpha\Psi)^{\lambda}]^{\frac{\lambda-1}{2\lambda}}} \tag{24}$$

and for frozen, saturated soils:

$$K_r(t) = \frac{\left\{1 - \dfrac{-(\alpha ft)^{\lambda-1}}{[1 + (-\alpha ft)^{\lambda}]^{\frac{\lambda-1}{\lambda}}}\right\}^2}{[1 + (-\alpha ft)^{\lambda}]^{\frac{\lambda-1}{2\lambda}}} \tag{25}$$

CONCLUSION

A surprisingly large number of sites in cold regions in the Northern Hemisphere are contaminated. There is a need to incorporate the fundamental physical, chemical, and hydrological processes that govern contaminant hydrology into the numerical models that are used to assist in the remediation of these sites. It is hoped that this paper assists in that process. The physical and chemical processes that determine the fate of contaminants in cold regions are just now being understood comprehensively. As with any new area of understanding, this is a challenging process, but it is also an exciting area at the limits of the understanding of the dynamic behavior of complex, heterogeneous materials.

RESEARCH PRIORITIES

The literature survey presented here has revealed important gaps in scientific information that will impede the development of contaminant-transport models for cold regions:

1. A consistent thermodynamic treatment of the hydrostatics of liquid water in frozen porous media, a critical need, has yet to be developed.
2. Aside from permeability, the capillary pressure-saturation relation for fluids in porous media is the most critical physical function for modeling the transport of fluids in variably saturated media. It has yet to be resolved entirely how temperature affects this relationship. A satisfactory understanding of the effect of temperature on soil retention curves for water and other liquids needs to be developed.
3. A coordinated research effort should be pursued to determine the temperature effects on the physics of insoluble and sparingly soluble nonaqueous phase liquids in porous media.
4. In frozen ground, the movement of solutes and water in response to osmotic and thermal gradients may be significant. Relations by which the transport of water, solutes, and nonaqueous phase liquids in response to thermal and osmotic gradients may be estimated reliably should be derived or developed.
5. The Pitzer model provides a powerful method by which to model the thermophysical behavior of electrolyte solutions below the freezing point of water. Unfortunately, there are few measurements with which to apply this tool. Physical-chemical properties of aqueous electrolyte solutions at subzero temperatures (constant-pressure heat capacities, molar volumes, and viscosities) are needed.

NOTATION

Symbol/Name (Definition)		*Equation First Cited*
A	cross-sectional area	(3)
c_j	aqueous concentration of the jth solute	(2)
$\mathbf{D}$	dispersivity tensor	(2)
g	acceleration due to gravity	(1)
h	height or width of a system	(3)
h	total head	(1)
$\Delta_s^l H_m^*$	molar enthalpy of melting, pure substance	(9)
k	(specific) permeability	(3)
$\mathbf{k}$	permeability tensor	(1)
$\mathbf{K}$	hydraulic conductivity tensor	(1)
p	pressure	(1)
p_c	capillary pressure	(11)
p_i	pressure gradient across ice-liquid-water interface in water-saturated porous media	(13)
q	seepage velocity	(3)
r	mean radius, largest undrained pore class	(5)
t	Celsius temperature ($\equiv T - 273.15$)	(17)
T	thermodynamic temperature	(9)
T^{l+s}	freezing temperature of pure solvent	(9)
$\mathbf{v}$	Darcian flow velocity vector	(1)
V_m^{α}	molar volume of α phase	(9)
$\Delta_s^l V_m^*$	molar volumetric change with fusion	(9)
z	vertical distance above datum	(1)
α	parameter in van Genuchten equation	(20)
γ^{wa}	interfacial tension of water against air	(6)
γ^{wi}	interfacial tension of ice against water	(15)

θ_r	residual liquid-water content	(21)
θ_s	saturated liquid-water content	(21)
Θ	reduced liquid-water content	(20)
λ	parameter in van Genuchten equation	(20)
ν	viscosity	(1)
ρ	density	(1)
ϕ	water-air contact angle at solid	(5)
Φ	porosity	(2)
θ	volumetric liquid-water content	(4)
Ψ	matric potential	(4)
Ψ_i	p_i expressed in terms of height of liquid water	(15)

ACKNOWLEDGMENT

Financial support by the U.S. Army Corps of Engineers, Waterways Experiment Station; the Cold Regions Research and Engineering Laboratory (Work Unit AT24-SC-FO2); and the U.S. Department of Defense Strategic Environmental Research and Development Program (SERDP) is acknowledged. The author warmly thanks S. E. Hardy, Y. Nakano, P. B. Black, and E. Wright for carefully reviewing this paper in manuscript.

REFERENCES

1. Bates, R. E., and M. A. Bilello. *Defining the Cold Regions of the Northern Hemisphere.* CRREL Technical Report 178. Cold Regions Reseach & Engineering Laboratory, Hanover, N.H., 1966.
2. Marigold, D. C., and C-F. Tsang. A Summary of Subsurface Hydrological and Hydrochemical Models. *Reviews in Geophysics,* Vol. 29, 1991, pp. 51–79.
3. Osipov, Y. A., B. V. Zheleznyi, and N. F. Bondarenko. The Shear Viscosity of Water Supercooled to −35°C. *Russian Journal of Physical Chemistry*, Vol. 51, 1977, pp. 748–749.
4. Zbeng, Q., D. J. Durben, G. H. Wolf, and C. A. Angell. Liquids at Large Negative Pressures: Water at the Homogeneous Nucleation Limit. *Science,* Vol. 254, 1991, pp. 829–832.
5. Perfect, E., P. H. Groenevelt, and B. D. Kay. Transport in Frozen Porous Media. In Transport Processes in Porous Media (J. Bear and M. Y. Corapcioglu, eds.), Kluwer Academic Publishers, Boston, 1989.
6. Everett, D. H. The Thermodynamics of Frost Damage to Porous Solids. *Journal of the Chemical Society, Faraday Transactions,* Vol. 57, 1961, pp. 1541–1551.
7. Haar, L., J. S. Gallagher, and G. S. Kell. *NBS/NRC Steam Tables.* Hemisphere Publishing Corporation, New York, 1984.
8. Nimmo, J. R., and E. E. Miller. The Temperature Dependence of Isothermal Moisture vs. Potential Characteristics of Soils. *Soil Science Society of America Journal*, Vol. 50, 1986, pp. 1105–1113.
9 McGlashan, M. L. *Chemical Thermodynamics.* Academic Press, New York, 1979.
10. Koopmans, R. W. R., and R. D. Miller. Soil Freezing and Soil Water Characteristic Curves. *Soil Science Society of America Proceedings,* Vol. 30, 1966, pp. 680–685.
11. Scheidegger, A. E. *The Physics of Flow Through Porous Media,* 3rd ed. University of Toronto Press, 1974.
12. Ketcham, W. M., and P. V. Hobbs. An Experimental Determination of the Surface Energies of Ice. *Philosophical Magazine,* Vol. 19, 1969, pp. 1161–1173.
13. Van Genuchten, M.Th. A Closed-form Equation for Predicting the Hydraulic Conductivity of Unsaturated Soils. *Soil Science Society of America Journal*, Vol. 44, 1980, pp. 892–898.

Publication of this paper sponsored by Committee on Physicochemical Phenomena in Soils.

PART 3

Management of Unpaved Surfaces

Factors Influencing the Transferability of Maintenance Standards for Low-Volume Roads

GERARD LIAUTAUD AND ASIF FAIZ

Among the many parameters that influence the selection of maintenance strategies for unpaved roads, two factors have been selected in this paper to illustrate that caution needs to be exercised when attempting to transfer policies or standards from one set of conditions to another. These two factors are *factor costs* (not budgets) and *material resources*. Broadly speaking, the definition of a maintenance policy for an unpaved network implies that besides routine activities such as vegetation control and ditch and culvert cleaning, consideration should be given to the frequency of grading and also to the timing of graveling operations. Drawing from the experience collected in two widely different environments, one in the equatorial forest region of central Africa—where maintenance costs are high and gravel resources scarce—and the other in northeast Brazil, it is shown that maintenance standards are highly dependent not only on traffic volume but also on the properties of surfacing materials and the unit cost of grading. As shown and explained in this paper, the optimum grading frequency derived from economic analyses for a given volume of traffic may vary by a factor of 5, ranging between 2 and 10 times per year. Similarly, the threshold value of traffic volume at which surfacing an earth road with gravel becomes economically justified can range from below 20 to more than 100 vehicles per day, depending on cost of graveling and physical properties of the subgrade to be graveled. Such wide variations suggest the need for a careful definition of local conditions before an attempt is made to transfer maintenance standards across countries or even across regions within a country.

Even under the best maintenance policy, vehicle operating costs on unpaved roads are usually 10 to 30 percent higher than those on well-maintained paved roads, mostly because of differences in average surface roughness conditions. Furthermore, the neglect of maintenance on an unpaved network may cause vehicle operating costs to increase by a factor of 2 to 3, because roughness can rise quickly from 5 m/km international roughness index (IRI) (on a newly graded road) to upward of 20 m/km within a few weeks if traffic volume is high. On paved roads, the situation is different: not only is the rate of progression of roughness slower, but also a smaller range of values is observed between a pavement in good condition (IRI = 3) and the same pavement at the end of its useful life, that is, in poor condition (IRI = 6 to 8), with the difference in vehicle operating costs generally not more than 30 percent.

Therefore, maintaining a network of unpaved roads requires relentless attention as well as a well-defined program of recurrent activities in order to keep the level of service of the roads within acceptable limits. Among the recurrent activities to be carried out, grading and graveling operations are the primary maintenance-related determinants of road conditions, and in turn of the cost of operating vehicles.

The World Bank, 1818 H St. N.W., Washington, D.C. 20433.

The frequency at which bladings are to be performed and the timing at which an unpaved road is to be surfaced or resurfaced with gravel constitute the basic requirements of any rationally designed maintenance program, and methods are now available that enable the definition of optimum standards both for grading frequencies and for appropriate timing of gravel surfacing (*1–3*). However, these standards are strongly dependent upon local conditions and a number of parameters such as traffic, level of service required, the importance of the road, climate (in particular, rainfall), budget constraints, material resources, and unit costs of grading and graveling. In this paper, the effect of the last two parameters is evaluated.

EFFECT OF MATERIAL RESOURCES ON MAINTENANCE STANDARDS

Grading Frequency

Depending on the availability of materials, the wearing course of unpaved roads may consist of a wide variety of soils, ranging from fine-grained silts or clays to fairly coarse gravel. Although the rate of surface deterioration is mostly influenced by traffic volumes, roughness progression is also governed by the physical and geotechnical properties of the surfacing material, that is, its particle size distribution and plasticity. Table 1, giving the mean rate of progression of roughness observed for various types of materials (*2,4,5*), shows, for example, that a surface course consisting of a sandy soil will, under the same traffic volume and similar climatic conditions, deteriorate some 20 times faster than a lateritic gravel wearing course. Consequently, and assuming that both roads were to be maintained at an identical level of service (i.e, at a given level of roughness), the frequency of grading in the first case would be substantially higher. Economic considerations suggest that an optimum level of service is governed not only by traffic volume but also by the expenditure corresponding to the number of gradings necessary to keep the long-term average roughness of the road within acceptable limits.

Figure 1 shows the difference in maintenance standards adopted for two regions in the same African country (Gabon); in one region the predominant soils were sandy clays with a mean rate of roughness progression of 0.5 m/km IRI per 1,000 vehicles, and in the other region the predominant soils were well-graded lateritic gravel with a rate of roughness progression of 0.08 m/km IRI per 1,000 vehicles. For the sandy clay surface road, the optimal grading frequency was about once every month, with a resulting average roughness of 8 m/km IRI. For the laterite road, the

TABLE 1 Mean Rate of Roughness Progression for Various Types of Materials (*4–6*)

Materials	Max. particle size, in mm	Plasticity Index	Soaked CBR at 95% Mod.AASHO	Increase in IRI/1000 veh, m/km
Fine-Grained				
Sands	2	< 10	5-20	1.3 to 1.8
Silts, silty clays	1	5-20	5-15	0.8 to 1.2
Clays	0.1	10-50	< 10	0.3 to 0.6
Coarse-Grained				
Silty gravel	10	16	> 15	0.07
Lateritic gravel	15-25	5-25	10-50	0.04 to 0.19
Crushed calcareous rock	30	10	85	0.09
Sandstone gravel	25-30	6-8	> 15	0.18
Quartzitic gravel	20-30	14-20	10-35	0.10 to 0.25
Cinder gravel	20	N.P.	> 20	0.20
Basalt gravel	30-75	20-30	> 20	0.20 to 0.24
Volcanic gravel	30	17	7-28	0.08 to 0.24

optimum grading frequency was about once every 4 months, with a resulting average roughness of 5 m/km IRI. Both roads had an average daily traffic (ADT) of 200. Similarly, and assuming that two roads have a gravel wearing course, the optimum grading frequency will depend upon the nature of the gravel material: for example, if the ADT is 200 vehicles and the desired year-round maximum roughness on these roads were to be fixed at 8 m/km IRI, a lateritic gravel course would need to be bladed three times a year, whereas a quartzite gravel course (with a greater maximum particle size, rounder aggregates, and less plasticity) would require grading eight times a year.

Graveling Threshold

The faster the rate of roughness progression on a road (as may result from poor geotechnical properties of the surfacing material), the closer will be the intervals between gradings needed to meet a given standard of roughness and consequently the higher will be the maintenance cost. In the Gabonese experience related above, embedding 1/2-in. stone in the silty clay subgrade at a rate of 10 L/m^2 proved effective in reducing the rate of roughness deterioration from 0.5 m/km to 0.24 m/km. As a result of this improvement, threshold values of traffic volumes at which full thickness graveling (15 cm) was justified changed from about 20 veh/day to nearly 50 veh/day. Since traffic volumes in that area were generally below this threshold and naturally occurring gravel is scarce, the economic return resulting from "nailing" the clay with a moderate amount of single-sized stones was very high.

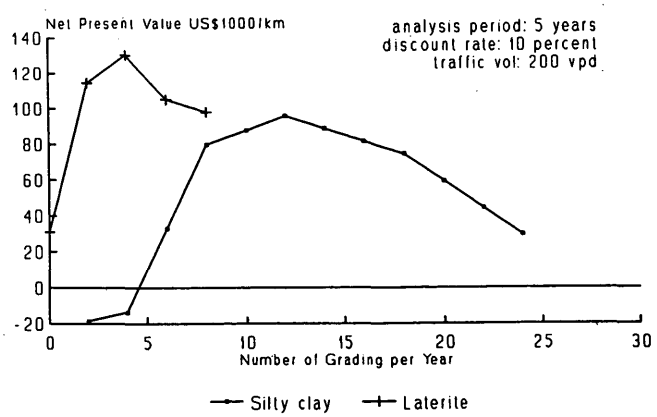

FIGURE 1 Influence of material properties on grading frequency.

EFFECT OF UNIT COSTS ON MAINTENANCE STANDARDS

By any standards, Gabon stands out as a country where unit costs of road construction and maintenance are exceedingly high because of particularly difficult physical and environmental conditions: predominance of dense primary forests, high rainfall, rolling or mountainous terrain, poor subgrade soils, and relatively high cost of labor. Assuming that the maintenance standard to be met corresponds to about 7 m/km IRI average roughness, the average cost of maintaining 1 km of unpaved road, including periodic regraveling, ranges between U.S.$20,000 and U.S.$30,000 for traffic volumes of 50 and 200 vehicles per day, respectively. By way of comparison, and to comply with the same standard, the average maintenance cost for 1 km of unpaved road located in northeastern Brazil varies between U.S.$2,000 and U.S.$3,000 for the same traffic volume, 10 times less. In either case, the average unit costs of maintenance are from competitive bids and include the cost of labor, materials, and equipment rental as differentiated below:

	Unit	*Brazil*	*Gabon*
Labor	U.S.$/hr	0.50	3
Gravel material	U.S.$/m^3	5	25
Grader rental	U.S.$/hr	35	125

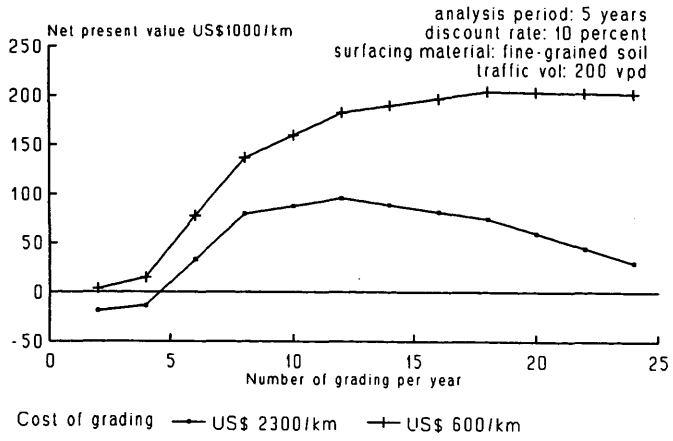

FIGURE 2 Influence of cost on optimum frequency of grading.

Under Gabonese conditions, and more generally wherever road maintenance and construction costs are high, competitive procurement procedures and careful evaluation of bids can result in substantial cost reductions. For example, under one maintenance contract, the lowest evaluated bid proposed a unit cost of grading equivalent to U.S.$600 per km, whereas the average cost submitted by other bidders was U.S.$2,000 per km. Economic analyses showed that awarding the contract to the lowest bidder meant that the unpaved network could be graded once every 15 days, thereby maintaining a level of roughness of about 6 m/km IRI throughout the year. Had the contract been awarded to the average bidder, the same network would have been graded about once a month with only a fair to poor level of roughness, about 9 m/km IRI, for an ADT of 200 vehicles per day (see Figure 2).

The magnitude of graveling costs can also have a significant impact upon the standard of maintenance. As in many other countries, there are large areas in Gabon where naturally occurring gravels are difficult to find and the cost of haulage of the material over long distances can more than double the total cost of graveling operations. In areas where lateritic gravels are abundant, the average unit cost of graveling is of the order of U.S.$15/m^3. In the eastern part of the country, where sands are predominant, the cost of providing 1 m^3 of gravel may be as high as U.S.$40. In the latter case, graveling thresholds would increase from about 25 veh/day to 45 veh/day, thereby introducing a significant change in the maintenance policy.

TABLE 2 Differences in Maintenance Standards Between Gabon and Northeast Brazil

Costs	Brazil	Gabon	
		low case	high case
Vehicles operation US$/veh*km			
for IRI=2	0.24	0.82	0.82
IRI=5	0.31	0.93	0.93
IRI=10	0.46	1.16	1.16
IRI=15	0.67	1.43	1.43
IRI=20	0.98	1.78	1.78
Graveling US$/ cu.meter	5.0	15	40
Grading US$/ km	200	600	2000
Standards			
Optimum number of grading/year			
for ADT=50	5	3	2
ADT=100	10	4	3
ADT=150	14	6	5
ADT=200	19	8	6
ADT=300	23	10	8
Gravelling threshold (ADT) vpd	10	25	45

Note: The above grading frequencies apply to a gravel surface having an average rate of roughness progression of 0.14 m/km per 1,000 vehicles, and will result in a maintenance level of service corresponding to an average 5 to 6 m/km IRI throughout the year.

COMPARISON OF OPTIMAL BLADING FREQUENCY AND GRAVELING THRESHOLD

To illustrate the differences in maintenance standards that may occur between two widely different environments, a comparison was made using the results of two studies on optimal grading frequencies for Gabon and northeastern Brazil. In both cases, vehicle operating costs were calculated with the HDM III model (*6,7*), duly calibrated for local conditions. Assuming a lateritic gravel wearing course for both cases, the optimal blading frequency was taken as the value that yielded the maximum net present value, discounted at 10 to 12 percent. Table 2 gives the results of the comparison and shows, for example, that for an average traffic volume of 100 vehicles per day, the appropriate grading frequency would be 10 times a year under Brazilian conditions and only 3 to 4 times a year under Gabonese conditions. The corresponding maintenance level of service was an average 4 to 5 m/km IRI for Brazil and an average 6.5 to 7 m/km IRI for Gabon.

Regarding graveling operations, the sheer difference in unit cost for graveling between Gabon and Brazil had a significant impact upon the graveling threshold. The cost of providing 1 m^3 of gravel in Gabon (when borrow pits are readily available) is about U.S.$15, as compared with a cost in Brazil of about U.S.$5 under similar material availability conditions. Calculations show that a cost ratio of this magnitude (about 3) would entail a graveling threshold ratio varying between 1.5 and 2, depending on the rate of roughness progression of the earth road before graveling is carried out. In other words, if graveling were justified in Brazil whenever the ADT reached 50 vehicles, such justification in Gabon would only occur for an ADT between 75 and 100 vehicles.

CONCLUSIONS

A comprehensive maintenance policy embodying appropriate standards for grading frequencies and graveling thresholds cannot be properly formulated unless due consideration is given to local conditions, in particular, to traffic volumes, materials resources specifications, and unit costs of blading and graveling operations. The optimum level of service to be aimed at, in terms of year-round average roughness on the network, cannot be determined by simply transferring maintenance standards from one country to another country or from one geographical region within a country to another. For example, blading frequencies applicable in one country may be well above the optimum values in another country, leading to substantial economic losses should such standards be transferred without an analysis of local conditions.

Management of unpaved road requires not only reliable traffic volume data and unit costs of maintenance activities but also regular condition surveys aimed at assessing surface material properties and the rates of roughness progression for the major types of wearing course materials constituting the unpaved road system. The reliability of factors influencing maintenance service levels for unpaved roads suggests several distinct maintenance standards or strategies that should be evaluated for each specific set of cost and material resources parameters peculiar to a region.

REFERENCES

1. Harral, C., and A. Faiz. *Road Deterioration in Developing Countries: Causes and Remedies.* The World Bank, Washington, D.C., 1988.
2. Patterson, W. D. O. *Road Deterioration and Maintenance Effects.* World Bank, Johns Hopkins Press, 1987.
3. Callao, R. A. *HDM Manager Version 2".* Transport Division, The World Bank, Washington, D.C., 1993.
4. Parsley, L. L., and R. Robinson. *The TRRL Road Investment Model for Developing Countries (RTIM2).* TRRL Laboratory Report 1057, Transport and Road Research Laboratory, Crowthorne, Berkshire, England.
5. Liautaud, G. Le Comportement des Routes en Afrique Occidentale et Centrale: Synthese de 20 Ans d'Observations. World Bank, Washington, D.C., 1993.
6. Watanatada, T., C. G. Harral, W. D. O. Patterson, A. M. Dhrareshwar, and K. Tsunokawa. *The Highway Design and Maintenance Standards Model, Volume 1: Description of the HDM-III Model.* World Bank, Washington, D.C., 1987.
7. Watanatada, T., C. G. Harral, W. D. O. Paterson, A. M. Dhareshwar, A. Bhandari, and K. Tsunokawa. *The Highway Design and Maintenance Standards Model, Volume 2: User's Manual for the HDM-III Model.* World Bank, Washington, D.C., 1987.

Publication of this paper sponsored by Committee on Low-Volume Roads.

Operational Unpaved Road Management System in the Cape Province of South Africa

A. T. VISSER, E. M. DE VILLIERS, AND M. J. J. VAN HEERDEN

The Roads Department of the Cape Province of South Africa manages a rural road network that includes 16 900 km of paved roads and 51 750 km of unpaved roads. Unpaved roads are usually considered of lesser importance, because in the Cape Province these roads typically carry between 20 and 300 vehicles per day. The expenditure on their maintenance is, however, the same as that for paved roads. The aim of this paper is to present the characteristics of the unpaved road management system, which includes a gravel management system; to demonstrate the relationship of these systems in the planning process; and to document the experience gained with implementation of the system. The Maintenance and Design System (MDS) was used as a basis for the management system, although extensive adjustments were made to cater to local practice and requirements. It has been 3 years since the system was implemented. To date, 38 000 km of the unpaved network has been evaluated, and the information has been entered into the data base. The system has already proved its worth and is being used in compiling the annual budget and providing strategic prioritized input to facilitate the scheduling of activities at the project level. It has also helped to ensure an equitable distribution of maintenance funds among the 20 Regional Services Council (RSC) areas, through which the gravel road maintenance is executed on an agency basis. On the basis of experience in the Cape Province, the management of unpaved roads should be an integral part of the management process of any road authority.

The Roads Department of the Cape Province of South Africa manages a rural road network that consists of 16 900 km of paved roads and 51 750 km of unpaved roads. These roads include

- Trunk roads that primarily serve the larger centers,
- Main roads joining cities and smaller towns and important centers, and
- Divisional roads acting as access and link roads in the rural areas and being generally important for agriculture.

The last two types form the bulk of the unpaved network. In addition, 84 000 km of minor roads is currently not included in the formal management systems. The total rural road network serves an area of 656 641 km^2, which comprises nearly 58 percent of the area of the Republic of South Africa.

Since 1981, a pavement management system for the paved network has been in use, and the positive results from this system led to the implementation of a management system for the unpaved network. Unpaved roads are usually considered of lesser importance, because these roads in the Cape Province typically carry between 20 and 300 vehicles per day. The expenditure on their maintenance is, however, of the same magnitude as that for paved roads, but it is justified particularly where roads serve the mining industry, major agricultural producing areas, and tourism.

The aim of this paper is to present the characteristics of the unpaved road management system, which includes a gravel management system; to demonstrate the relationship of these systems in the planning process; and to document the experience gained with the implementation of the system. The unpaved road management system provides

- Routine maintenance requirements, such as blading;
- Special maintenance requirements for roads that cannot be maintained routinely, for example, reworking to remove or reduce oversize materials or reshaping;
- Regraveling requirements;
- Budget requirements and the implications of alternative budgets; and
- Optimization of the use of borrow pits for regraveling, and the implications of using scarce natural resources from the gravel management system.

The Maintenance and Design System (MDS) (*1,2*) was used as a basis for the management system, although extensive adjustments were made to cater to local practice and requirements. It has been 3 years since the system was implemented. Since the Roads Department did not have enough staff to collect the information to operate the system, eight consulting engineering firms were appointed, each to a region. To date, 38 000 km of the unpaved network has been evaluated and the information has been entered into the data base. The system has already proved its worth and is being used in compiling the annual budget and providing strategic prioritized input to facilitate the scheduling of activities at the project level. It has also helped to ensure an equitable distribution of maintenance funds among 20 Regional Services Council (RSC) areas, through which gravel road maintenance is executed on an agency basis.

The structure of the management system is presented first, and then examples of the outputs are provided. The operational aspects of implementing and operating the system are discussed. Finally the value of using the system is discussed, and recommendations for other road authorities are given.

A. T. Visser, Department of Civil Engineering, University of Pretoria, Pretoria, 0002, South Africa. E. M. de Villiers, Materials, Roads and Traffic Administration Branch, Cape Provincial Administration, P.O. Box 2603, Cape Town, 8000, South Africa. M. J. J. van Heerden, van Heerden and van der Vyver Inc., P.O. Box 95256, Waterkloof, 0145, South Africa.

UNPAVED ROAD MANAGEMENT SYSTEM

Introduction

The length of the unpaved road network prohibits its being monitored by sophisticated and expensive means. Consequently, visual monitoring was adopted to evaluate the condition of the road and the need for specific actions. Ideally, such visual inspections could be done by the district road superintendents during their three-monthly visits to the roads under their jurisdiction. Setting up the system was beyond the staff capabilities of the Roads Department, and a consulting engineering group was appointed for the implementation in each of the eight regions. Another consulting group was appointed for software development and data processing.

Installing a reference system on the unpaved road network proved to be a major task. To date, about a third of the implementation cost has been expended on placing location markers in the field so that all observations could be tied to the reference system. Markers were placed at the start and end of each road section, as well as every 5 km along the section, and at boundaries of the different regions as well as at marked changes in topography. The basic building blocks for assessment purposes are the 5-km segments. Subsegments primarily involving marked changes in topography, notably in mountain passes, are also accommodated.

The unpaved road management system is essentially a network-level tool. The network is monitored to determine the global deterioration over time as well as to identify, prioritize, and determine approximate budgets for the network as a whole. The coarse network evaluation is then used as a strategic input for the detailed project-level investigations where the actual design is determined with the aid of further refined investigations and tests. Because the focus was at the network level, care was taken to collect only the information that was relevant and required at the network level.

The collected information was then processed in a computer data base to provide the outputs for top management for strategic and budgeting purposes as well as for maintenance engineers for tactical planning and execution purposes. These outputs will be discussed below.

Visual Assessment

The visual assessment is carried out by means of the evaluation form shown in Figure 1. Four different attributes of the road section are considered:

- Fixed information,
- Structural assessment,
- Functional assessment, and
- General information.

These attributes will be discussed briefly.

Fixed Information

Fixed information includes location, such as region, road number, and start and end kilometer distances. The road type typically defines the road width, and the width is used to confirm the data. Traffic counts are very costly, and three categories of traffic had to be used based on vehicles encountered on the section, knowledge of the area, and discussions with the local people. Less than 50 vehicles per day (vpd) is considered light traffic, medium is from 50 to 300 vpd, and heavy is more than 300 vpd. Terrain is designated as flat, rolling, or mountainous, according to broad guidelines. The moisture regime at the time of evaluation is important because it could accentuate or mask certain types of deterioration and is used where significant differences with previous assessments are encountered. Finally, a distinction is made between a gravel road and a nonengineered earth road, because the latter would normally receive no additional gravel. In addition, information such as the nature of agricultural activities is also collected to facilitate a strategic plan to curb the impact of dust in a prioritized manner; for example, a high earner of foreign exchange would receive a high priority for paving.

Structural Assessment

Structure The structural assessment is related to the ability of the pavement to carry the traffic loads. Although there may be arguments about the inclusion of other aspects or the exclusion of some of the evaluated factors, the process is aimed at identifying structural needs such as regraveling, ripping and recompaction,

CAPE PROVINCIAL ADMINISTRATION

ASSESSMENT (GRAVEL ROADS)

AREA : A B C D E F G H
RSC :
ROAD NO :
SECTION : FROM ____ km
: TO ____ km
WIDTH (m) 6 - 7.9 | 8 - 9.9 | 10 - 12

DATE :
ROUTE : TRUNK | MAIN | DISTRICT
TRAFFIC : LIGHT | MEDIUM | HEAVY
TERRAIN : F | R | M
MOISTURE : WET | MOIST | DRY
TYPE OF ROAD: GRAVEL | EARTH

STRUCTURAL ASSESSMENT

STRUCTURE		DEGREE MINOR 1	2	3	4	SEVERE 5	EXTENT SELDOM 1	2	3	4	FREQUENT 5
POTHOLES	0										
CORRUGATIONS	0										
RUTTING	0										
LOOSE MATERIAL	0										
DUST	0										
STONINESS : FIXED	0										
: LOOSE	0										
GENERAL CONDITION		VERY GOOD		GOOD		FAIR		POOR			VERY POOR

GRAVEL PROPERTIES					
GENERAL	FERRICRETE	CALCRETE	QUARTZITE	CHERT	DORBANK
MATERIAL TYPE	SANDSTONE	GRANITE	SHALE	DOLERITE	SAND
MAXIMUM SIZE (mm)		> 50	> 25-50	> 13-25	< 13
CLASSIFICATION		COARSE	MEDIUM	FINE	
APPROXIMATE PI		< 6	6 - 15	> 15	
GRAVEL THICKNESS (mm)					

FUNCTIONAL ASSESSMENT

RIDING QUALITY	VERY GOOD	GOOD	FAIR	POOR	VERY POOR
SKID RESISTANCE		GOOD	FAIR	POOR	
EROSION : LONGITUDINAL DIRECTION		NONE	MINOR	SEVERE	
: CROSS DIRECTION		NONE	MINOR	SEVERE	
DRAINAGE : ON THE ROAD		> 4%	2 - 4%	0 - 2%	
: SIDE OF THE ROAD		GOOD	FAIR	POOR	
: PROBLEMS	CULVERTS	SIDE DRAINS	MITRE DRAINS	TOO LOW	

GENERAL INFORMATION

WEEKS SINCE LAST GRADED

PROBLEMS WITH:		YES	NO
	DUST		
	SKID		

NORMAL GRADING (EVERY ? WEEKS)	
WET SEASON	DRY SEASON

FIGURE 1 Field inspection form.

and reshaping or special blading. The way in which the visual assessment is conducted requires the use of technicians skilled in materials and unpaved roads. Assessments should preferably not be made while there is water on the road surface.

All the aspects are assessed in terms of severity and extent. Three anchor values are used to define severity, namely,

1: Visually noticeable, but still minor, usually isolated;
3: Needs attention, but not urgent; and
5: Needs urgent attention.

If the assessment is intermediate to the above anchor values, either 2 or 4 is noted. If there are no defects, a zero is noted without an extent. The extent is given on a five-point scale, as follows:

1: 0 to 5 percent,
2: 5 to 20 percent,
3: 20 to 60 percent,
4: 60 to 80 percent, and
5: 80 to 100 percent.

The occurrence is estimated, and no lengths are measured.

The condition attributes that are evaluated, according to clearly defined guidelines in the evaluation manual, are the following:

- Potholes, which are local depressions;
- Corrugations, which are regular undulations transverse to the direction of travel;
- Rutting, which defines the wheelpath and is caused by wear or compaction in the wheelpath;
- Loose material deposited adjacent to the wheelpaths or occasionally in the wheelpath after maintenance;
- Dustiness, as an indicator of safety; and
- Stoniness, which, when the stones are embedded, reflects the ability of the motor-grader to maintain the road, and when stones are loose, reflects rapid and severe ravelling.

In addition, the observer gives a general impression of the quality of the road, which is used to validate the other attributes.

Gravel Properties Detailed testing of the gravel characteristics of the complete network would have been prohibitive. Initially the most important characteristics were evaluated visually, namely, type of gravel, maximum size, type of grading, and plasticity index. As part of the gravel management program, the available sources were tested, and when one is placed on the road, the data base is updated. Fortunately, the maintenance strategy is not highly sensitive to small variations in material properties (actual versus estimated visually), and this approach gave a working solution for the initial stage of implementation. No doubt, for long-term planning of regraveling, the more accurate data will yield more reliable predicted gravel loss.

The gravel thickness was measured at least five times within a section, or every 1 km, by making a hole and measuring the thickness of the gravel. This information is used to determine regraveling needs.

Functional Assessment

The functional assessment evaluates the service that the road provides to the user. Riding quality is assessed by driving over the section, and the qualitative descriptors are linked to roughness measurements. Skid resistance on unpaved roads is difficult to measure, particularly since it is unlikely that the worst conditions are encountered at the time of measurement. Comments from the district staff or local users about skidding during the wet are used to flag potential problem materials. Erosion could make a road unserviceable, and both the erosion on the road as well as that alongside the road are assessed. Any defects would have to be corrected apart from the structural aspects of the road. Any specific problems are also highlighted.

General Information

Observations related to the general condition of the road are also noted. These include normal blading frequencies, time since last blading, and dustiness and slipperiness. This information is primarily used to judge observations that are significantly different from the general trend.

Evaluation of Special Activities

Special activities are those that are not carried out routinely but are executed in response to a deficient condition. Special activities include regraveling, ripping and recompacting, and reshaping and special grading. A flowchart showing the evaluation process is given in Figure 2. The underlying philosophy is that a higher-order action is only executed if a lower-order action would not be effective. Generally a higher order would be more expensive than a lower order. In this manner a road with a large number of rocks protruding through the surface would only be regraveled if there is insufficient gravel. Otherwise it would be ripped, the coarse stones would be removed (or if feasible, reduced to the specified maximum 37.5-mm size using gridroller or rockbuster techniques), and the road would then be recompacted.

Regraveling

The regraveling need is identified first. A regraveling score is calculated as a function of the minimum required gravel thickness to carry the loads, annual gravel loss, existing or predicted gravel thickness, and the traffic volume. The needs are prioritized by ordering the regraveling scores, and the roads are treated until the allocated budget has been expended. Five-year regraveling programs can be compiled in this manner and long-term underfunding identified at an early stage. Ideally the volume of material lost annually should be replaced to maintain a balance between wear and replacement.

Ripping, Reworking, and Recompacting

Ripping, reworking, and recompacting are triggered by the extensive presence of coarse stones that render blader maintenance ineffective. The product of severity and extent of stoniness greater than 12 triggers this need. In the event of a lack of binder, represented by less than 14 percent passing the 0.075-mm sieve, or the product of severity and extent of loose material greater than 12, additional binder has to be placed after ripping.

Reshaping

If the gravel layer is less than 75 mm, it is ineffective to try and rip the wearing course to remove the coarse stones. In such cases the wearing course is only reshaped and recompacted, because regraveling will be required within a relatively short period. The same approach would be taken if the shape of the road was poor and drainage on the road was classified as poor.

Special Blading

There are cases in which none of the foregoing actions would be triggered, but nevertheless the road is in poor condition, possibly because of neglect in maintenance. The situation often cannot be remedied by routine maintenance, and a special maintenance action is required. The road is considered in poor condition if the riding quality is poor or very poor or the product of severity and extent of potholes, rutting, or corrugations is greater than 11. In the cases of special maintenance, slippery areas in steep terrain, represented by a plasticity index greater than 15 and fine material, may be rectified by the addition of coarse material.

Evaluation of Routine Maintenance Activities

Once the network is in such condition that routine maintenance can be effectively executed, the routine maintenance needs are determined. These include the routine blading at an economic frequency, and the volume of gravel that needs to be replaced to balance the material lost.

Details of the procedure used to calculate grader maintenance were presented previously by Visser and Curtayne (*1*) and the models used by Paige-Green and Visser (*2*), and they will not be repeated. From this procedure the economically optimal allocation of motor-graders and resources for any given budget can be determined. The sum of the cost of maintenance and the road user costs is used to define economic optimality. The resources are allocated to the network such that the expenditure of an additional unit of costs would result in the same benefit on every road.

The volume of gravel lost is calculated for the gravel roads of the network using the process and models presented previously (*1,2*). Once the volume of material lost annually is known, the budget can be defined on the basis of the volume that has to be replaced to keep up to date. The roads on which the gravel would be placed are identified from the special maintenance evaluation.

Gravel Management Subsystem

Good quality road-building materials are usually relatively scarce. In a given area the better-quality materials are invariably used first, with the result that later only poorer-quality gravels are available for use as a wearing course. The situation is even worse when the gravel road has to be upgraded to the paved-road standard, and expensive processed gravels have to be purchased if the local materials are not good enough. The gravel management subsystem was implemented to handle this situation.

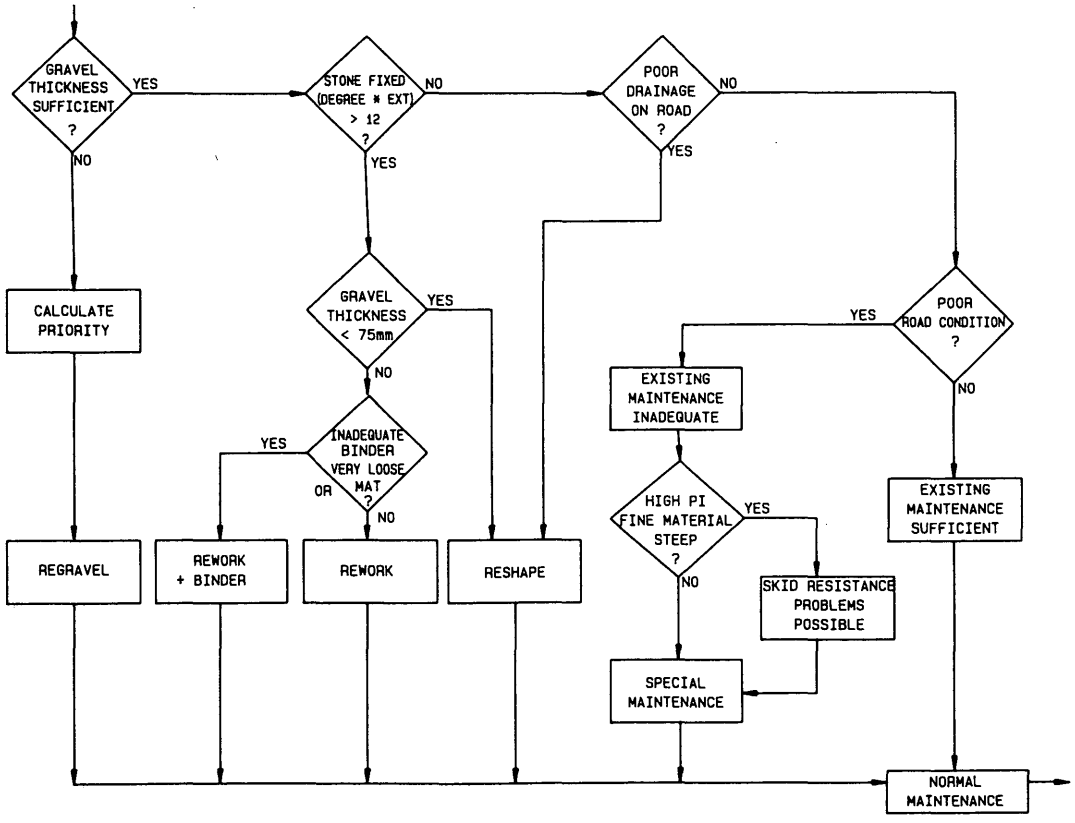

FIGURE 2 Flow chart for determining special maintenance requirements.

The gravel management subsystem contains information about the location of existing or potential gravel borrow pits and the properties and volume of the available materials. A special effort was made by the consulting engineering groups to identify all potential borrow pits within an economic haul distance of the road network. For the first time, an overall view is available as to the availability of materials. Gravel materials are also allocated to specific roads taking into account the quality of gravel, the consequent routine maintenance costs and road quality, and location of the borrow pits. This allocation process is done manually, and no formal optimization is used.

Besides the quality of the gravel, the performance of the roads on which specific materials have been used is monitored to confirm or modify the performance prediction equations. This monitoring also provides the opportunity for mixing materials from different borrow pits to obtain one that would provide the best economic performance. Consequently, planning for regraveling has been significantly enhanced.

Another major benefit of the gravel management subsystem is that, particularly in areas with limited gravel resources, the cost of bringing in processed materials can be considered. In some cases it would warrant paving the road to retain the scarce gravel resources. This would enhance long-term management of the network.

OUTPUTS GENERATED BY UNPAVED ROAD MANAGEMENT SYSTEM

Introduction

Outputs have been tailored to the specific needs of the different levels of management within the Cape Roads Department and of the Regional Services Councils (RSCs). This is particularly important because the Chief Executive Officer needs to know the financial and economic implications, whereas the maintenance engineer in a district wishes to know the sections of road where special maintenance is required and the evaluated condition that triggered this need. The different types of output that are prepared are discussed next, starting with the detailed outputs for the field staff and progressing to that required by top management.

Detailed Outputs

Detailed printouts of the input and processed information are prepared for use by the field staff. These are in typical computer printout formats and because of the large amount of data are not reproduced here. The information is also presented as a strip chart for each road, as shown in Figure 3. This is a handy format because it contains all the relevant information for the road and is normally compiled as a book for each of the 20 regions. It shows the homogeneous sections that were assessed, the traffic volumes, and the existing gravel thickness. From the analyses, a 5-year regraveling program was developed. From this overall perspective it may be decided from an operational point of view to regravel the short sections programmed for successive years in one year.

Parts of the road identified for ripping, reworking, and recompacting or reshaping are also shown, together with the assessment that triggered the need. Although some parts are due for immediate regraveling, they have also been flagged for reshaping if regraveling has to be postponed. Before the work is executed, the exact limits of each activity will be determined by a detailed field inspection at the project level, which is obviously beyond the scope of the unpaved road management system.

Management Information

Management is interested in strategic and financial implications, and the summary information has to address these requirements. One of the most easily understood formats for presenting data is graphically, and this was widely used.

Figure 4 shows the information about regraveling needs for each RSC area as well as for the complete network. Because the output is repetitive, only part of it is presented. For each RSC area the network length and annual gravel loss are shown. The regraveling needs for the next 3 years are indicated. By comparing the length of the bars for regraveling, taking into account the road length and annual loss, an immediate indication can be gained about the severity of the needs and potential backlogs.

At the end of the output, a summary is given for the complete network together with the annual gravel loss. In Figure 4 it is evident that a backlog equal to one year's regraveling has developed and that this backlog can be reduced by the recommended annual program. From inspection of the plot for the whole network, it was evident that the backlog was isolated particularly in one large RSC area. With the managerial information, this matter can be readily rectified.

A further diagram, presented in Figure 5, shows the distribution of gravel thickness as a histogram and the annual change in average gravel thickness as a trend resulting from loss and regraveling. The latter is particularly useful in determining whether the situation is being kept under control. Such plots are developed for each RSC area, for each road category, and for the network as a whole. As a further plot (not shown), the average gravel thickness for each RSC area is plotted as an arrow on a horizontal axis of gravel thickness from 0 to 150. It is possible to see at a glance where the problem areas with low average gravel thickness are located.

Special maintenance needs are also plotted as a series of bar charts for each RSC area (Figure 6). Beside the bars, numerical values are given for the length of road that requires ripping and recompacting, reshaping, or special blading. Although the needs in some areas appear large, invariably they are for large networks. In due course the special maintenance needs should decrease significantly when better control over the quality of regraveling materials is exercised, and effective routine maintenance is applied. However, the corollary is also true, namely, that routine maintenance cannot be effective if the road conditions are inappropriate.

A routine grader maintenance budget is determined from the marginal benefit/cost curve as a function of blading budget, as shown in Figure 7. For public authorities it is impossible to spend an amount on maintenance such that for an additional unit of expenditure the road user would save one unit. Analysis of public authority operations has showed that invariably one additional unit of cost is spent on maintenance for each three to five units of benefit derived by the road user. The impact of a reduction in the recommended budget can then be determined by expressing it as the additional cost incurred by the road user.

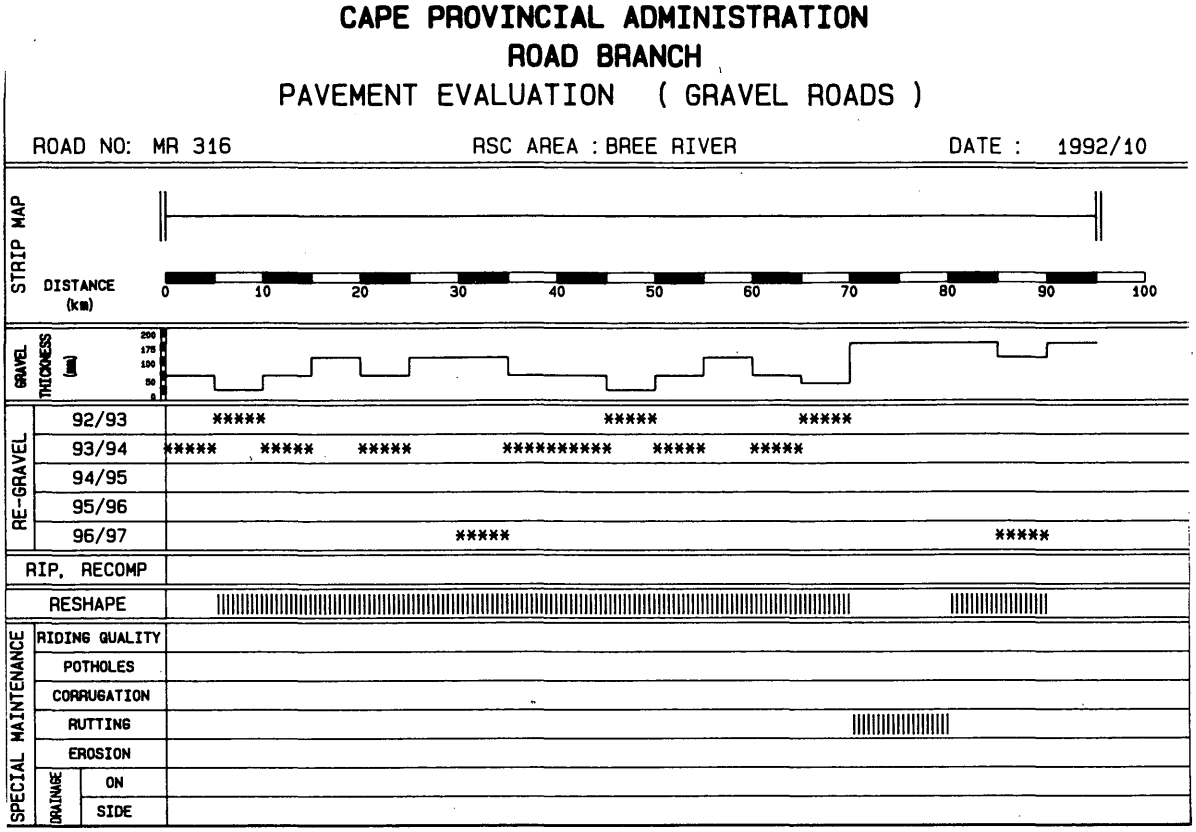

FIGURE 3 Strip chart showing condition and special maintenance needs.

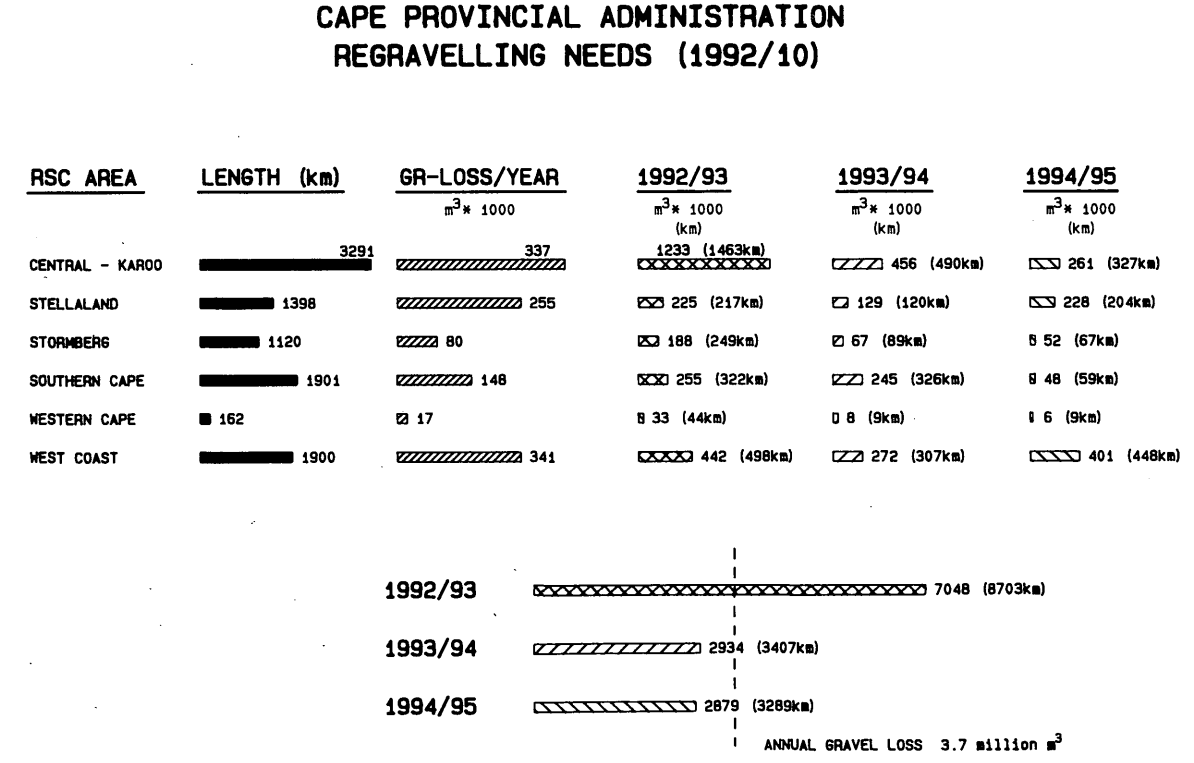

FIGURE 4 Summary chart of regraveling needs.

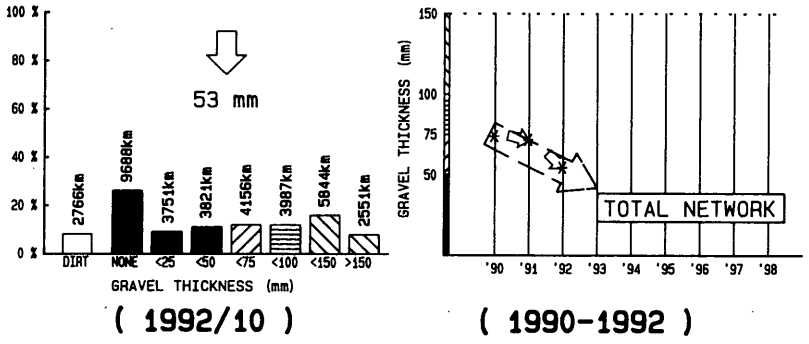

FIGURE 5 Histogram distribution of gravel thickness and changes over time.

IMPLEMENTATION AND OPERATIONAL CONSIDERATIONS

In the implementation phase of the unpaved road management system, a workload beyond the capabilities of most organizations develops. The approach adopted in this study of dividing the Cape Province into eight regions and allocating each region to a consulting engineering group has worked well. In this manner the experience of the individual groups was also harnessed to the benefit of the overall project. The coordination, data processing, and reporting constituted a further major task, and allocating this task to another consulting engineering group ensured that there was good correlation among groups. Ideally one set of assessors should be used to ensure uniformity of procedures. The magnitude of the task, however, prohibited the application of the ideal situation. The coordinating group held regular training sessions with the assessors to ensure a uniform approach to the evaluations and also to ensure that the same standard as that in previous years was being maintained.

Although at first glance the data collection phase appears prohibitively expensive and would unnerve most organizations, there are ways of overcoming the time lag for useful implementation and cost implications. It is important that the system generate useful information at an early stage. Roads that carried more than 150 vpd as well as roads previously identified as problem roads and roads scheduled for immediate regraveling were considered to be the first priority. Information relevant to these roads—that is, information that had a significant influence on managerial outputs— was collected, and the less important information was estimated from local conditions. The relevant information is road length and width and traffic volumes. Within a few months it was possible to provide a fairly good indication of the needs. As regraveling takes place the properties of the gravel wearing course are substituted for the estimated material properties, and the system is updated. In this manner valuable management information is generated at an affordable cost.

Operationally there may be some additional data collection required. A system of sending as-built information to the data base manager has been instituted. In this way all regraveling information is captured. In those cases where special maintenance is executed, the team foreman sends a report to the data base manager. The routine evaluation of the network on a 3-year cycle is expected to remain the responsibility of the consulting engineering groups. This will at the same time strengthen the technical input to the RSCs, because much of the work would be carried out in close liaison with them.

The application of maintenance funds to those areas in which they are required, thus ensuring that the complete network benefits, far outweighs the cost of operating the unpaved road management system. The Cape Roads Department would recommend that all road authorities implement unpaved road management systems on the basis of the benefits of this system that have already accrued within the short period of its use.

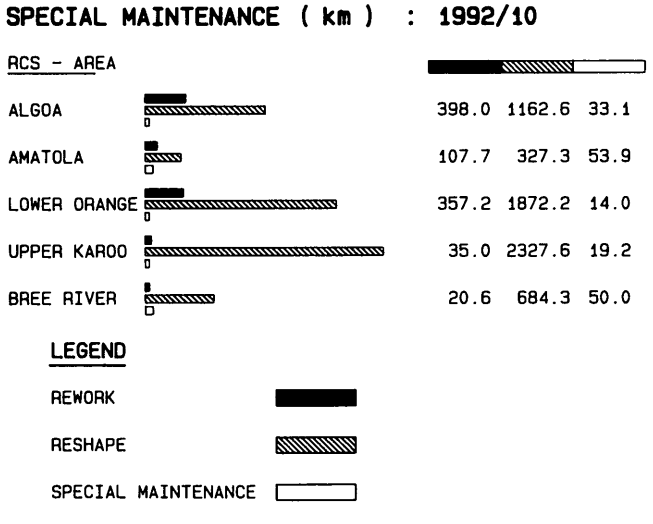

FIGURE 6 Summary chart of special maintenance needs.

CONCLUSIONS AND RECOMMENDATIONS

An unpaved road management system was installed in the Cape Province of South Africa. Since implementation 3 years ago, 38 000 km, or about two-thirds of the proclaimed unpaved network, has been placed on the system. The information is being used to compile the annual budget and to provide strategic prioritized input to facilitate the scheduling of activities at the project level.

One of the system outputs relates to the regraveling needs and allocation of the regraveling budget on a priority basis for a 5-year planning horizon. Special maintenance needs in terms of ripping, reworking, and recompacting; reshaping; and special blading are also identified from a visual assessment of uniform links. The special maintenance is required to bring the road to a

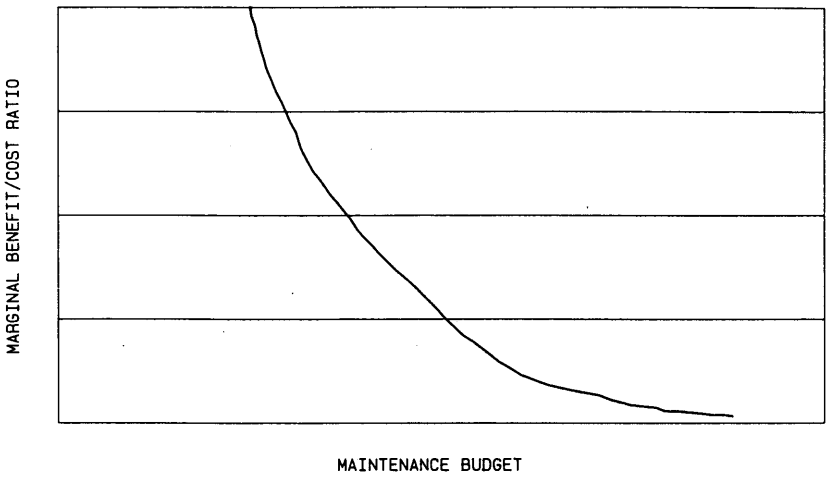

FIGURE 7 Marginal benefit cost ratio curve for determining the appropriate maintenance budget.

condition such that routine blading can be executed effectively. The routine blading budget is determined by considering the effect of maintenance on total transport cost on the network. By using the marginal benefit/cost ratio curve, the effect of changes in the recommended budget can be demonstrated in economic terms.

A gravel management subsystem is an integral part of the unpaved road management system. This is a feature that has not previously been reported as being part of an unpaved road management system. It provides powerful information for the strategic management of a road network, particularly for determining warrants for paving in areas where gravel materials are scarce.

The system has proved its worth in managing the Cape Province unpaved road network, particularly to ensure an equitable distribution of maintenance funds between 20 RCSs that execute maintenance on an agency basis. On the basis of the experience gained, the formal Unpaved road Management System should become an integral part of the road management system of any rural road authority. The process of implementation and operation adopted and presented in this paper can be recommended to other authorities.

ACKNOWLEDGMENT

The authors wish to thank the Provincial Roads Engineer of the Roads and Traffic Administration Branch of the Cape Provincial Administration for permission to publish this paper.

REFERENCES

1. Visser, A. T., and P. C. Curtayne. The Maintenance and Design System: A Management Aid for Unpaved Road Networks. In *Transportation Research Record 1106,* Vol. 1, TRB, National Research Council, Washington, D.C., 1987.
2. Paige-Green, P., and A. T. Visser. Comparison of the Impact of Various Unpaved Road Performance Models on Management Decisions. In *Transportation Research Record 1291,* Vol. 2, TRB, National Research Council, Washington, D.C., 1991.

Publication of this paper sponsored by Committee on Low-Volume Roads.

Quality Assurance Procedures Related to Administration of Unsurfaced Roads

JACOB GREENSTEIN AND STUART W. HUDSON

The principle that the delivery of safe and effective road services is a duty owed to the road users provides the impetus for a quality assurance (QA) program. QA refers to all of the criteria and activities used to verify and audit road performance. Road conditions are measured in terms of pavement distress extent and severity, structural capacity, and riding quality. The most dominant surface distresses are roughness, potholes, dust, and rutting (plastic deformation under the wheel path). Simplified QA criteria are presented related to surface distress severity, traffic loading, maintenance expenditures, vehicle operating cost (VOC), and economic indicators such as net present value and internal rate of return. Construction and maintenance work procedures and their QA and quality control (QC) procedures are introduced. The choice between using rougher surfaces with more severe potholes and dust distresses and higher VOC is compared with the use of smoother roads that require higher maintenance and rehabilitation costs but save the users money. As an example, when the average daily traffic is equivalent to fifteen 12-ton trucks, road owners have a choice between (*a*) a dirt road that requires U.S.$2,800 in annual maintenance expenditures and will develop surface roughness of 14 m/km and medium to high severity of dust and potholes or (*b*) a silty sand surface with roughness of 10 m/km with a lower level of potholes and dust but higher rehabilitation and maintenance costs. Although the economic return of upgrading the dirt road to a silty sand surface is 12 percent, the road's owners may select to postpone the road improvement and spend less on rehabilitation and maintenance and allow a higher VOC. On any given road network the trade-off between spending on routine maintenance and saving in VOC should be carefully evaluated to provide a balance among user cost considerations, agency costs, and acceptable road performance.

Poorly built and maintained roads are expensive and inconvenient to taxpayers. The quality of work performed on roads is directly related to service life, future maintenance costs, level of service, and user costs. The principle that the delivery of safe and effective road services is a duty owed to the taxpayer or user is the basis for a quality assurance (QA) program. To obtain a reasonable degree of QA, proper design standards and specifications acceptable to the users should be established and enforced. Recognition of the inherent variability of construction requires establishment of a comprehensive set of design standards, long- and short-range work plans, material specifications, sampling and testing guides, and maintenance standards.

The term *quality* is that characteristic of a road network that provides a well-defined and acceptable level of performance in terms of service and life. "Quality" does not mean "perfection." If the objective of a roadway surface is to carry the anticipated traffic safely (service) for five years (life), then "quality" refers to those characteristics of the surface that are necessary to achieve that objective.

Inter-American Development Bank, 1300 New York Avenue, N.W., Washington, D.C. 20577.

Quality control (QC) ensures that proper materials and procedures are used and placed in a definite manner so that the end product will have the desired level of performance in terms of service and life. QC activities are specific steps taken during construction and maintenance to control the quality of materials and work.

QA refers to all of the activities necessary to verify, audit, and evaluate quality. It may also refer to the quality of data collected for use in a road surface management system.

The quality of a road network is influenced by activities other than field operations, as shown in Figure 1. Broad quality objectives are established in the planning stages of a project. Design implements those objectives and sets the specific levels of quality to be achieved. Finally, the preparation of plans and specifications establishes the rules under which the quality will be achieved. QA is concerned with all of these activities and how they affect the final quality of the product.

ENGINEERING CLASSIFICATION OF UNSURFACED ROADS

Experience indicates that unsurfaced roads can be classified into five principal categories (*1–5*). Type 1 is designated for natural earth roads built with limited engineering input using either labor-intensive methods or limited use of a motor-grader during the rainy season. These roads are frequently impassable, depending on whether they are in semiarid or subtropical areas, whether good or poor drainage conditions exist, and whether adequate maintenance is provided. Type 2 roads are composed of compacted silty sand constructed usually to widths of from 4 to 6 m. The thickness of the surface course on these roads varies between 10 and 30 cm and the design California bearing ratio (CBR) varies from 7 to 15, depending on the local environmental and drainage conditions. These roads usually have a surface life of 2 to 5 years if adequately maintained. Type 3 roads are constructed with a gravel or laterite surface from 12 to 35 cm thick and 4 to 6 m wide. These roads have a surface life of approximately of 5 to 7 years before resurfacing (pavement rehabilitation). Type 4 roads have stone surfaces with a range of width from 3 to 6 m and require minimum maintenance. These roads have a surface life of 20 to 30 years before strengthening or rehabilitation is necessary. Type 5 roads are normally about 7.2 m wide with high-quality screened or crushed gravels or stones that have a CBR of more than 40 and a surface life of 7 to 10 years.

The quality performance of unsurfaced roads is determined from the following primary pavement defects:

1. *Loose sand or gravel*: gravel or sand surface compacted loosely; gravel or sand in wind-rows parallel to the direction of traffic;

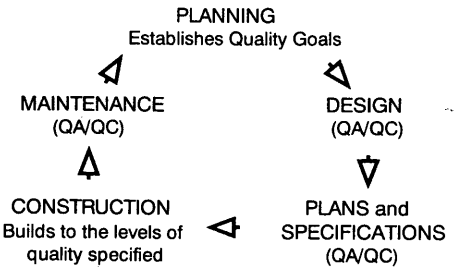

FIGURE 1 Quality assurance activities.

2. *Dust*: traffic action creating a dust cloud;
3. *Potholes*: bowl-shaped depressions in the road surface;
4. *Breakup*: subgrade soils coming up through the gravel surface, most likely to occur in the wheel tracks;
5. *Roughness*: series of closely spaced crests and valleys, usually more pronounced in the wheel tracks;
6. *Rutting*: surface depression in the wheel path;
7. *Flat or reverse crown*: slope of road flat, nonexistent, or reversed, with road edges higher than the center portion of the road surface;
8. *Distortion*: any deviation of road surface from its original shape (other than described for roughness or rutting), such as humps or dips; and
9. *Shoulder distress manifestation*: excessive height, ponding, vegetation growth, and so forth.

The possible causes of each defect (distress) and definitions of severity and extent are presented in the literature (*5–8*). Failure of unsurfaced roads is defined as rutting to a depth of 75 cm to 150 mm, roughness of 17 m/km (international roughness index), or more than 50 percent of the roadway surface affected by severe potholes (*3,9,10,12*).

CONSTRUCTION AND MAINTENANCE WORK PROCEDURES

The construction and maintenance responsibility of governmental agencies can be discussed in terms of who actually performs the work: a contractor or the agency's own forces (in-house projects).

The agency must establish the necessary procedures to ensure that construction and maintenance will be of an acceptable quality, regardless of who performs the work. These procedures will usually be formalized by ordinances, regulations, standard operating procedures, manuals, specifications, and contracts.

Road construction and maintenance contracts are usually let on a low-bid basis and must ensure adequate surface performance during the useful life of the road network. In other words, the contract establishes the work to be performed, the amount of reimbursement, specifications, and QA/QC procedures to be performed during the project's lifetime and the duties and responsibilities of the authorities and the contractor.

SPECIFICATIONS AND QUALITY CONTROL

Specifications are written instructions or precise descriptions of the product desired. Specifications answer the question "How do we order it?" and translate quality levels established by design into specific quality requirements. There are two common uses of the term *specifications*: general specifications and product specifications.

General specifications relate to contract requirements such as bidding conditions, control of work, legal responsibilities, payment, prequalification of contractors, and other considerations. Product specifications establish the requirements that the material, product, or services being purchased must meet. In construction, product specifications can be classified into the two general categories, recipe and performance.

Recipe Specifications

Also referred to as method specifications, recipe specifications describe what is wanted and how it is to be obtained. For a gravel pavement, the engineer would specify the CBR, moisture-density relationship, plasticity range, gradation and other requirements of the aggregate, the general types of equipment to be used, hauling, placing, rolling, and degree of compaction. Recipe specifications are currently the more frequently encountered type of product specification in the road industry and are primarily developed by experience. Disadvantages of recipe specifications include the following:

- Natural product variability is not adequately accounted for,
- Little or no recourse is available if the specifications were followed but the results were unsatisfactory,
- Materials sampling often does not yield a statistically significant or reliable result, and
- Little opportunity for innovation is allowed on the part of either contractor or engineer.

Advantages of recipe specifications are as follows:

- The inspectors and contractors involved with construction are familiar with the specifications,
- They are relatively easy to understand, and
- Clear guidelines are provided for those who are inexperienced in planning, supervising, and inspecting construction activities.

Performance Specifications

Also referred to as end-result specifications, performance specifications describe how the completed product must perform, in other words, what kind of surface defects (loose gravel, dust, potholes, breakup, rutting, and roughness) will be allowed during the project lifetime and an acceptable level of their severity. Performance specifications give the contractor considerable freedom in choosing how to satisfy the requirements, and the primary responsibility for quality control is placed on the contractor. The engineer monitors the contractor's quality control and accepts or rejects the work and the contractor invoice. Performance specifications are statistically oriented and are based on random sampling techniques, with acceptance on a lot-by-lot basis (a lot being a given quantity of material, i.e., 1,000 tons of material or a day's production).

Disadvantages of performance specifications include the following:

- Full implementation requires statistical procedures that may be difficult for small governments to administer;
- The additional responsibilities placed on the contractor may result in higher bid prices, at least initially; and
- The lack of specific "how to" specifications requires experienced and competent inspectors and contractors.

Advantages of performance specifications include the following:

- A realistic picture of the true quality of a product or material is provided to the engineer;
- The relative freedom allowed contractors encourages innovation, which should eventually result in lower prices; and
- There should be a decrease in inspection requirements and expenses.

Enforcement

Specifications establish contractual requirements; road authorities and contractors must assume that the contracted price fairly compensates the successful bidder for all costs associated with complying with the specifications. In terms of QA, performance goals cannot be met if any step in the process falls short. Specifications establish requirements that represent the culmination of planning and design efforts. Inspection, sampling, and testing are QC procedures designed to enforce the specifications and to monitor and achieve acceptable levels of surface distress. In other words, on the basis of the actual road conditions (in terms of the development of potholes, rutting, roughness, and dust) during the lifetime of the project, a decision is made to approve or reject the contractor invoice.

Road Surface Inventory Information

Planning the Inventory

The road surface inventory is the process of collecting and assembling data to properly implement a surface management program (*1,2,8*). Most agencies probably already have some type of inventory. It might be simply a map showing all roads maintained by the agency or complete construction project files containing information such as date of construction, project length, width, and pavement type. An inventory, in a format that can be easily recalled and used, should contain all the basic information that identifies and describes each section and is needed to make sound management decisions. Inventory data, once established, do not change often. They will only change as maintenance, rehabilitation, or reconstruction changes basic section characteristics or as traffic levels change. Condition information, on the other hand, is constantly changing and will require updating at regular intervals.

A good inventory does not require the use of a sophisticated computer system. A carefully planned inventory can be as simple or as sophisticated as the user desires. Data forms and system files can be designed to permit manual operation initially and also to provide a smooth transition to computer applications at some point in the future. Whether to use a manual file or a computer is strictly a local choice.

Defining Section Boundaries

The first step in an inventory is to divide the road system into manageable segments called sections. The minimum number of sections that adequately define the road network will be the most economical and easiest to maintain.

Sections are defined so that the pavement within their boundaries is consistent in terms of physical characteristics and factors that contribute to deterioration. Any of the following would define the boundary between two sections: (*a*) a change in road width or in pavement surface type and (*b*) traffic, drainage, and subgrade characteristics. In addition, geographic or man-made boundaries may offer or force section limits, such as rivers or streams, city or township limits, and county or district lines. In deciding where to locate section boundaries, it should be remembered that once established, boundaries take on a somewhat permanent nature. Every effort should be made to reference sections to permanent, recognizable, and safe landmarks. The concept of dynamic segmentation may also be used if section limits are expected to change because of construction project overlap or subdivision into smaller sections.

Essential Information

The inventory process should be as simple as possible while still collecting the required information. Assembling inventory information should be accomplished in three phases: (*a*) determine the types of data needed, (*b*) determine which data currently exist in office records, and (*c*) determine the remaining data that must be gathered by the survey team. The essential information to be considered includes section description (boundaries and name and number of route), functional and administrative classification, surface structure (thickness and material characteristics), construction and maintenance history, cost data, traffic, geometry and drainage characteristics, and other data (signs, guardrails, location of utility drainage structures, etc.).

Describing and Delineating Sections

Identification of sections used for inventory and data collection to uniquely describe the area of influence within the road network is a critical first step that can have long-term repercussions if not done in a logical manner. Once the sections are described, thought must be given to assigning a numbering or naming system to them. It is important in assigning section identifiers to consider how the inventory data will be stored and how the section identifier will be used to easily recall data. There are several recommended methods for setting up sections and assigning numbers. These include using existing street names or route numbers, assigning coded numbers to sections, using a link-node system, setting up a unique alternative numbering system, or using a computerized geographical information system.

Geographical Information Systems

A geographical information system (GIS) provides a modern method of numbering and locating sections using computer technology. A coordinate system is used to store the network-wide

map on the computer. The sections are then defined by the coordinates of the end points. Sections can be selected or identified directly on the computer screen map by pointing to the correct road or circling a group of roads in a certain area. GIS is becoming more and more popular, but it is still considered a highly advanced technology, which may not be appropriate for some local governments.

Automated Data Collection

A data format does not necessarily require written documentation. However, once it has been determined what information will be collected and how that information will be organized, an economical and convenient process may be to program a simple data collection routine on a hand-held computer. Such a device can be readily used in the field to directly enter the inventory data. The data can then be electronically transferred to a microcomputer in the office for processing and storage. This procedure significantly reduces the volume of documentation, labor, and errors associated with the use of paper forms. The entire step of data entry from the forms into the computer and checking the entries is eliminated. Hand-held, notebook-style computers are relatively inexpensive and easy to program. They are ideally suited for field data compilation as part of a road surface management system. Road survey vehicles are also available for use in automating the inventory data collection. On-board computers are used to accept the data directly in the field.

Conducting an Inventory

Whether an automated or manual inventory procedure is used, certain basic principles should be followed. A two-person survey team should be used to conduct the physical inventory. The team members should have a basic knowledge of (*a*) road location and classification, (*b*) the inventory data format, (*c*) the concept of sections and reference points, and (*d*) the existing record system of the agency.

Road Surface Condition Information

Surface Condition Survey

A condition survey is the process of collecting data to determine the surface structural integrity; type, amount, and severity of distress; and overall riding quality of the roadway. Unlike inventory information, surface condition changes constantly and must be reevaluated on a regular basis. Condition surveys provide a rational and consistent method of allocating limited resources. By monitoring the road surface condition using the methods described here, the local agency should be able to (*a*) prioritize maintenance activities, (*b*) prepare long-range programs, (*c*) determine effects of budget reductions and deferred maintenance, (*d*) schedule future surface maintenance activities, and (*e*) track performance of various surface designs and materials.

Types of Surveys

Three types of condition surveys are applicable to unpaved surfaces: distress survey, roughness evaluation, and structural testing. The distress survey involves identifying the various distress types and the extent and severity of each. Roughness evaluation measures the ride quality of the roadway. Roughness is itself only an important distress type as well as an indicator of other distress. It can also be used to prioritize visual distress surveys. According to World Bank research on the Highway Design and Maintenance (HDM) Model, roughness and material loss from the surface are the primary types of distresses that characterize the deterioration of unpaved roads (*10*).

Since the AASHO Road Test (1965), several measurement procedures have been developed to quantify roughness levels on road surfaces. Many of these measures are summary statistics derived from precise measurements of road profile. Others involve measurement of the response of a roughness meter. Once a roughness meter is calibrated to one of the profile-based statistics, the direct output of the roughness meter can be converted to an estimate of the standardized roughness statistic. Currently, the most widely accepted roughness statistic is called the international roughness index (IRI). Other similar statistics include the quarter-car index (QI) and the standard Mays meter number (MO). All of these statistics are similar in derivation in that they are initially obtained by a mathematical manipulation of the surface profile elevations.

Structural testing may be destructive or nondestructive. Destructive testing involves soil borings or test pits with a materials analysis to determine bearing values. Nondestructive testing consists of measuring either deflections or load response and correlating the results to known values. Structural data are not routinely collected for network-level surface monitoring by most agencies. Normally these date are used for structural evaluation and design on an individual-project basis. Exact location and frequency of structural testing within specified road sections should be carefully determined before seeking testing services. The tests should be limited to locations where distress and roughness surveys indicate potential structural problems. The results of these tests reflect the degree of structural adequacy that exists in the pavement structure.

Planning Roughness Surveys

Surface condition data are needed to adequately assess maintenance and rehabilitation needs. It is necessary to accurately and methodically determine the current surface conditions to ensure that decisions for scheduling and implementing maintenance and rehabilitation projects are based on the best and most recent information. This information must be collected using standard procedures so that results can be compared over time.

It is recommended that the entire network be surveyed for roughness initially and the resulting data be correlated with the distress data by surface type. With this information, roughness can be used as an indicator of other problems and can help prioritize sections needing more expensive distress surveys. Roughness alone can be used to determine maintenance strategies. However, greater benefits result when roughness data are evaluated along with other types of surface distress data.

An educated decision should be made as to the method of roughness surveying. For continuity of information and to allow comparison of results to determine deterioration, the same method and equipment should be used from year to year. If a change in method is necessary, a method of correlating results will be needed.

Survey Frequency

The frequency of surveys depends upon several factors. These include surface type, age, current condition, average daily traffic, axle loadings, drainage characteristics, and weather factors. Of these factors, current condition, axle loadings, and drainage are the most important.

Traffic loadings are usually relatively consistent within each road class. Therefore, if traffic and axle loading data are not readily available, it may be reasonable to assign survey frequency by functional classification. For instance, principal roads might be inspected annually, secondary roads every 2 years, and penetration roads every 4 years. Routine maintenance inspections may be required more often because of the relatively rapid deterioration experienced on unpaved surfaces.

Frequency also depends on the surface condition of individual sections. New roads or roads in good condition require less frequent inspections than roads that are experiencing high rates of deterioration.

Environmental Considerations

Rural road administration, including construction, improvement, rehabilitation or maintenance work, and environmental protection or remediation activity, is a complementary aspect of the same agenda (*11,12*; Greenstein and Ehrlich, another paper in this Record). The inclusion of environmental QA/QC in road development is well recognized. QA procedures specify cleaner and safer project sites for the local communities and the construction workers during both the rehabilitation and operation of roads and bridges. These QA procedures should address applicable environmental regulations known to be getting more rigorous.

In order to optimize expenditures and develop practical environmental QA and QC procedures for any given project, it is common to adopt an environmental classification system. According to the Inter-American Development Bank (IDB) (*11*), projects are classified in four environmental impact categories: beneficial, neutral, moderate or potentially negative, and significantly negative. The World Bank (IBRD) classifies projects in three categories:

- Complete environmental analysis is required because the project may have diverse and significant environmental impacts,
- Limited environmental analysis is appropriate because the project may have well-identifiable and manageable environmental impacts, and
- Environmental analysis is not usually necessary because the project is unlikely to have significant environmental impacts.

For each type of rural road or bridge project, QA/QC should identify and address the protection procedures related to

1. Protection of areas with endangered fauna or flora or with particularly vulnerable ecosystems;
2. Elimination of barriers to movement in areas with conservation-worthy or particularly large wildlife populations;
3. Protection of areas with significant historic and cultural remains or landscape elements of importance to the local population;
4. Prevention of regressive or progressive erosion;
5. Minimization or prevention of the use of scarce material resources;
6. Limitation of accessibility to protected areas or to vulnerable natural resources;
7. Legal and physical protection of the local population with regard to cultural conservation, land use, and ownership of land;
8. Minimization of changes in traditional resource exploitation related directly or indirectly to the project;
9. Modifications of natural drainage patterns and groundwater characteristics and quality;
10. Air and water pollution control related to road or bridge construction and maintenance;
11. Minimization and control of noise and dust during the construction, maintenance, and operation (use) stages;
12. Minimization of the effects of increased motorized traffic on nonmotorized transportation economy;
13. Prevention of illegal timber cutting and illegal land clearing;
14. Prevention of illegal invasion by squatters poaching on the homelands of indigenous people;
15. Preservation of wetland;
16. Control of soil and water contamination and management of construction and hazardous materials;
17. Enhancement of employee and workplace safety features;
18. Protection of archeological sites, and
19. Management of ecosystems and conservation of biodiversity.

Environmental QA is obtained through the implementation of a set of guidelines that describe the above environmental impact prevention procedures and mitigating prevention or correction procedures related to road administration, allocation of responsibilities, and cost recovery of environmental damage.

Environmental QC procedures are the site-specific or detailed environmental requirements that, together with the general guidelines, are an integral part of the project specifications. These specifications must precisely define the environmental parameters and the ways to measure changes during the implementation and operation of the project, for example, the allowable levels of noise and dust during the construction period and methods of measurement, methods and parameters to monitor water quality before and after construction, means to design erosion control measures taking into consideration soil and climatic characteristics; optimum gradation and plasticity to reduce dust during traveling after construction of unpaved roads, and optimum size of embankment and drainage facilities to minimize alteration to the natural drainage pattern and obstacles to wildlife. The environmental QA guidelines and the QC procedures should be constantly updated to meet international and local standards and legislative requirements.

Maintenance Management

The main objective of road maintenance planning is to determine the relationship between the projected surface conditions and the most economical and affordable level of rehabilitation and maintenance expenditures that the road users are able and willing to incur. To achieve this goal, it is necessary first to determine the relationship between the projected traffic and surface performance. In predicting surface performance, each failure criterion should be developed to take care of each specific distress, namely, surface deformation (roughness, rutting, flat or reverse crown, distortion);

surface defects (loose sand or gravel, dust, potholes, breakup); and shoulder distress. Once the allowable surface distress during the road's operation are determined, an economic analysis is carried out to select the most practical construction and maintenance activities together with the appropriate QA procedures.

As an example, a projected traffic volume range from 27,000 to 216,000 medium-sized 12-ton trucks may be selected to analyze the performance of an unsurfaced road network. For a life expectancy of 15 years, the foregoing traffic volumes vary from 5 to 40 trucks (12-ton) per day, respectively, or between 25 and 200 average vehicles per day (*1–3,7*). The selected quality criteria of the road network are as follows:

1. Maximum allowable roughness should be 10 to 17 for adequately maintained to rough surfaces, respectively. Usually, the higher the traffic volume is and the better the surface materials are, the lower is the maximum allowable roughness;
2. The maximum allowable amount of potholes should not exceed 50 percent of the roadway surface and the dimensions of individual potholes should not exceed 300 mm in width and 100 mm in depth (*3,5,10*). (Note: The roughness and pothole *failure* criteria are compatible and are usually associated with subgrade or pavement rutting of 75 to 100 mm under the wheel path.)
3. Less than 50 percent of the roadway should be affected by dust, and the severity of the dust cloud should be moderate or slight so that vehicles are still visible to other vehicles in front or behind or to on-coming traffic.

The engineering classifications for the road network surface materials are (*a*) silty clay (A-6) with a design CBR of 5 to 6, (*b*) silty sand (A-2-4) with a design CBR of 12 to 14, and (*c*) local gravel materials (A-1) with a design CBR of 18 to 20. The life expectancy in terms of number of axle passes on these types of surface materials is determined according to the following equation (*8,13*):

$$C = 0.1138N^{0.172}P^{0.580}Q^{0.490}$$

where

C = soaked CBR of surfacing material, in percent (C varies between 4 and 20);
N = design number of cumulative equivalent single wheel loads of P;
P = 40 kN and tire pressure Q;
Q = 550 kPa (equivalent approximately to that of a medium-sized 12-ton truck).

According to the equation, the life expectancy in terms of cumulative 12-ton trucks is 50, 10,000, and 140,000 repetitions for a surface CBR of 5, 12.5, and 20 of silty clay, silty sand, and gravel, respectively. For these three typical materials, Table 1 presents the relationship between the projected average daily traffic (ADT) of representative trucks (12-ton); type of surface; net present value (NPV) of construction, maintenance, and VOC calculated for a project lifetime of 15 years and discount rate of 10

TABLE 1 Cycle Cost Analysis Versus Surface Roughness

	DIRT ROAD			SILTY SAND ROADS					GRAVEL ROADS				
	NPV*$1000			NPV*$1000					NPV*$1000				
ADT 12 tons	Roughness M/KM	Rehab./ Maint.	VOC	Roughness M/KM	Const./Rehab.	Maint.	VOC	IRR %	Roughness	Const./ Rehab.	Maint.	VOC	IRR %
5	10	12.2	13.4	10	11.3	4.2	13.4	<5					
10	10	21.3	26.8	10	14.6	7.6	26.8	<5	10	22.7	11.4	26.8	<5
15	14	21.3	49.7	10	21.5	9.1	40.2	12	10	28.0	13.7	40.2	<5
20	17	21.3	77.0	10	30.3	12.2	53.7	68	10	28.0	15.2	53.7	7
25				12	39.9	11.4	74.6		10	28.0	17.5	67.0	24
30				14	39.9	13.7	99.4		10	28.0	19.0	80.5	37
40				17	49.4	21.3	153.3		10	28.0	20.5	107.3	102

ADT = Average Daily Trucks of 12 Tons.

NPV = Net Present Value (15 years of life expectancy, 10 percent discount rate).

IRR = Internal Rate of Return.

percent; road roughness; and economic analysis in terms of internal rate of return (IRR). The procedures to determine construction, maintenance, and VOC costs are presented elsewhere (*7,9,13*).

Table 1 summarizes the planning options for the road network. For example, for a low traffic volume of 5 to 10 trucks, which is equivalent to 10 to 60 vehicles per day, it appears that the use of dirt roads is feasible. With an annual maintenance cost of $1,600 to $2,800/km, it is possible to comply with the specified QA criteria, namely, roughness of 10 and less than 50 percent of roadway surface affected by small to medium-sized potholes. When the traffic volume increases to 15 and 20 trucks per day, maintenance is not sufficient to keep the surface in the desirable condition. Under elevated annual maintenance costs of $2,800 daily, a traffic increase to 15 and 20 trucks will cause an increase of roughness from 10 m/km to 14 and 17 m/km, respectively. These elevated roughness levels are associated with moderate potholes (20 to 50 percent of the surface affected) and extensive potholes (over 50 percent of the roadway surface affected). The dimensions of severe potholes usually exceed a width of 300 mm and a depth of 100 mm. The VOC increases 237 and 43 percent with the increase of surface roughness index from 10 to 14 and 17 m/km, respectively. In these circumstances, the economic return of upgrading the dirt road to a better pavement of silty sand is 12 and 68 percent for an ADT of 15 and 20 trucks per day, respectively. In these cases, the road users or owners may select between lower construction and maintenance costs and higher VOC.

As an example, for an ADT of 15 trucks, the required annual maintenance cost of a dirt road to maintain the surface roughness at a level of 14 m/km and moderate to low potholes and dust is $2,800. On the other hand, to maintain a roughness level of not more than 10 m/km on a silty sand, it is necessary to invest $5,250 for pavement resurfacing each third year in addition to an annual expenditure of $1,200 for routine maintenance. The annual VOC is $6,534 for the dirt road (roughness = 14) and $5,292 for the silty sand surface (roughness = 10) (Table 1). Although the economic return of upgrading a dirt road to a silty sand road is 12 percent when the ADT equals 15 trucks, the road users may select to invest less in rehabilitation and maintenance and more in VOC. A similar conclusion is applicable to the improvement of a silty sand road to a gravel road when the ADT equals 25 trucks. In this case (see Table 1), although the economic return to improve the silty sand road to a gravel surface is 24, the users may want to avoid the initial improvement cost of $25,000/km and the average annual maintenance cost of $2,300 and pay a higher annual maintenance and resurfacing cost ($6,750/km) and higher VOC for the rougher surface (12 m/km versus 10 m/km). When the daily traffic volume increases to 40 trucks or more, the silty sand surface cannot meet the quality criteria of roughness not to exceed 17 m/km and pothole severity not to exceed 50 percent of the roadway surface with individual potholes less than 300 mm in diameter and less than 100 mm deep. In this case, the economic return of upgrading the silty sand surface to a gravel surface is 102 percent (see Table 1).

Once the different types of road surface are implemented, the trade-off decision of spending on maintenance versus saving on VOC, it should be left to the road users to analyze the cycle cost options of road network maintenance and the consequent ramifications for the quality of traveling. As an example, to ensure a representative roughness of 10 m/km and medium to low severity of potholes and dust on a silty sand surface serving an ADT of 15 trucks (12 tons), it would be necessary to invest $1,200/(year·km) in routine maintenance and $5,250/km each second year on pavement resurfacing and rehabilitation. In this case, the estimated annual VOC is $5,292 and the total net present value of rehabilitation, maintenance, and VOC for a 15-year life expectancy is $21,500/km, $9,129/km, and $40,251/km, respectively (see Table 1). Reduction of the biannual resurfacing cost from $5,250 to $3,600 and $3,100 results in an increase of surface roughness from 10 to 13 and 14, respectively. Consequently, the annual VOC increases from $5,292 to $6,210 and $6,534, respectively. This reduction of the resurfacing costs during a lifetime period of 15 years results in a negative economic return of 23 and 36 percent, respectively.

Road users should select between optimizing the expenditures of maintenance and VOC versus reduction in maintenance costs, which accelerates surface deterioration and increases VOC. Each rural road network should be administered according to the needs and financial capabilities of its users.

REFERENCES

1. Greenstein, J. Issues Related to Administration of Low-Volume Roads in Developing Countries. Presented at the 71st Annual Meeting, Transportation Research Board, Washington, D.C., 1992.
2. Greenstein, J., and H. Bonjack. Socioeconomic Evaluation and Upgrading of Rural Roads in Agricultural Areas of Ecuador. In *Transportation Research Record 898*, TRB, National Research Council, Washington, D.C., 1983.
3. Greenstein, J., and M. Livneh. Pavement Design of Unsurfaced Roads. In *Transportation Research Record 827*, TRB, National Research Council, Washington, D.C., 1981, pp. 21–26.
4. Inter-American Development Bank. *Agricultural Sector Investment Program in Venezuela.* Washington, D.C., 1992.
5. Berger, L., and J. Greenstein. Simplified Procedures to Manage the Maintenance of Low-Volume Roads. In *Transportation Research Record 1106*, Vol. 2, TRB, National Research Council, Washington, D.C., 1987, pp. 201–210.
6. Chong, C. G., and G. A. Wrong. *Manual for Condition Rating of Gravel Surface Roads.* Research and Development Branch, Ministry of Transportation, Ontario, Canada, 1989.
7. *Pavement Maintenance Management for Roads and Parking Lots.* Technical Report M-294. U.S. Army Corps of Engineers, Oct. 1981.
8. *Pavement Condition Rating Guide.* FHWA, U.S. Department of Transportation, May 1985.
9. Watanatada, T., C. Harral, W. Paterson, A. Dharceshwar, A. Bhandari, and K. Tsunokawa. *The Highway Design and Maintenance Standard Model.* World Bank, Washington, D.C., 1987.
10. Paterson, W. D. O. *Road Deterioration and Maintenance Effects.* World Bank, Washington, D.C., 1987.
11. Inter-American Development Bank. *Application of Environmental Procedures in the Transportation Sector: Guidelines.* Washington, D.C., April 1991.
12. *Environmental Assessment Sourcebook.* Technical Paper 140. World Bank, Washington, D.C., Dec. 1991.
13. *Local Low-Volume Roads and Streets.* Federal Highway Administration; American Society of Civil Engineers, Nov. 1992.

Publication of this paper sponsored by Committee on Low-Volume Roads.

Institutional Aspects of Environmental Management in Road Development

JACOB GREENSTEIN AND MARKO EHRLICH

Environmental protection and remediation are integrated activities of road administration. International lending agencies such as the Inter-American Development Bank and the World Bank and the lawmakers of both developed and developing countries insist that all projects be environmentally sound. To achieve this goal, road departments need adequate institutional capacity to address and resolve all the environmental issues in a timely and cost-effective manner to reduce or avoid remedial costs. Experience with the administration of environmental units within road departments is detailed in this paper. The principal responsibilities of such a unit are the administration of environmental impact assessments; research, development, and adaptation of new technologies; and education and training of the department's managerial and technical staff. This kind of environmental management is set within a defined legal and regulatory framework and requires interinstitutional cooperation and coordination. In order for this program to succeed, institutional strengthening is required for the development of human resources, improvement of the organizational set-up, implementation of environmental policies related to road administration, and improvement of the administration of environmental impact assessments. A typical institutional set-up and its responsibilities are presented.

In road administration, construction, improvement, rehabilitation or maintenance, and environmental protection or remediation are complementary aspects of the same agenda. The inclusion of environmental considerations in road development is being recognized by road planners and engineers as a legitimate concern to (*a*) promote better highway planning, design, and construction and (*b*) benefit society as a whole through protection of the environment and prevention of the loss of recognized environmental values (from aesthetic values to biodiversity). In other words, the era of classifying environmental considerations as a "required nuisance" seems to be over. A few indicators that strengthen this conclusion are as follows (*1–6*):

- Local communities are demanding cleaner and safer construction sites, especially in projects related to rehabilitation or improvement of existing roads and bridges. This concern comes waxes and wanes, but there is an overall upward movement.
- Environmental regulations are getting stricter and will continue to get more rigorous.
- New economic instruments—taxes, charges, and tradeable permits—are rewarding "clean" companies. Business in general is calling for the increased use of such instruments.
- International lending agencies such as the Inter-American Development Bank (IDB) and the World Bank (IBRD) insist that all projects be environmentally sound and that the executing agency have adequate institutional strength to properly address all the environmental issues (*2–4,6*).
- Commercial banks are more willing to lend to companies that prevent pollution rather than paying for expensive clean-ups. There are two main reasons for this. First, there is growing concern among bankers about their liability for the environmental misdeeds of borrowers. Second, a company that is unlikely to be liable for large clean-up bills is a company more likely to be able to repay its loans on schedule.

Considerable progress has been achieved at integrating environmental concerns into standard engineering practice, and road economic evaluation increasingly includes a greater portion of environmental mitigation as part of the road construction costs. Although environmental quality of road development has probably benefited from this progress, much still needs to be done to secure and improve these achievements and to institutionalize environmental work as an integral part of infrastructure administration. A simplified institutional framework for an environmental unit (EU) and its set-up and function within the organizational structure of a road department is presented.

GENERAL OBJECTIVES AND TASKS

The main tasks of an EU are to (*a*) ensure proper analysis of project alternatives during the planning process; (*b*) perform adequate quality assurance (QA) and quality control (QC) procedures during the project construction and operation; (*c*) where needed, implement protection measures to prevent or reverse negative environmental impacts in order to reduce or avoid remedial costs by addressing the issues in a timely and cost-effective manner; and (*d*) participate in the development and implementation of environmental policies related to road administration. Research, development, and adaptation of new technology to be used by the department's managerial and technical staff, consultants, and contractors who provide advice and services to the department form another principal task. Education and training are other important activities needed to relate the daily work of the road administration to environmental regulations.

Environmental Impact Assessment

As part of its QA function, the EU needs to be closely (though not necessarily directly) involved in the preparation of environmental impact assessments (EIAs). Specifically, the unit's task is to prepare the EIA's terms of reference in order to make it a comprehensive and flexible management tool tailored to the entire range of the department's activities (i.e., construction, rehabilitation, maintenance) in the different environmental conditions of the

Inter-American Development Bank, 1300 New York Avenue, Washington, D.C. 20577.

state or country under its jurisdiction. Although there is no fixed inventory of issues to be evaluated in any particular project, it is usually necessary to coordinate the EIA preparation with other public institutions directly responsible for environmental issues at both the central and regional levels. In order to ease decision making and optimize expenditures dedicated to evaluating the environmental quality of any given project, it is common to adopt an environmental classification system. According to the IDB (*2,3*), projects are classified in four environmental impact categories: beneficial, neutral, moderate or potentially negative, and significantly negative. The IBRD classifies projects in three categories: complete environmental analysis is required because the project may have diverse and significant environmental impacts, more limited environmental analysis is appropriate because the project may have well-identifiable and manageable environmental impacts, and environmental analysis is not usually necessary because the project is unlikely to have significant environmental impacts. Such a classification system is useful to determine work priorities and assign the necessary funds and personnel needed to properly carry out the EIA or environmental analyses (*2,5,6*) and to determine whether the project

1. Affects areas with animal or plant life worthy of protection or areas with particularly vulnerable ecosystems;
2. Creates barriers to movement in areas with conservation-worthy or particularly large wildlife populations;
3. Affects areas with significant historic and cultural remains or landscape elements of importance to the local population;
4. Causes regressive or progressive erosion;
5. Leads to high rates of consumption of scarce material resources;
6. Leads to increased accessibility to protected areas or vulnerable natural resources;
7. Changes the way of life of the local population in such a way that it leads to an increased pressure on the natural resource base;
8. Leads to major conflicts with regard to existing land use and ownership of land;
9. Obstructs or leads to changes in the traditional resource exploitation patterns either directly or indirectly affected by the project;
10. Modifies the natural drainage patterns and groundwater characteristics and quality;
11. Contributes to air and water pollution;
12. Increases noise and dust impact on the local population, especially along unpaved roads;
13. Affects the increase of motorized transportation (with possible increased dependency on imported fuels);
14. Affects the nonmotorized transportation economy because of changes in land use, increased availability of motorized alternatives, or both;
15. Causes illegal timber cutting and illegal land clearing; and
16. Causes illegal invasion by squatters and poachers of homelands of indigenous peoples.

The preparation of the EIA usually requires coordination with other governmental departments and nongovernmental organizations to ensure compliance with national and international standards related to road administration minimize overall expenditures. To achieve so many ambitious goals, the EU must ensure that the department's managerial and technical staff and the consultants and contractors that provide advice and services are educated in environmental concerns and qualified to carry out their duties. In other words, the EU should help all involved with the department's activities to understand how their work relates to the environment.

Resources Needed To Prepare EIA

The time required to prepare an EIA and the resulting cost vary with the local, sociocultural, and environmental conditions (e.g., fragile tropical forest area versus semiarid zone); the type, size, and complexity of the project and its characteristics (e.g., new construction versus rehabilitation); and the amount and quality of environmental data already available. Experience indicates that EIAs need as much time as do feasibility studies, of which the EIA is essentially a part, and usually take from less than 5 months to more than 18 months to complete (*2,4–6*). Implementation of EIAs does not usually delay projects; on the contrary, in many cases, the EIA has shortened the total time from identification to operation by promptly revealing environmental issues that might have halted work altogether had they emerged at a later stage. In other words, whether a particular EIA actually delays a project depends largely on how well it is coordinated with feasibility studies and other preparation activities.

EIA preparation cost rarely exceeds 1 percent of the total capital cost of the project and is frequently less than that. The cost of implementing mitigating measures can range from 0 to 10 percent of total project cost, with 3 to 5 percent being common (*4*). These estimates do not take into account possible remediation cost savings resulted from a cost-effective environmental analysis.

CONCEPTUAL FRAMEWORK

As mentioned earlier, environmental concerns permeate every stage of road development from planning to design, to construction and supervision, to operation and maintenance. They also involve a great many different actors within both the public and the private sectors. Concretely, transportation-related environmental considerations involve the different levels of decision making, such as the road department, national and local governments, and other autonomous agencies (i.e., agrarian and forestry institutions, national parks, and wildlife agencies). Other concerned groups include local residents, tourists, and recreational travelers. In other words, environmental considerations in road administration are cross-institutional issues that need to be addressed through an interdisciplinary and participatory approach involving a wide range of public and private interest groups.

INSTITUTIONAL STRUCTURE

Given the interdisciplinary, interinstitutional, and intersectoral nature of environmental management, the EU must be positioned sufficiently high in the organizational structure of the road department to effectively administer the policy and the technical and managerial work. The EU must support the top management decision-making level with proper technical advice and constantly update policies, guidelines, and QA and QC procedures. To do so, EU must work closely with the legal and planning departments in

order to affect decision making early in the project cycle and within the appropriate legal and regulatory framework. Whenever necessary, the EU will provide essential inputs to the planning and legal departments in order to develop a coherent and effective road development strategy. The EU must also participate in the decision making at the technical level, including the programming, design, construction, supervision, and road maintenance departments. Technical specialists of the EU work closely with all the technical units to assist in the project implementation and operation monitoring and, when needed, all remediation work.

COMPOSITION AND FUNCTION OF EU

The three principal institutional criteria that the EU must fulfill are (*a*) adequate location in the organizational structure of the road department, (*b*) qualified personnel, and (*c*) sufficient budgeting. Moreover, a variety of fields of expertise need to be addressed by the EU, including, among others, ecology, hydrogeology, geography, regional planning, rural sociology, forestry and natural resources management, civil engineering, and hazardous waste management. It is always a challenge to integrate this many skills into the routine activity of the road department. Teamwork and a constructive exchange of information are needed to break traditional barriers and preconceived ideas to assess and improve (*a*) the type and quality of the mitigating and corrective measures, (*b*) their timing and most effective application mechanism, (*c*) the requirement of the EIA process as a result of field analysis, and (*d*) the proper and most effective monitoring procedures. Close cooperation between the EU and the other professional and managerial personnel from the department is necessary, in addition to effective cooperation with other public- and private-sector institutions, affected communities, and the population at large. Such an institutional composition and structure would require approximately 60 to 80 professional person-months per annum to administer the environmental activities related to a road network of 7,000 to 10,000 km (*7–9*).

QA AND QC PROCEDURES

Environmental QA is obtained through the implementation of a set of guidelines that describe the impact prevention procedures and mitigating measures related to construction, rehabilitation, improvement, and maintenance of roads and bridges (*7,8*). This set of guidelines covers, among other things, construction specifications; employee and workplace safety features; extraction, processing, and use of construction materials; management of hazardous materials; air pollution and water and soil contamination; noise control; preservation of wetlands; erosion and sedimentation control; acquisition of land and property; conservation of the right-of-way zone; protection of indigenous groups; protection of archeological sites; ecosystem management and biodiversity conservation within the project influence area; prevention, mitigation, and correction procedures related to road administration; and allocation of responsibility and cost recovery for environmental damage.

The QC procedures are the site-specific or detailed environmental requirements that, together with the general guidelines, are an integral part of the project specifications. These specifications must define precisely the environmental parameters and the ways to measure changes during the implementation and operation of the project, for example, what the level of noise and dust should be during the construction period and how it should be measured; methods and parameters to monitor water quality before and after the construction; means to design erosion control measures taking into consideration soil and climatic characteristics; optimum gradation and plasticity to reduce dust during traveling after completion of the construction of unpaved roads; and optimum size of embankment and drainage facilities to minimize alteration to the natural drainage pattern and minimize obstacles to wildlife. The EU with the assistance of legal and technical advice should constantly update the QA guidelines to meet international and local standards and legislation requirements.

INSTITUTIONAL SET-UP FOR ENVIRONMENTAL MANAGEMENT

There seems to be no universal model or institutional set-up that will be satisfactory in every situation of the highway department. In addition, the effectiveness of the EU within the highway department depends on the existence of a national process and the expertise of (*a*) environmental policies and laws, (*b*) the degree of incorporation of environmental concern into the planning and budgeting of investment and maintenance programs, (*c*) the coordination and cooperation with the central authorities or ministry of environment on relevant issues, (*d*) the establishment of clear guidelines for the EIA, and (*e*) the provision for independent review and approval of EIAs as well as monitoring programs. The preparation and review of the EIAs are very important aspects of environmental management and usually reflect the strengths and weaknesses of the institutional structure and its capabilities to carry out sound environmental recommendations related to road administration. The range of typical institutional problems is wide, and the questions that can be asked are correspondingly varied. Fundamental questions include the following:

1. What EIA procedures apply to the specific road department? Are there guidelines to make them operational? Are they being carried out properly by the EU?
2. How is the environmental information assembled and analyzed and by whom (i.e., consultants versus force account)?
3. How is the information used in selecting, planning, designing, and executing projects?
4. When intersectoral issues arise, such as with the agricultural department rural development program, which also includes a road component, how are they resolved? Are the mechanisms for resolution formal or informal?
5. What are the procedures for monitoring, evaluating, and reporting on project impacts during the construction or the operation stage?
6. How clearly are the responsibilities and authorities of the EU defined?
7. What are the formal and informal lines of communication between the EU and other units of the department?
8. Is there evidence of political and managerial commitment (adequate funding and other resources, leaderships, etc.) to accomplish the desired objectives?

INSTITUTIONAL STRENGTHENING

Institutional strengthening is the permanent activity of updating and improving the environmental managerial capability of the

highway department to administer the EIA and to ensure that investment and maintenance projects are environmentally sound and sustainable. To achieve this goal, the EU should have or be able to obtain the capacity to produce a satisfactory EIA, incorporate the EIA findings into designs and implementation plans and specifications, monitor and manage the construction and operation of the project, and evaluate the results in order to improve future activities.

To identify the scope of institutional strengthening, a diagnostic is done to determine the specific weaknesses that can impair the effectiveness of the environmental administration. The five principal institutional weaknesses are discussed in the following sections (*4,7,8*).

Human Resources

The most common institutional problems in any environmental organization stem from shortages of qualified personnel or deficiencies in the management of the personnel available, or both. The causes are frequently found to be some combination of lack of managerial capacity, low salaries, low job status, lack of strong leadership, and inadequate resources for education and training.

Organizational Structure

The most obvious structural shortcomings affecting the environmental administration are the absence of a strong coordination unit to perform key functions, such as EIA review, technical supervision, monitoring, or regulation, and the fragmentation of responsibility for key functions among the other units of the department without an effective mechanism to coordinate them. Other common weaknesses stem from structures that do not integrate environmental considerations into development planning, especially when intersectoral issues are involved.

Environmental Policy, Laws, and Regulations

Common problems with legal instruments include the absence of (or lack of commitment to) a clear national policy, lack of up-to-date laws and inconsistent regulations of environmental management, lack of implementation of QA/QC guidelines, and improper laws and sanctions that are inadequate to promote compliance with environmental requirements.

Environmental Management Procedures

It is frequently the case that national procedures of environmental management have not been defined. Even when the necessary institutions exist, there may be a need to strengthen the decision-making processes whereby programs and procedures are identified, assigned priority, and implemented to get results. Often monitoring programs, if any, have not provided adequate baseline data for environment-related decisions. Successful interagency coordination, without which many environmental issues cannot be resolved, is difficult to achieve in the absence of established procedures. Many projects that result in adverse environmental impacts in spite of proper planning and design do so because of weak or nonexistent programs essential to sound implementation—monitoring and supervision, operation and maintenance, and community involvement are the ones most frequently cited in this regard.

Financial Issues

Financial factors may be the basis for many of the human resource, organizational structure, and procedural weaknesses discussed above. Funding for the environmental administration (planning, supervision, implementation of mitigation plans, monitoring, measurement of impacts, feedback, etc.) may be inadequate, either because the environment has been given low priority in economic planning and budget preparation or because the available resources are not being managed effectively. Poor project performance can often be traced to insufficient provision of operating and maintenance costs.

Once the principal weaknesses have been determined, the institutional strengthening of the EU may include the following:

- Organizational mechanisms to ensure that environmental policies are followed in all programs and projects;
- Interagency and interdepartment coordination on environmental issues;
- Follow-up to the National Environment Strategy and the environmental action plans;
- Assistance for other units of the department in strengthening their own capacity to deal with environmental issues and develop environmentally sound guidelines, specifications, and procedures of QC and QA;
- Definition of overall needs for environmental education, information, promotion, and training;
- Programs for adequate operation and maintenance, including funding, staffing, facilities, and equipment;
- Rational and equitable cost recovery system to sustain the operation and maintenance functions; and
- Planning, authorizing, and funding processes that provide decision makers with adequate information to meet their environmental protection responsibilities.

INSTITUTIONAL STRENGTHENING OF COLOMBIAN ROAD DEPARTMENT

As part of an effort jointly supported by the IDB and the IBRD to modernize the country's transportation sector, the Ministry of Public Works (MOP) of Colombia has established an EU within its roads department organizational structure (*7,9*). Coordinated and financed jointly by both banks, the EU will receive technical assistance, training, and equipment to become a key player in the establishment and implementation of the MOP's environmental policy. The technical assistance component will consist of consultant services directed to (*a*) review and reformulation of the legal, regulatory, and administrative framework related to environmental management in road projects; (*b*) development of effective and efficient EIA procedures covering the entire project cycle; (*c*) establishment of administrative and normative procedures to supervise the proper application of environmental protection, mitigation, and remediation at the different stages of road administration; (*d*) development of effective environmental

monitoring procedures; and (*e*) establishment and monitoring of institutional mechanisms for interdepartmental and interinstitutional coordination and cooperation as well as for public participation on environmental and sociocultural issues related to road development.

The EU institutional strengthening program includes specialized training both locally as well abroad on such topics as EIA administration, natural resource planning and conservation, environmental monitoring, environmental QA and control, sociocultural aspects of road development, field survey and research and data base management and training.

Logistical support to be provided by the IDB and the IBRD includes all field and office equipment, such as office furniture and hardware (including photocopiers, printers, and facsimile machines), computer software, four-wheel drive vehicles, and field motorcycles.

Additional institutional support will be provided by the Colombian Institute of Natural Resources and Environment (INDERENA) specifically directed at (*a*) standardizing EIA procedures, including project classification and impact evaluation criteria and methodology; (*b*) improving mechanisms of interinstitutional coordination and cooperation; (*c*) staff training and development of educational and promotional programs for field technicians, municipal or local government workers, and community groups; (*d*) preparing field manuals; and (*e*) developing conceptual framework and methodology for conducting applied research on environmental aspects of road administration.

Special attention is given to the preparation of environmental studies of potential road projects in fragile areas such as the Amazon basin or the Pacific coastal region. These studies offer the opportunity to (*a*) train EU staff in dealing with complex environmental issues related to road administration; (*b*) plan land use and sustainable resource development in anticipation of road construction in an undeveloped region; (*c*) consider cultural and indigenous issues as well as biodiversity before unplanned land settlement and habitat degradation and resource depletion occur; and (*d*) allow for public involvement and community participation at an early stage in the decision-making process when it is still feasible to make changes. Through financial support for the institutional strengthening of MOP's own environmental management capability, the IDB and IBRD expect to contribute significantly to environmental protection and sustainable development in Colombia.

CONCLUSIONS

The following conclusions may be stated:

1. Environmental protection and remediation are integrated and principal components of road administration. In other words, environmental expertise is incorporated during the planning, design, construction, and project operation.

2. The main tasks of an EU within the road department are to ensure a thorough analysis of project alternatives, perform adequate QA and QC procedures, and implement protection measures to prevent, mitigate, and remediate adverse environmental effects. In addition, the EU is responsible for research and development, training, and the raising of environmental awareness.

3. Environmental assessment procedures including project classification, impact evaluation, mitigation and remediation measures, and monitoring methods are integral components of a road development project.

4. Adequate allocation of human and financial resources to prepare EIAs avoids unnecessary delays in project preparation and does not significantly raise cost and at the same time can improve project quality and reduce future remediation cost.

5. To effectively incorporate environmental responsibility into the structure of the roads department, the EU must be located simultaneously at the highest managerial and technical decision-making levels.

6. To optimize the functional integration of the EU within the structure of the road department, it is necessary to address environmental issues in a interdisciplinary and participatory manner. The participatory process should include units inside the department, such as planning, design, construction, maintenance, and more important, other governmental, nongovernmental, and community-based interest groups.

7. Environmental management depends upon legal and regulatory frameworks, existing institutional capacity, public awareness, and interinstitutional cooperation and coordination.

8. Institutional strengthening is an ongoing activity essential to adequate performance and an environmentally sound road project. Key elements to be considered under institutional strengthening are (*a*) human resources development, (*b*) an organizational structure that allows efficient administration of the work (done mostly by consultants), (*c*) an environmental policy related to road administration, (*d*) formulation and implementation of EIA procedures, and (*e*) updating and improvement of evaluation and monitoring systems to optimize the allocation of financial resources to perform the unit responsibilities.

REFERENCES

1. *IFC and the Environment: Annual Review.* International Finance Corporation, Washington, D.C., Sept. 1992.
2. *Application of Environmental Procedures in the Transportation Sector: Guidelines.* Inter-American Development Bank, Washington, D.C., April 1991.
3. *Strategies and Procedures on Socio-Cultural Issues Related to the Environment.* Inter-American Development Bank, Washington, D.C., n.d.
4. *Environmental Assessment Sourcebook.* Technical Paper 140. World Bank, Washington, D.C., Dec. 1991.
5. Greenstein, J., P. Pedersen, and T. Terhune. Simplified Techniques of Evaluation and Remediation of Contaminated Paved Areas. Presented at the 70th Annual Meeting, Transportation Research Board, Washington, D.C., 1991.
6. Greenstein, J. Issues Related to Administration of Low-Volume Roads in Developing Countries. Presented at the 71st Annual Meeting, Transportation Research Board, Washington, D.C., 1992.
7. *Colombia: Transport Corridor Program.* Inter-American Development Bank, Washington, D.C., 1992.
8. *Ecuador: National Road Program.* Inter-American Development Bank, Washington, D.C., 1992.
9. *Colombia: Third National Road Sector Project.* The World Bank, Washington, D.C., 1992.

Publication of this paper sponsored by Committee on Low-Volume Roads.